Role of kindlin and talin in the fibrillogensis of fibronectin by platelet integrins exposed to fluid shear forces

Inaugural dissertation

for the attainment of the title of doctor
in the Faculty of Mathematics and Natural Sciences
at the Heinrich Heine University Düsseldorf

presented by

Huong T. T. Nguyen
from Dong Nai/Vietnam

Dusseldorf, October 2015

from the Institute of Hemostasis, Hemotherapy, and Transfusion Medicine
at the Heinrich Heine University Düsseldorf

Published by permission of the
Faculty of Mathematics and Natural Sciences at
Heinrich Heine University Düsseldorf

Supervisor: Prof. Dr. Rudiger Scharf
Co-supervisor: Prof. Dr. Dieter Willbold

Date of the oral examination: 21 October 2015

ACKNOWLEDGEMENT

There have been many individuals who have helped me on my journey here in Germany and at Heinrich Heine University of Dusseldorf. I want to express my deepest appreciation and gratitude to those individuals.

First of all, I would like to acknowledge my dissertation supervisory committee, Prof. Dr. Rudiger E. Scharf and Prof. Dr. Dieter Willbold for letting me work on this very interesting project and their enduring support, their simulating ideas and their critical feedback throughout this project.

I am also heavily indebted to Dr. Volker Stoldt and Dr. Khon Huynh. Thank you for your unyielding support and contribution since the very first stage of this draining yet beautiful journey. This work could not have been done without you two whom I am grateful the most.

I am grateful to Joanna Ventura, Dr. Melanie Eberhard, Dr. Marianna Gyenes, Elisabeth Kirchhoff, Gunda Grosse, Beata Maruhn-Debowski, Maria Völkl, and other staffs as well as MD students at IHHTM for being my best colleagues over all these years. My life in the lab would not have been so joyful and efficient without their friendship and support. Thanks to them for helping me to solve the difficulties in scientific and personal life.

I also thank Martin Wolff, Institute of Physical Biology, for supporting me in experiments with circular dichroism spectrometer.

I would like to acknowledge NRW Research School Biostruct and IHHTM for their financial assistance, both through scholarship awards and the research funding provided. Especially, I deeply appreciate the administrative support from Dr. Cordula Kruse over these years.

I would also like to thank my dear friends and relatives who have encouraged me to pursue my dreams throughout the years.

I deeply appreciate for the love and support given to me by my parents and my sister. Throughout my struggles, they have been an incredible source of encouragement and strength. For their many sacrifices, I dedicate this work to them.

For any errors or inadequacies that may remain in this work, of course, the responsibility is entirely my own.

SUMMARY

This work focused on the roles of adaptor proteins Talin-1 and Kindlin-3, which connect integrins with the cytoskeleton, in modulating Fn fibrillogenesis induced by flow-simulated shear forces. In this context, it was necessary to characterize the effect of fluid shear forces, physical properties of stainless steel of the rheometer, β3 integrins, and actin polymerization on the Fn unfolding.

Soluble plasma fibronectin (Fn) with its inactive compact structure requires unfolding to assemble into active fibrils, which play a role in hemostasis and thrombosis. Hence, deoxycholate solubility assay and Western blot were used as a tool to monitor Fn fibrillogenesis induced by dynamic shear simulating venous or arterial flow conditions. The presented data show that flow and resulting shear stress over a broad range of physiological and pathological rates (50 – 5000 s^{-1}) could induce conformational changes of plasma Fn. These Fn fibrils could support platelet adhesion. In addition, physical properties of metallic material modulate Fn fibrillogenesis.

Upon stimulation with agonists (e.g., ADP), integrins expressed in a low affinity state undergo conformational changes that results in increased affinity for their ligands (i.e., Fn, fibrinogen). Platelet integrins (αIIbβ3, αvβ3, and α5β1) were blocked by inhibitory antibodies to determine their contribution to shear-induced Fn fibrillogenesis. Hereby, αIIbβ3 plays a predominant role, while α5β1 has a minor part in terms of fibril formation. The dynamic of actin polymerization is also necessary for fibril formation of Fn. Disruption of the actin polymerization markedly diminished Fn unfolding and assembly. These observations lead to the conclusion that Fn-integrin αIIbβ3-cytoskeleton interaction is crucial for the assembly of plasma Fn matrix under flow conditions.

The cytoplasmic tail of integrin β subunit has been shown to interact with many signaling and cytoskeletal proteins, including Talin and Kindlin. A loss of β3 interactions with these intracellular adaptor proteins could cause defective signaling. Two β3 cytoplasmic tail mimetic peptides were used to abrogate the structure and functional link between the β cytoplasmic tail and adaptor protein, Talin-1 or Kindlin-3, in platelets. Data showed that these integrin mimetic peptides could penetrate into platelet cytoplasm and bind specifically to their adaptor proteins. In addition, it is demonstrated that β3 mimetic

peptides could impair platelet adhesion, platelet aggregation and integrin αIIbβ3 activation, resulting a reduction in Fn fibrillogenesis induced by shear.

ZUSAMMENFASSUNG

Diese Arbeit fokussiert sich auf die Rolle der Adapter-Proteine, Talin-1 und Kindlin-3, die die Integrine mit dem Zytoskelett verbinden und somit an der Fibrillogenese des Fibronektins unter flussdymanischen Scherkräften beteiligt sind. Im Rahmen dieser Arbeit war es notwendig neben dem Einfluss der Scherkräfte in der Flüssigkeit, auch die physikalischen Eigenschaften des eingesetzten rostfreien Stahls im Rheometer, der β3-Integrine und der Aktinpolymerization auf die Entfaltung des Fn zu untersuchen.

Lösliches Plasmafibronektin (Fn) mit seiner inaktiven, kompakten Struktur muss in aktive, unlösliche Fib-rillen überführt werden, damit es seine Funktion in Hämostase und Thrombose einnehmen kann. Unlös-liche Fibrillen des Fn können mittels Deoxycholate präzipitiert und im Immunoblotting dargestellt wer-den, um so die Dynamik der Fn-Fibrillogenese unter Simulation venöser oder arterieller Flussbedingun-gen nachzuvollziehen. Die Ergebnisse belegen, dass physiologische und pathologische Scherraten (50 - 5000 s-1) die Konformation des Fn verändern wobei fibrilläre Strukturen entstehen, die eine gesteigerte Thrombozytenadhäsion vermitteln. Die Oberfläche rostfreien Stahls trägt zur Fn-Fibrillogenese bei.

Als Antwort auf Agonisten (z.B. ADP) durchlaufen vormals nicht aktivierte, niedrig ligand-affine Integrine eine funktionsrelevante Konformationsänderung, wobei sich die Affinität zum Liganden (z.B. für Fibrino-gen oder Fn) erhöht. Die Beteiligung der thrombozytären Integrine αIIβ3, αvβ3 und α5β1 an der Fn-Fib-rillogenese wurde mittels ADP und unter Einsatz inhibitorischer Antikörper untersucht. Die Ergebnisse beweisen, dass das Integrin αIIβ3 in der Fibrillenbildung dominiert, während dem Integrin α5β1 eine Ne-benrolle zukommt. Die Aktinpolymerisation nimmt ebenfalls eine entscheidende Rolle ein, da ihre Blo-ckade das Entfalten und Fibrillogenese des Fn hemmt. Zusammengefasst legen die Beobachtungen den Schluss nahe, dass die Wechselwirkung zwischen Fn und dem Integrin αIIβ3 bzw. Integrin αIIβ3 und dem Zytoskelett für die Fibrillogenese einer plasmatischen Fn-Matrix von entscheidender Bedeutung sind.

Es ist bekannt, dass der zytoplasmische Schwanz der β3-Untereinheit mit einer Reihe von Proteinen der Signalwege und des Zytoskeletts – einschließlich Talin und Kindlin - interagiert. Der Verlust dieser β3-In-teraktion mit diesen regulatorischen Proteinen

verursacht Defekte in der Signalübermittlung. In dieser Arbeit wurden daher, abgeleitet von der Sequenz des zytoplasmatischen Schwanzes der β3-Untereinheit, mimetische Peptide eingesetzt, die an Talin-1 bzw. Kindlin-3 binden, um auf diesem Weg die Strukturen und Funktionen zwischen den Bindungspartnern - β3-Untereinheit und Adapter-Proteinen - aufheben. Die Ergebnisse legen dar, dass die mimetischen Peptide in den Thrombozyten eindringen und im Zyto-plasma spezifisch an ihre Adapter-Proteine binden. Weiterhin konnte gezeigt werden, dass β3-mimeti-sche Peptide die Thrombozytenadhäsion, -aggregation und die Aktivierung des Intergins αIIbβ3 beeinträchtigt und daraus resultierend eine Verminderung der scherkraft-induzierten Fibrillogenese des Fn vermitteln.

TABLE OF CONTENT

LIST OF TABLES AND FIGURES

page

LIST OF ABBREVIATION

ADP	adenosine diphosphate
AFM	atomic force microscopic
APS	ammonium persulfate
Ala	Alanine
Arg	Arginine
Asp	Aspartic acid
BSA	bovine serum albumin
CMFDA	5-chloromethylfluorescein diacetate
ECM	extracellular matrix
EDTA	ethylenediaminetetraacetic acid
DOC	deoxycholate
FERM	4.1, ezrin, radixin, moesin
Fg	fibrinogen
FlAsH	fluorescein arsenical hairpin binder
Fn	fibronectin
Fn488	Alexa Fluor 488 conjugated Fn
FRET	fluorescence resonance energy transfer
Gly	Glycine
GPTS	3-Glycidyloxypropyl trimethoxysilane
HEPES	4-(2-hydroxyethyl)-1-piperazineethanesulfonic acid
MD	membrane distal
MP	membrane proximal
NHS	N-hydroxysuccinimido
NMR	nuclear magnetic resonance
PBS	phosphate-buffered saline
PEG	polyethylene glycol
PH domain	pleckstrin homology domain
PRP	platelet-rich plasma
PTB	phosphotyrosine binding
RGD	Arginine-Glycine-Aspartic acid
SDS	sodium dodecyl sulphate

SDS-PAGE	sodium dodecyl sulfate polyacrylamide gel electrophoresis
TAT	trans-activator of transcription
TEMED	tetramethylethylenediamine
TM	transmembrane
Tyr	Tyrosine
UV	ultraviolet
vWF	von Willebrand factor
%	percent
°C	Celsius degree
g	gram
kDa	kilodalton
µg	microgram
µm	micrometer
µM	micromolar
mg	milligram
ml	milliliter
mM	millimolar
mPa s	millipascal-second
nm	nanometer
U/ml	unit (of activity) per milliliter
s^{-1}	inverse seconds

1. Introduction

1.1. Fibronectin

The extracellular matrix (ECM) is composed of diverse classes of adhesive and scaffolding molecules which form a rich variety of filamentous networks with distinct physical and chemical properties. Fibronectin (Fn) is one of the most abundant glycoproteins in the ECM, composed of two nearly identical subunits (230 – 270 kDa) connected by disulfide bonds near the C-termini (Petersen et al., 1983). This adhesive protein is divided into two groups: soluble plasma Fn and less-soluble cellular Fn (Pankov and Yamada, 2002). Plasma Fn is synthesized in the liver by hepatocytes and secreted into the blood plasma at a concentration of 300-400 μg/ml (Zardi et al., 1979), where it polymerizes during blood clotting following vascular injury. Cellular Fn is synthesized by many cell types (including fibroblasts, endothelial cells, chondrocytes, and myocytes) (Mao and Schwarzbauer, 2005a) and is organized into fibrils contributing to the insoluble extracellular matrix (To and Midwood, 2011).

1.1.1. Structure and domains of Fn

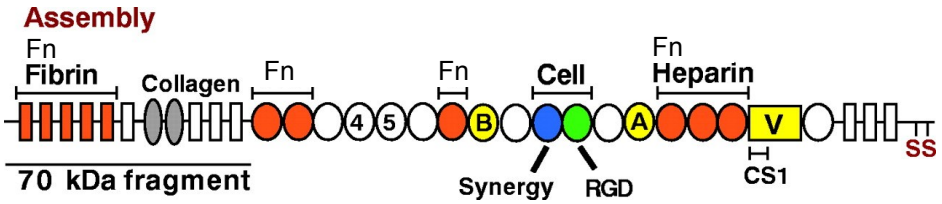

Figure 1.1. The domain structure of Fn.

Fn consists of type I (rectangles), type II (ovals) and type III (circles) repeats. Sets of repeats constitute binding domains for fibrin, Fn, collagen, cells and heparin, as indicated. Figure adopted from Wierzbicka-Patynowski and Schwarzbauer (2003).

Fn composes of three types of repeating globular modules (Figure 1.1): 12 type I modules, 2 type II modules, and 15-17 type III modules linearly connected by short chains of variable flexibility (Leahy et al., 1996; Petersen et al., 1983). Type I and type II modules contain two intrachain disulfide bonds stabilizing the folded structure of Fn, while type III modules, which comprise more than half of the protein, exhibit a seven-β-stranded sandwich motif (Johnson et al., 1999; Ulmer et al., 2008).

Each module of Fn comprises functional domains that mediate interactions with other ECM components, with cell surface receptors, and with Fn itself. Most of the binding activities that direct Fn to assembly sites is contained in the amino terminal 70-kDa region, in particular, within modules I1-I5. The type I modules 1–5 bind directly to Fn and mediate localization of fragments containing this domain to Fn matrix (McKeown-Longo and Mosher, 1985). Fn binds to integrin receptors through a cell adhesive site comprising modules III8-III10 (Bowditch et al., 1994). Fn also possesses many other adhesive sites for various substances, including collagen, fibrin, fibrinogen (Fg), heparin, factor XIII (Magnusson and Mosher, 1998).

1.1.2. Major steps of Fn matrix assembly

In the circulation, plasma Fn exhibits a compact form, however, intrinsic functions of Fn *in vivo* are prevalent to multimeric Fn fibrils. The creation and deposition of insoluble Fn fibrils, termed Fn fibrillogenesis or Fn matrix assembly, are tightly regulated. Plasma Fn does not form multimeric fibrils spontaneously *in vivo* and thereby prevents abnormal interactions with blood cells that may induce vascular occlusion by thrombi (Mao and Schwarzbauer, 2005a).

Cell-dependent Fn assembly is a stepwise process (Figure 1.2). Initiation of assembly of Fn is mediated by interaction of the N-terminal 70-kDa region of Fn with uncharacterized cell surface molecules (Xu and Mosher, 2011). Subsequently, inactive and compactly folded Fn binds to integrin receptors via the Arg-Gly-Asp (RGD) loop on module III10 and the neighboring sequence in module III9 (Mao and Schwarzbauer, 2005b). Integrin complexes soon become clustered in response to bivalent Fn (Dzamba et al., 2009). Integrin clustering recruits signaling and cytoskeletal proteins, resulting reorganization of the actin cytoskeleton. Tension generated by cytoskeleton contractility is transmitted via β integrin subunit to cell-surface-bound Fn (Dzamba et al., 2009). This cytoskeletal tension applied to Fn dimers can expand and unfold the subunits of Fn to expose cryptic Fn-Fn binding sites buried in the soluble structure, thus promoting the interaction of Fn with other Fn molecules (Zhong et al., 1998).

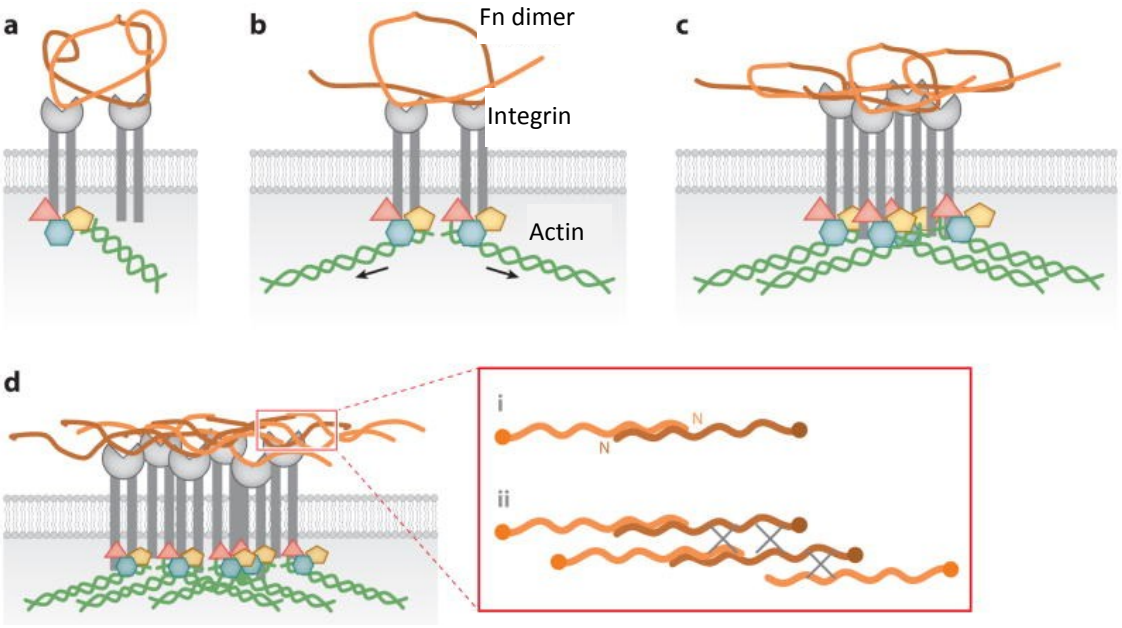

Figure 1.2. Major steps in Fn matrix assembly.

(a) A compact Fn dimer (orange) binds to integrins (gray). (b) Intracellular proteins (pink, yellow, blue) are recruited to integrin cytoplasmic domains and connected to the actin cytoskeleton (green). Cytoskeletal connections increase cell contractility (arrows), which induces conformational changes in Fn. (c) Integrin clustering and exposed Fn-binding sites promote Fn-Fn interactions and further changes in Fn conformation. (d) Finally, these events trigger formation of stable insoluble fibrillar matrix. The inset (red box) shows interactions between single subunits of Fn dimers. N indicates the N terminus of an Fn subunit. Fibrils form through (i) end-to-end association of Fn dimers, mediated by the N -terminal assembly domain, followed by (ii) lateral associations between fibrils that are likely to involve the other Fn-binding sites in III1–2, III4–5, and III12–14. Gray X's represent interactions between fibrils. Figure adopted from Singh et al. (2010).

Molecular dynamic simulation, biophysical, biochemical, and microscopic analyses have shown that changes in ionic strength or mechanical stretch may also induce conformational changes of Fn (Bushuev et al., 1985; Erickson and Carrell, 1983; Gao et al., 2003; Smith et al., 2007; Steward et al., 2011; Williams et al., 1982). In addition, Fn fibrils are formed by incubating soluble Fn dimers with anastellin (a Fn fragment of first type-III repeat which induces the formation of Fn multimers) or by denaturing soluble Fn with guanidine (Hocking et al., 1996; Morla et al., 1994). Low concentrations of chemical denaturants first destabilize ionic interactions between III2-3 and III12-14, leading to separation of crossed-over arms, and increasing denaturant concentrations finally unfold Fn (Smith et al., 2007). In addition, interactions with heparin or collagen fragments may induce conformational changes of Fn (Ugarova et al., 1995; Williams et al., 1982). These interactions are associated with an increase in the β-sheet content of the protein (Khan et

al., 1988), resulting a partial unfolding event and/or a global structural rearrangement of Fn (Bultmann et al., 1998; Ingham et al., 1997; Schwarzbauer, 1991). As a consequence, it exposes binding sites on the surface of the molecule and promotes Fn self-association and fibrillogenesis.

1.1.3. Characteristic of Fn fibrils

The organization of Fn within the fibrils is not well understood but probably involves intermolecular disulfide bonding or might result from highly stable protein–protein interactions (Chen and Mosher, 1996; Langenbach and Sottile, 1999; McKeown-Longo and Mosher, 1985). At early stages of assembly, Fn fibrils are short and usually extend between adjacent cells or from the cell to nearby substrate. Fn fibrils then become laterally associated into thicker fibrils (Dzamba and Peters, 1991). Further Fn-fibril interactions allow the formation of high-molecular-weight, complex, branched, and fibrillar Fn matrices, which are detergent-insoluble.

Chen et al. (1997) and Peters et al. (1998) used high-resolution cryo-scanning electron microscopy to study the structure and assembly of Fn fibril. They observed that Fn fibrils have two distinct conformations: nodules (10 – 13 nm in diameter) randomly spaced throughout the length of the fibril or very straight with smooth surfaces (with diameters between 6 and 15 nm). Both conformations existed within an individual fibril. In addition, the distribution of the nodular and smooth fibrils varied depending on whether the fibrils were formed in tissue culture or in the cell-free system. The majority of fibrils observed in culture were smooth fibrils. These smooth fibrils were always attached to the surface of fibroblasts, other matrix fibrils, or the substrate. In contrast, nodular fibrils were less prevalent in cultures and always had at least one free end. Immunolabeling studies revealed that these nodules represent discrete globular subdomains of III3 and 4 (Chen et al., 1978; Singer, 1979).

1.1.4. The function of Fn

Two studies (Ni et al., 2000; Ni et al., 2003) suggested that plasma Fn is an essential compensatory factor for hemostasis in afibrinogenemic patients. Patients deficient in Fg may have only a mild bleeding phenotype, despite the importance of the conversion of Fg to fibrin by thrombin and Fg binding to platelets for normal hemostasis (Acharya and

Dimichele, 2008). During megakaryocytopoiesis when Fg is lacking or unable to interact with αIIbβ3, Fn also can substitute Fg (Cho and Mosher, 2006c).

Fn involves in many ECM-dependent processes *in vivo*. For instance, Fn fibrils form the primitive ECM during wound healing (Hynes, 1990). Fn can support thrombosis and hemostasis by initiating platelet adhesion onto Fn on the injured vessel wall, mediating platelet aggregation, contributing to the fibrin clot, and enhancing thrombus growth and stability in flow conditions via Fn assembly on platelet surfaces (Cho et al., 2005; Cho and Mosher, 2006a; Olorundare et al., 2001). It is proposed that plasma Fn has context-specific functions in the hemostatic system such that this dimeric glycoprotein can both support hemostasis and inhibit thrombus formation (Maurer et al., 2010). It is due to the interaction of Fn with fibrin endowing plasma Fn with the capacity to switch from supporting hemostasis to inhibiting thrombosis/vessel occlusion, based on fibrin gradient (George et al., 1993; Pankov et al., 2000).

As mentioned, intrinsic functions of Fn *in vivo* are prevalent to multimeric Fn fibrils (Mao and Schwarzbauer, 2005a), mediated by interaction of Fn with integrins (Magnusson and Mosher, 1998). Integrin cytoplasmic tails also link with the intracellular cytoskeleton; such linkage permits the bi-directional transmission of force across the plasma membrane (Calderwood et al., 2000; Evans and Calderwood, 2007). Living cells are continuously exposed to mechanical forces, and can translate these bi-directional signals into biochemical information (e.g. mechanotransduction). Hence, the Fn-integrin-cytoskeleton interaction is crucial in many normal cellular functions, e.g. cell adhesion, hemostasis, migration, differentiation, and survival, as well as the progression of diseases such as cancer (Calderwood, 2004).

Abnormal cell behavior alters Fn function resulting in many implications. For example, diabetes-induced abnormal Fn behavior has been linked to increased thickness and permeability of basement membranes of various tissues (Qian et al., 2008; Tsilibary, 2003). These diabetes-induced complications often lead to diseases such as micro- and macroangiopathy as well as atherosclerotic lesions (Tsilibary, 2003). In addition irregular Fn function may also result in impaired wound healing (Brem and Tomic-Canic, 2007; Lerman et al., 2003), a coordinated process that involves inflammation, matrix deposition, and remodeling by fibroblasts.

1.2. Integrin receptors

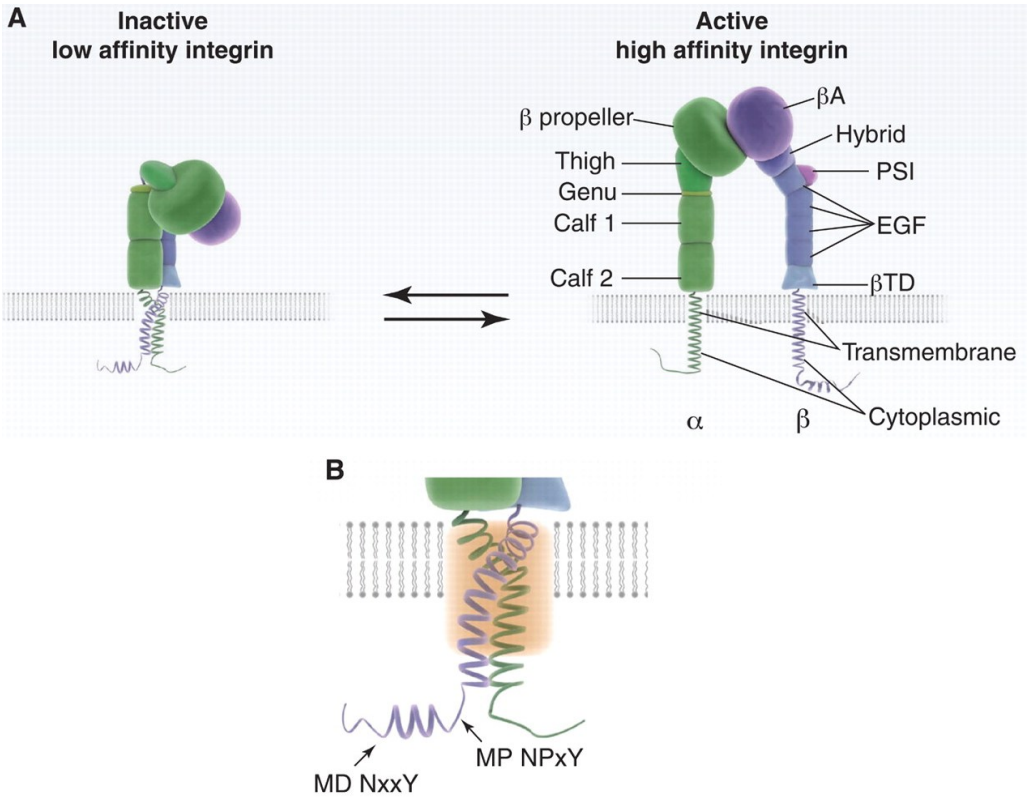

Figure 1.3. Integrin architecture and schematic representation of integrin activation.

(A) Specific contacts between the ectodomains, the transmembrane (TM), and cytoplasmic domains keep the integrin in its bent conformation. Separation of the integrin legs, TM, and cytoplasmic domains occurs during integrin activation, resulting in an extended integrin conformation. The α subunit is shown in green and the β subunit in violet. (B) A closer look at the interacting site (orange rectangle) between the TM and membrane proximal cytoplasmic domains of the α and β subunits. The membrane proximal (MP) and distal (MD) NPxY/NxxY motifs within the β tail are indicated. Figure adopted from Moser et al. (2009).

Integrins (Figure 1.3) compose of one α-subunit and one β-subunit, both of which have an extracellular ligand-binding region, a transmembrane helix domain and a generally short cytoplasmic tail (Calderwood et al., 2013). The α subunit seems to be a primary determinant of extracellular ligand binding specificity, whereas the β-tail is the main moderator of intracellular interactions (Hynes, 2002). The cytoplasmic domains are the sites of interaction with, and linkage to, the cytoskeletal and signaling partners of integrins.

In circulating cells and platelets, this heterodimeric adhesion receptor is present on the cell surface in an inactive conformation. A central concept for the function of integrins is their ability to shift between an inactive state with low affinity for ligand and high-affinity (operationally defined as activated) state, by alteration of the conformation of the extracellular domain (Humphries, 1996). Intracellular signaling events, such as the binding of adaptor proteins to β-integrin tails and acidic membrane phospholipids, could regulate the ligand binding affinity ("inside-out" signals) by reorganizing the α and β subunit cytoplasmic and transmembrane domains and affecting the structure and function of the extracellular domains (Harburger and Calderwood, 2009; Luo et al., 2007; Ma et al., 2006; Roberts and Critchley, 2009; Shattil et al., 2010; Wegener et al., 2007). Extracellular ligand binding also activates integrins and initiates "outside-in" signaling that regulates many cellular functions, including cell spreading and migration (Ginsberg et al., 2005; Hynes, 2002).

1.3. Adaptor proteins, Talin-1 and Kindlin-3

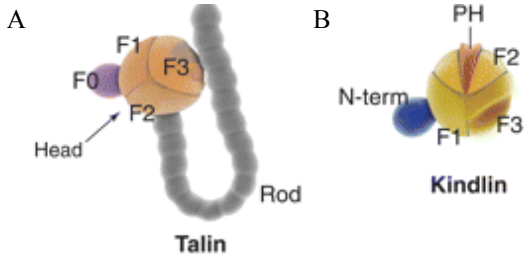

Figure 1.4. Integrin-activating proteins Talin and Kindlin.

Schematic drawings of the integrin-activating proteins Talin (A) and Kindlin (B). The FERM domains are depicted as balls subdivided into three subdomains, F1 to F3. Kindlins contain a pleckstrin homology (PH) domain inserted into the F2 subdomain. Domain sizes are not to scale, and Talin is shown as a monomer for simplicity. Figure adopted from Moser et al. (2009).

Tight regulation of integrin affinity is particularly crucial for blood cells, where signaling-independent integrin activation would have undesirable consequences, such as thrombosis (Banno and Ginsberg, 2008; Ratnikov et al., 2005). The β3 cytoplasmic tail contains two NXXY turn motifs, $NPLY^{747}$ and $NITY^{759}$, which are separated by a short helix containing a T/S cluster, the $TS^{752}T$ region (Xi et al., 2003). The β3 cytoplasmic tail has been shown to interact with many signaling and cytoskeletal proteins, including Src, Talin and Kindlin. A loss of β3 interactions with these intracellular regulatory proteins could

cause defective signaling and dysfunction (Moser et al., 2008; Petrich et al., 2007a; Petrich et al., 2007b).

1.3.1. Talin-1

Talin-1, a major cytoskeletal protein at integrin adhesion sites, is the only Talin isoform expressed in hematopoietic cells (Monkley et al., 2001). Talin consists of a large C-terminal rod-like domain and an N-terminal FERM (4.1, ezrin, radixin, moesin) domain with three subdomains: F1, F2 and F3 (Calderwood et al., 1999). The head domain is packed against the rod domain in its inactive state. Upon platelet activation by agonist, this interaction is disrupted and the phosphotyrosine-binding (PTB) subdomain in the F3 domain binds to two distinct regions in the β cytoplasmic tails, including membrane-proximal residues and $NPLY^{747}$ (Ma et al., 2006; Wegener et al., 2007). This interaction is sufficient for integrin activation *in vitro* (Calderwood et al., 1999; Wegener et al., 2007). Talin binding to the β-integrin tails was shown to be the final common step in αIIbβ3 integrin activation and ligand binding (Calderwood et al., 2002; Nieswandt et al., 2007; Tadokoro et al., 2003).

1.3.2. Kindlin-3

Kindlin-3, restricted to hematopoietic cells and particularly abundant in megakaryocytes and platelets, is another family of β-integrin tail-binding protein. This FERM-domain-containing protein also has key roles in integrin activation and signaling (Ussar et al., 2006). Like Talins, Kindlins have an F0 domain and a large unstructured insert in F1. However, unlike Talins, Kindlin F2 domains contain an inserted PH domain, which is required for Kindlin to promote integrin activation. The F3 subdomains of Kindlins have been found to share highest homology with the F3 domain of Talin (Kloeker et al., 2004). Kindlin binds the second NxxY motif (i.e., NITY) in β-integrin tails, that is distinctive from the Talin binding site. The F3 subdomain of Kindlin-3 is sufficient for this interaction and this interaction occurs in a direct manner. The Kindlin F0 domain, F1 loop, and the PH domain can each bind anionic phospholipids, and such binding is required for Kindlin to fully co-activate αIIbβ3 integrin (Liu et al., 2011; Perera et al., 2011; Yates et al., 2012b).

1.3.3. The role of Kindlins and Talins in regulation of integrin activation

Talins play key roles in inside-out and outside-in signaling. Upon interaction, Talin F3 forms a salt bridge with the conserved membrane-proximal Asp residue in β-integrin (Asp723 in β3) (Anthis et al., 2009), disrupting the inhibitory interaction of the β-integrin tail with the conserved Arg995 residue in the αIIb subunit. The binding of F2-F3 domains of Talin to β3 cytoplasmic tail causes tilting and reorientation of the β-integrin transmembrane domain helix, and dissociation of the α-subunit and β-subunit transmembrane domain contacts (Kalli et al., 2011). This FERM domain may participate in integrin outside-in signaling by either promoting integrin clustering and/or acting as an adapter for signaling pathways downstream of integrins such as focal adhesion kinase (Bledzka et al., 2013). Conditional knockout of Talin in mouse platelets impairs agonist-induced αIIbβ3 integrin activation and causes a severe bleeding diathesis (Nieswandt et al., 2007; Petrich et al., 2007b). Knocking in a Talin mutant which is defective in binding to β tail substantially reduces the ability of Talin to strengthen integrin adhesion to the ECM in Drosophila (Tanentzapf and Brown, 2006).

Kindlin-3 knockout causes bleeding phenotype in mice (Malinin et al., 2010), while knockdown model impairs integrin adhesion and spreading (Bialkowska et al., 2015), and Kindlin overexpression model does not activate integrins and in some cases can even suppress activation (Harburger et al., 2009). As described earlier, Talin binding is sufficient to activate membrane-embedded αIIbβ3 integrins (Ye et al., 2010). However, Kindlin knock out, knockdown and overexpression data, along with data on the function of integrin mutants defective in Kindlin binding, all implicate that a direct interaction of Kindlin with the β tail is required for integrin activation (Calderwood et al., 2013). The detailed mechanisms by which Kindlins exert their effects on integrin activation remain uncertain. In cells, Kindlins alone have little effect and can only synergize with Talin to activate integrins (Harburger et al., 2009; Ma et al., 2008). *In vitro*, the Talin head, Kindlin and β tails form a ternary complex (Bledzka et al., 2012; Yates et al., 2012a). This formation may be essential for integrin activation, although the sequential binding of these components, or their binding to adjacent integrins (Moser et al., 2009), has not been excluded. This has led to suggestions that Kindlin influences events occurring after Talin recruitment to integrins (Kahner et al., 2012). Such events might include: (Malinin et al., 2010; Moser et al., 2009; Shattil et al., 2010)

- Post-translational or structural changes in Talin or αIIbβ3 that promote Talin interactions with membrane-proximal residues in the β3 tail or with membrane phospholipids;
- Displacement of a negative regulator of integrin signaling that competes with Talin for critical interactions with αIIbβ3;
- Interaction of Talin and Kindlin together with as yet unidentified factor(s) to promote integrin activation.

1.4. Fluid shear forces and shear flow-dependent protein unfolding

Fluid mechanical shear could change secondary and/or tertiary structures of proteins. It is reported that the conformation of proteins can change at shear rate as low as 10 s^{-1}. In contrast, other researchers found no indication of shear-mediated unfolding even at shear rate of 5000 s^{-1}. The explanation of this contradiction could be the longer the molecule and the more extended its conformation, the larger effect shear forces have on its stability. In general, it is much easier to induce conformational changes in long protein molecules than in much shorter one. In addition, multi-unit proteins are more susceptible to shear (Piotr and Marek, 2011). Modeling studies have suggested that application of sufficient force promotes gradual unfolding of individual type III repeats of Fn, which are not stabilized by disulfide bonds. Breakage of hydrogen bonds between β-strands in type III modules could lead to partial or eventually complete unraveling (Krammer et al., 1999).

Shear flow is a combination of elongational and rotational components of equal magnitude. Upon shear exposure, polymer chain undergoes a tumbling motion, a series of subsequent stretching and coiling events with frequent changes in the orientation of the chain with respect to the shear axis (Doyle et al., 2000; Schroeder et al., 2005; Teixeira et al., 2004). While the elongational component of the flow is stretching the molecule, its rotational component aligns it along the shear axis, leading to the collapse of the chain due to the decreased hydrodynamic drag. An important role in this dynamic is played by Brownian fluctuations, which cause the chain segments to cross the streamlines into the regions of higher or lower flow which results in further stretching or collapse of the chain, respectively. In particular, the fluctuations may tip the polymer in such a way that its two ends lie in the regions of opposite flow direction, which results in a tumbling event, in which one polymer end moves over the other (Piotr and Marek, 2011). Images of the

polymers molecules can be digitized, and a computer-generated cursor is used to measure (by inspection) the maximum extension of the molecule along the shear direction (Smith et al., 1999).

Tzima et al. (2001) reported that fluid shear stress due to blood flow induces conformational activation of integrins followed by their increased binding to ECM ligands. Fluid shear stress due to blood flow is a major determinant of vascular remodeling, arterial tone and atherosclerosis. The endothelial monolayer *in vivo* acts as a signal transduction interface for hemodynamic forces; these forces determine the shape, cytoskeletal organization and function of endothelial cells, allowing the vessels to cope with physiological or pathological conditions (Davies et al., 1997). Hydrodynamic forces-induced conformational changes could be a self-regulatory repair mechanism of blood vessel walls (Kroll et al., 1996). For instance, in the case of damage, the shear stresses increase, inducing transitions of the von Willebrand factor (vWF) structure that seem to be necessary for the initiation of platelet adhesion (Kroll et al., 1996).

1.4.1. Shear stress induces vWF unfolding

Several lines of evidence (Siediecki et al., 1996; Vincentelli et al., 2003) suggest that the structure and function of vWF may be altered by changes in hemodynamic conditions. When exposed to physiological shear rates (up to 2000 s^{-1}), vWF undergoes subtle changes in molecular structure. These changes probably involve rearrangement of protein domains within the globular section of vWF. At shear rates > 2300 – 6000 s^{-1}, dramatic alterations in vWF occur, resulting in the exposure of hydrophobic domains (Singh et al., 2009). Barg et al. (2007) described the self-assembly of plasma vWF multimers into a network of fibers on a collagen matrix. This self-assembly of soluble vWF does not require the presence of cellular membrane receptors. In addition, formation of vWF fibers depends on flow dynamics, concentration of soluble vWF, and a suitable binding surface.

In addition, Fn and vWF support platelet adhesion under flow-dynamic conditions (Beumer et al., 1994; Kroll et al., 1996; Thurlow et al., 1990). At shear rates below 1000 s^{-1} (such as in veins and larger arteries), platelet adhesion involves interaction with Fn. At shear rates above 1000 s^{-1} (such as in small arteries, the microvasculature, atherosclerotic and stenotic vessels), the interaction between the platelet surface receptor glycoprotein Ibα and vWF becomes critically important to induce

tethering of rapidly circulating platelets, i.e. to slow down their speed at sites of vascular injury (Broos et al., 2011; Savage et al., 1998).

1.5. Stainless steel

Metals are widely used in cardiovascular interventions or surgical implants and have appropriate biofunctionality and biocompatibility. Stainless steel, in particular, is the most commonly used metal for endovascular devices (Oeveren et al., 2000). Metallic surfaces have been reported to bind components of the intrinsic pathway of hemostasis (Hong et al., 2005). Physical surface properties can also influence the molecular structure of Fn upon adsorption (Bergkvist et al., 2003). Consequently, artificial surfaces may trigger conformational changes in Fn with subsequent formation of biological active fibrils (Salmeron-Sanchez et al., 2011).

1.6. Objectives and the importance of the present study

The process of Fn fibril assembly involves Fn binding to cell receptors, biomechanical coupling of Fn to the cytoskeleton by integrins (e.g., αvβ3, αIIbβ3, α5β1), exposure of self-assembly sites via contractile cell forces, and elongation of fibrils by Fn polymerization (Hynes, 2002; Schwarzbauer and Sechler, 1999). Hence, interactions between Fn binding integrins and an intact actin cytoskeleton are critical for the assembly of a Fn matrix (Wu, 1997). Few have connected this effect to other modes of mechanical stimulation, such as fluid shear forces. In addition, there is evidence that physical surface properties can influence the molecular structure of Fn upon adsorption (Bergkvist et al., 2003).

Besides, the β3 cytoplasmic tail has been shown to interact with many signaling and cytoskeletal proteins, including Talin and Kindlin. A loss of β3 interactions with these intracellular regulatory proteins could cause defective signaling. Blockade of ligand binding to αIIbβ3 by orally administered antagonists is ineffective in thrombosis protection, possibly because of the need to limit dosage to avoid pathological bleeding, associated with complete lack of αIIbβ3 function (Chew et al., 2001; Quinn et al., 2003). In contrast, blockade of Talin binding to αIIbβ3 inhibits thrombosis with less pathological bleeding than complete lack of αIIbβ3 function. Several studies have proposed that Kindlin-3 and Talin-1 may serve as a potential target for design of therapeutics aimed at specifically disrupting integrin activation in platelets (Moser et al., 2008).

In this work, I propose to use specific β3 cytoplasmic tail mimetic peptides that bind to Talin-1 or Kindlin-3 and therefore, abrogate the structure and functional link between the β cytoplasmic tail of platelet integrins (αIIbβ3, αvβ3, and α5β1) and these adaptor proteins. These integrins are crucial both for the assembly of Fn and for the adaptor proteins Talin-1 and Kindlin-3. The use of specific β subunit mimetic peptides may provide a novel antithrombotic strategy, which, in contrast to conventional drugs, leaves normal hemostasis intact.

The overall objective of this research is to explore the roles of Talin-1 and Kindlin-3 in modulating Fn fibrillogenesis on platelets under flow dynamic conditions. We will focus on the changes in the fibrillogenesis of Fn on platelets upon exposure to shear stress and study systematically the consequences, when integrin-Talin and integrin-Kindlin interactions are disrupted.

Our overall hypotheses are:

1. Flow dynamic conditions can modulate conformational changes of Fn.
2. Shear-dependent Fn fibrillogenesis on platelet is mediated by distinct platelet integrins and actin cytoskeleton.
3. Blocking the interaction of integrin-Talin or integrin-Kindlin will cause quantitative changes in Fn fibril formation on platelets under different flow dynamic conditions.

2. Materials and methods

2.1. Materials

2.1.1. General equipment

Aggregometer (APACT4, Diasys Greiner,), Centrifuge (5415R, Eppendorf, Hamburg, Germany), Centrifuge (universial 320, Hettich, Tutttingen, Germany), cone-plate rheometer (Haaka Rheostress 1, Thermo Scientific, Karlsruhe, Germany), Dry Block Heater (Thermomixer 5436, Eppendorf, Hamburg, Germany), Flow cytometer (FACSCalibur, BD, USA), Fluoroskan Ascent Microplate Fluorometer (Thermo Scientific, Helsinki, Finland), Mini Trans-Blot® Electrophoretic Transfer Cell (Bio-rad, CA, USA), Haematology analyzer (KX-21N, Sysmex, Kobe, Japan), Laser scanning microscope (LSM 510, Carl Zeiss, Jena, Germany), Milligram balance (LA1200S, Sartorius, Gottingen, Germany), Molecular imager (Chemidoc XRS, Bio-rad, CA, USA), pH meter (pH540GLP, Multical, Weilheim, Germany), Power supply (Pac universial, Bio-rad, CA, USA), Shaking incubator (MaxQ400, ThermoScientific, OH, USA), Spectropolarimeter (J-715, Jasco, Gross-Umstadt, Germany), UV/VIS Spectrophotometer (Genesys 10S, Thermo Scientific, Madison, USA), Water bath (SW-20C, Julabo, Seelbach, Germany), Ultrasonication (S10H, Elma, Germany).

2.1.2. General chemicals and materials

30 % Acrylamide/ 0.8 % Bisacrylamide (National Diagnostics, Atlanta, USA), acetone (Sigma, Steinheim, Germany), ADP (Sigma, Taufkirche, Germany), APS (Sigma, St. Louis, USA), Apyrase (Sigma, St. Louis, USA), BSA (Sigma, St. Louis, USA), $CaCl_2$ (Merck, Darmstadt, Germany), 5-chloromethylfluorescein diacetate (CMFDA, Invitrogen, Darmstadt, Germany), Coomassive Brilliant Blue R-250 staining solution (Bio-rad, USA), Dextrose (Sigma, Steinheim, Germany), diisopropylethylamine (Aldrich, Steinheim, Germany), EDTA (Sigma, St. Louis, USA), ethanol (VWR, Fontenay-sous-Bois, France), EZ-Link Sulfo-NHS-Biotinylation Kit (Thermo Scientific, IL, USA), fresh frozen plasma (Blood center, University of Duesseldorf), Gelatin sepharose (Sigma, St. Louis, USA), Glacial acetic acid (VWR, Fontenay-sous-Bois, France), Glycerol (Roth, Karlsruhe, Germany), 3-Glycidoxypropyltrimethoxysilane (GPTS, Aldrich, Steinheim, Germany), Glycine (Roth, Karlsruhe, Germany), HEPES (Sigma, St. Louis, USA), H_2O_2 (Sigma, Steinheim, Germany), H_2SO_4 (Sigma, Steinheim, Germany), KH_2PO_4 (Sigma, Steinheim, Germany), K_2HPO_4 (Sigma, Steinheim, Germany), Methanol (VWR, Fontenay-sous-Bois, France), n-methyl-2-pyrrolidone (Sigma, Steinheim, Germany),

methylene chloride (Sigma, Steinheim, Germany), $MgCl_2.6H_2O$ (Merck, Darmstadt, Germany), NaCl (Merck, Darmstadt, Germany), NaH_2PO_4 (Merck, Darmstadt, Germany), NaN_3 (Merck, Darmstadt, Germany), Polyethylenglycol (Mn = 1,500 g/mol, Fluka, Steinheim, Germany), Protein ladder (Bio-rad, USA), SDS (Sigma, Steinheim, Germany), sodium citrate (Sigma, Steinheim, Germany), Sodium deoxycholate (Sigma, Steinheim, Germany), Supersignal West Dura Extended Duration Substrate solution (Thermo Scientific, IL, USA), TEMED (Sigma, St. Louis, USA), toluene (Sigma, Steinheim, Germany), Tris base (Sigma, St. Louis, USA), Tween-20 (Merck, Hohenbrunn, Germany), Urea (Sigma, Steinheim, Germany).

2.1.3. Antibodies, ligands and fluorescence dyes

10E5 (a gift from Barry Coller (Rockefeller University, New York, NY, USA)), Abciximab (Reopro, Lilly, Bad Homburg, Germany), Alexa Fluor 488 succinimidyl ester (Molecular Probes, Darmstadt, Germany), Collagen (Sigma, St. Louis, USA), Cytochalasin D (Sigma, St. Louis, USA), TC-FlAsH^{TM} II In-cell Tetracysteine Tag Detection Kit (Life Technology, USA), horseradish peroxidase-conjugated anti-rabbit antibody (GE Healthcare, Buckinghamshire, UK), Jasplakinolide (Calbiochem, Darmstadt, Germany), IgM-FITC (BD, San Jose, USA), LM609 (Millipore, Schwalbach, Germany), N-terminal 70kDa fragment, P1D6 (Abcam, Cambridge, UK), PAC-1 FITC (BD, San Jose, USA), PE mouse antihuman CD42a (BD, San Jose, USA), polyclonal rabbit anti-human Fn antibodies (Abcam, Cambridge, UK), precision protein streptactin-HRP conjugate (Bio-rad, Germany).

2.1.4. Peptide sequences

Sequences of β3 subunit cytoplasmic tail which contain NPxY for binding to Talin (^{739}WDTAN**NPLY**KEA^{750}) or NxxY for binding to Kindlin (^{751}TSTFT**NITY**^{759}) were used for peptide synthesis. These sequences had been fused to a TAT sequence (^{47}YGRKKRRQRRR^{57}), which is known to facilitate uptake of mimetic peptides into platelets. Synthetic peptides harboring mutations that prevent interaction with Talin or Kindlin as well as peptide containing only TAT (^{47}YGRKKRRQRRR^{57}) sequence were used as control peptides. All peptides were synthesized by Peptides&Elephants company (Postdam, Germany) and, except mentioned elsewhere, were dissolved in PBS pH 7.3 and stored at -20^{o}C.

For fluorescence microscopic imaging and experiments investigating the penetration of peptides, a tetracysteine sequence (CCPGCC) was put into the peptides' sequence and was used in combination with a membrane-permeant fluorogenic biarsenical dye named FlAsH (Fluorescein Arsenical Hairpin binder). FlAsH is used as a nonfluorescent complex with ethanedithiol, and it becomes fluorescent on binding to this tetracysteine sequence (Hoffmann et al., 2010).

Table 2.1. Peptide nomenclature

	Peptide sequence	**MW** (KDa)
Peptide for Talin-1 binding site	YGRKKRRQRRRWDTANNPLYKEAT-NH_2	2.99
Peptide for Kindlin-3 binding site	YGRKKRRQRRRTSTFTNITYT-NH_2	2.69
Peptide for Kindlin-3 binding site-tetracysteine	YGRKKRRQRRRHRWCCPGCCKTFTSTFTNITYT-NH2	4.11
Control peptide for Talin-1 binding site	YGRKKRRQRRRWDTANNPLAKEAT-NH_2	2.9
Control peptide for Kindlin-3 binding site	YGRKKRRQRRRTSTFTNITAT-NH_2	2.6
TAT peptide	YGRKKRRQRRRT-NH_2	1.66
TAT peptide-tetracysteine	YGRKKRRQRRRHRWCCPGCCKTFT-NH2	3.08

2.1.5. Other materials

96-well plate (Costar, Corning Incorporated, USA), blood collection set (BD vacutainer, Franklin Lake, USA), blood collection tube (BD vacutainer, Plymouth, UK), stainless steel cone (C60/1^{o} Ti L, Thermo Scientific, Karlsruhe, Germany), nitrocellulose membranes (0.45 μm, Bio-Rad, Germany), PD-10 desalting column (GE healthcare, Buckinghamshire, UK), Polystyrene plates (Sarstedt, Germany), 220 – 1600 nm cuvettes (Eppendorf, Hamburg, Germany), Sephadex G-25 gel filtration columns (GE healthcare, Buckinghamshire, UK).

2.1.6. Buffer and SDS-PAGE gel compositions

- PBS buffer: 137 mM NaCl, 2.7 mM KCl, 8 mM Na_2HPO_4, and 2 mM KH_2PO_4, pH 7.3
- PBS-T: PBS buffer containing 0.1% Tween-20
- 100 ml 10mM potassium phosphate buffer pH 7.0: 61.5 ml 10mM K_2HPO_4 + 38.5 ml 10mM KH_2PO_4
- HEPES Tyrode's buffer: 136.5 mM NaCl, 2.7 mM KCl, 2 mM $MgCl_2.6H_2O$, 3.3 mM $NaH_2PO4.H_2O$, 10 mM HEPES, 5.5 mM dextrose and 1 g/l fatty acid-free albumin, pH 7.4
- 2% DOC lysis buffer: 2 % sodium deoxycholate, 20 mM Tris-Cl pH 8.8
- 1% SDS solubilization buffer: 1 % SDS, 20 nM Tris-Cl pH 8.8,
- SDS-PAGE running buffer (10X): 30 g Tris-base, 142 g glycine and 10 g SDS dissolved in 1 L of double distilled water.
- Destaining buffer: 100 ml methanol, 100 ml glacial acetic acid and 800 ml H_2O distilled water
- Separating gel (6 % acrylamide): 3 ml Acrylamide/Bisacrylamide, 3.75 ml 4X Tris HCl/SDS pH 8.8, 0.1 ml APS 10%, 0.01 TEMED and 8.25 ml distilled H_2O.
- Stacking gel (3.9 % acrylamide): 0.65 ml Acrylamide/Bisacrylamide, 1.25 ml 4X Tris HCl/SDS pH 6.8, 0.05 ml APS 10%, 0.005 TEMED and 3.05 ml distilled H_2O.
- Towbin buffer (10X): 30 g Tris-base, 144 g glycine dissolved in 1 L of double distilled water.
- Towbin buffer (1X): 100 ml Towbin (10X), 200 ml methanol, 2.5 ml SDS 20% dissolved in 1 L of double distilled water.

2.2. Methods

2.2.1. Purification of plasma Fn

Human plasma Fn was isolated by a modified procedure from previously described gelatin-sepharose chromatography (Engvall and Ruoslahti, 1977). Briefly, frozen human plasma obtained from the Heinrich Heine University Blood Center of Dusseldorf was thawed at 37^{o}C and supplemented with 10 mM EDTA and 0.02 % NaN_3. Plasma was then applied onto a gelatin-sepharose packed column. The column was washed with PBS pH 7.3 until there was no detectable protein in the eluant (absorbance at 280 nm). Washing was continued with 1 M NaCl followed by 1 M urea. Finally, Fn was eluted by

50 mM sodium citrate at pH 5.5 and subjected to dialysis overnight in PBS at pH 7.3 with 10% glycerol to remove sodium citrate. Its purity and concentration were examined by SDS-PAGE and UV measurement at 280 nm, respectively.

2.2.2. Platelet preparation

Human blood from healthy adult volunteers was collected into acid-citrate-dextrose containers. Whole blood was subjected to centrifugation at 307 *g* for 10 min to obtain platelet-rich plasma (PRP). Thereafter, 2 ml PRP was transferred to a plastic tube containing 2 ml PBS, pH 6.5, and 2.5 U/ml apyrase, followed by centrifugation at 854 *g* for 6 min. A platelet pellet was obtained and resuspended in 500 µl of 4-(2-hydroxyethyl)-1-piperazineethane-sulfonic acid (HEPES) Tyrode's buffer at room temperature. Platelet number was counted using a hematology analyzer.

2.2.3. Secondary structure of mimetic peptides

To study the secondary structure of mimetic peptides, synthesized peptides in powder were dissolved in 10 mM potassium phosphate buffer pH 7.0. Subsequently, 0.1 mg/ml of peptide containing TAT sequence only, peptide for Talin-1 binding sites, or peptide for Kindlin-3 was subjected to circular dichroism measurement in 1 cm pathlength cell. Spectra were acquired over the wavelength range 185 to 260 nm, with 0.1 nm step size at 0.25 seconds per data point. Myoglobin and potassium phosphate buffer pH 7.0 were used as control. Data were then analyzed by program CONTINLL (CDPro package). Reference set was SMP50.

2.2.4. Peptide biotinylation

100 µM mimetic peptides in PBS were incubated with 2 mM Sulfo-NHS-Biotin solution for 1 hour, at room temperature. Subsequently, the solution was applied to desalting column and subjected to buffer exchange by centrifugation at 1000 *g* for 2 min. Concentration of biotinylated peptides was measured by 4'-hydroxyazobenzene-2-carboxylic acid (HABA) assay according to manufacturer's protocol.

2.2.5. Platelet Adhesion Assay

Fn, which was exposed or not exposed to shear generated by untreated cones, at different concentrations (5, 10, 25, or 50 µg/ml), was coated onto wells of a 96-well plate. Protein-coated wells were subsequently blocked with 1% BSA. Washed platelets (10^8/ml) were

labeled with 10 μM 5-chloromethylfluorescein diacetate (CMFDA) for 1 h at room temperature. HEPES Tyrode buffer (200 μl) containing CMFDA-labeled platelets (10^7/ml) and 2 mM $CaCl_2$ was placed on Fn-coated wells and incubated for 30 min at 37°C. Non-adherent platelets were washed away by PBS buffer. Adherent platelets were quantified based on the fluorescence signal of CMFDA and recorded by a microplate fluorometer. Wells coated with 1% BSA or Fn which was not exposed to shear were used as controls.

In parallel experiment, soluble Fn (50 μg/ml) was coated onto wells of a 96-well plate. Protein-coated wells were subsequently blocked with 1% BSA. Washed platelets (5 x 10^8/ml) were labeled with 10 μM CMFDA for 1 h at room temperature. Fluorescent-labeled platelets (2.5 x 10^8/ml platelets) were subsequently treated with mimetic peptides, containing the binding site for either Talin-1 (400 μM) or Kindlin-3 (200 μM) for 15 min at room temperature. HEPES Tyrode buffer (200 μl) containing treated platelets (5 x 10^7/ml) and 2 mM $CaCl_2$ was placed on Fn-coated wells and incubated for 30 min at 37°C. Non-adherent platelets were washed away by PBS buffer. Adherent platelets were quantified based on the fluorescence signal of CMFDA and recorded by a microplate fluorometer. As control experiments, platelets without peptides or with control peptides were used.

2.2.6. Platelet aggregation assay

Platelets (2 x 10^8/ml) in PRP prepared from peripheral venous blood of apparently healthy volunteers, were incubated with 800 μM mimetic peptides for 15 min at room temperature. Subsequently, peptide-treated platelets were stimulated by 2.5 μM ADP, an activated agonist. Their response was recorded on an aggregometer, with continuous stirring. For control experiments, washed platelets alone or platelets treated with control peptides were tested for aggregation, in the presence or absence of ADP. The maximal aggregation, achieved within 3 min after the addition of the agonist, was determined and expressed as a percentage of 100% light transmission calibrated for each specimen (maximal percentage of aggregation). All aggregation assays were conducted within 3 hours after venipuncture.

2.2.7. PAC-1 binding assay by flow cytometry

Platelets (2 x 10^8/mL) in PRP were preincubated with mimetic peptides (800 μM). Treated platelets were then incubated with 0.5 μg/ml FITC-conjugated PAC-1 antibody, in the presence of 100 μM ADP, for 1 hour in the dark; diluted (1:10, v/v) with 10 mM PBS, pH 7.4 and immediately analyzed by flow cytometry. Platelets were gated according to staining for the platelet specific antigen CD42a. As control experiments, isotype control or platelets treated with control peptides were used.

2.2.8. Surface modification of stainless steel

The cone (Diameter: 60 mm, cone angle: 1.016°, truncation: 0.051 mm) in cone – plate apparatus is made of stainless steel. To study the effect of physical properties of stainless steel on Fn fibril formation, the surface of the cone was grafted with *O,O'*-Bis(amino-propyl) polyethylene glycol (PEG), a hydrophilic polymer, using a modified procedure by Kang and Lee (2007). Briefly, the cones were subjected to silanization with epoxy-functionalized silane (GPTS) in a 10% (v/v) GPTS/toluene solution at 55°C for 48 h. Grafting of the PEG polymer was then carried out in a 10 mM PEG/n-methyl-2-pyrrolidone solution at 50°C for 24 h. The polymer-grafting step was performed twice. The amount of Fn adsorbed onto stainless steel cones, which were treated or untreated, was quantified.

Quantification of adsorbed Fn. To evaluate the effect of surface modification on the Fn adsorption, PEG-grafted and ungrafted cones were incubated with 100 μg/ml Fn in 10 min at room temperature (under static conditions). Those cones were also used to generate shear rates for 10 min. Adsorbed Fn was then harvested using 1% sodium dodecyl sulphate (SDS) and loaded onto 6% SDS-PAGE under reducing conditions. Western blot and densitometric analysis were used to quantify the amount of adsorbed protein.

2.2.9. Exposure to shear

For the exposure to shear, different experimental settings were used. In all experiments, except mentioned elsewhere, cones grafted with PEG were used to generate shear. Flow conditions were simulated by dynamic shear rates stepwise increasing from 50 s^{-1} to 5000 s^{-1} within 5 min and subsequently decreasing from 5000 s^{-1} to 50 s^{-1} within 5 min using a

cone-plate rheometer. Viscosities (mPa s) of shear-exposed solutions were recorded over 10 min.

2.2.9.1. Impact of stainless steel on conformational changes of Fn

Fn isolated from fresh frozen human plasma was added, at different concentrations (10, 50 or 100 μg/ml), to plates pre-coated with 100 μg/ml of soluble Fn, collagen or BSA. Subsequently, the solutions were exposed to shear generated by different stainless steel cones with bare surfaces or with cones pre-grafted with PEG to reduce non-specific adsorption of plasma proteins.

2.2.9.2. Role of platelet and platelet integrins in Fn fibril assembly

To study the effects of platelet on conformational changes of Fn, soluble Fn (100 μg/ml), in the absence or presence of washed platelets (2.5 x 10^7/ml or 2.5 x 10^6/ml), was exposed to shear. For microscopic analysis, Alexa Flour 488-conjugated Fn was used. In parallel experiment, 70 μg/ml N-terminal 70kDa fragment of Fn was incubated with 100 μg/ml soluble Fn at room temperature for 20 min before shear exposure.

To examine the role of distinct platelet integrins in fibril formation of Fn, washed platelets (2.5 x 10^8/ml) were incubated with the monoclonal antibodies LM609, P1D6, 10E5, or C7E3 (10 μg/ml, each) for 30 min at room temperature to block αvβ3, α5β1, αIIbβ3, or both αIIbβ3 and αvβ3, prior to the addition of Fn and subsequent shear exposure.

2.2.9.3. Effect of platelet cytoskeleton and adaptor proteins on Fn fibrillogenesis

To study the effect of cytoskeleton forces on Fn fibrillogenesis, washed platelets (2.5 x 10^8/ml) were pre-incubated with actin-modifying reagents, 1 μM jasplakinolide or 10 μM cytochalasin D for 30 min at room temperature to promote or disrupt actin polymerization, prior to the addition of Fn and subsequent shear exposure.

To determine the potential involvement of adaptor proteins in Fn fibril formation, washed platelets (2 x 10^8/ml) were preincubated with mimetic peptides (800 μM), prior to the addition of Fn and subsequent shear exposure. For control experiments, control peptides were used.

2.2.10. Quantification of fibril formation

To quantify the amount of fibril formation, a (deoxycholate) DOC solubility assay and Western blotting were performed. The solutions that were exposed to shear conditions were removed from the BSA-, collagen- or Fn-immobilized plates and precipitated with 2% DOC solution in eppendorf. The DOC-insoluble pellets containing Fn fibrils were isolated by centrifugation at 19019 *g* for 20 min at 4°C. The supernatant was removed and saved as the DOC-soluble fraction, whereas the pellet was washed with 2% DOC buffer and resuspended in 1% SDS buffer.

For Western blotting, insoluble and soluble Fn were resolved in a 6% SDS-PAGE under reducing conditions and blotted onto nitrocellulose membranes. The membranes were blocked for 1 h at room temperature using 5% (w/v) nonfat dry milk in PBS containing 0.1% Tween-20 (PBS-T). The blot was subsequently incubated for 2 h with polyclonal rabbit anti-human Fn antibodies, diluted 1:2500. The membranes were washed twice in PBS-T and incubated with horseradish peroxidase-conjugated anti-rabbit antibody at room temperature for 90 min. The blot was washed three times in PBS-T and subsequently incubated with Supersignal West Dura Extended Duration Substrate solution according to the manufacturer's protocol. Densitometric analysis of immunoreactive bands was conducted using Chemidoc XRS imager and Quantity one software.

2.2.11. Statistics

All experiments were conducted in at least 3 independent experiments and carried out using blood of different volunteer blood donors. Data were expressed as the mean ± SD of at least 3 independent experiments. One way ANOVA was used for comparison of 2 groups. Differences were considered significant at $p < 0.05$.

3. Results

3.1. Fn unfolding upon fluid shear forces

Plasma Fn is in a direct contact with blood flow. However, less is known about the contribution of fluid shear forces to the conformational changes and the fibrillogenesis of Fn. In order to investigate how flow and resulting shear solely modulate the conformational changes of Fn, plasma Fn, at different concentrations (10, 50 or 100 µg/ml), was exposed to dynamic shear rates simulating venous or arterial flow conditions. As shown in Figure 3.1 and Table 3.1, upon exposure to dynamic shear for 10 min, the viscosities of Fn solutions at the concentration of 50 or 100 µg/ml increased significantly, while at the concentration of 10 µg/ml, the viscosities did not change (Figure 3.1 and Table 3.1).

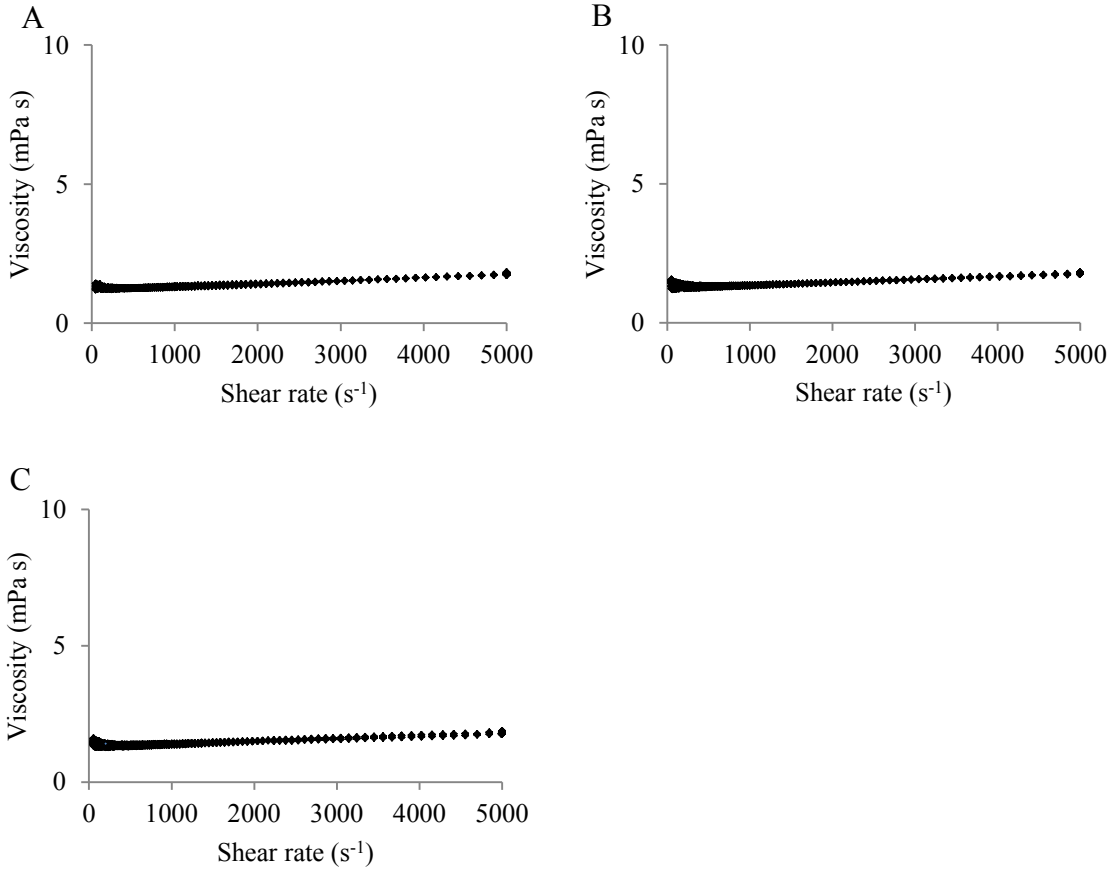

Figure 3.1 Changes in viscosity of Fn in solution exposed to shear.

Soluble plasma Fn, at different concentrations (10, 50, and 100 µg/ml), was added to plates pre-coated with BSA, collagen, or soluble Fn. Subsequently, Fn solutions were exposed to stepwise increasing shear rates from 50 s^{-1} to 5000 s^{-1} within 5 min (lower curves) and subsequently decreasing from 5000 s^{-1} to 50 s^{-1} within 5 min (upper curves) generated by untreated cones. 10 µg/ml Fn on BSA (A). 10 µg/ml Fn on collagen (B). 10 µg/ml Fn on Fn (C). Depicted are data of at least 4 independent experiments.

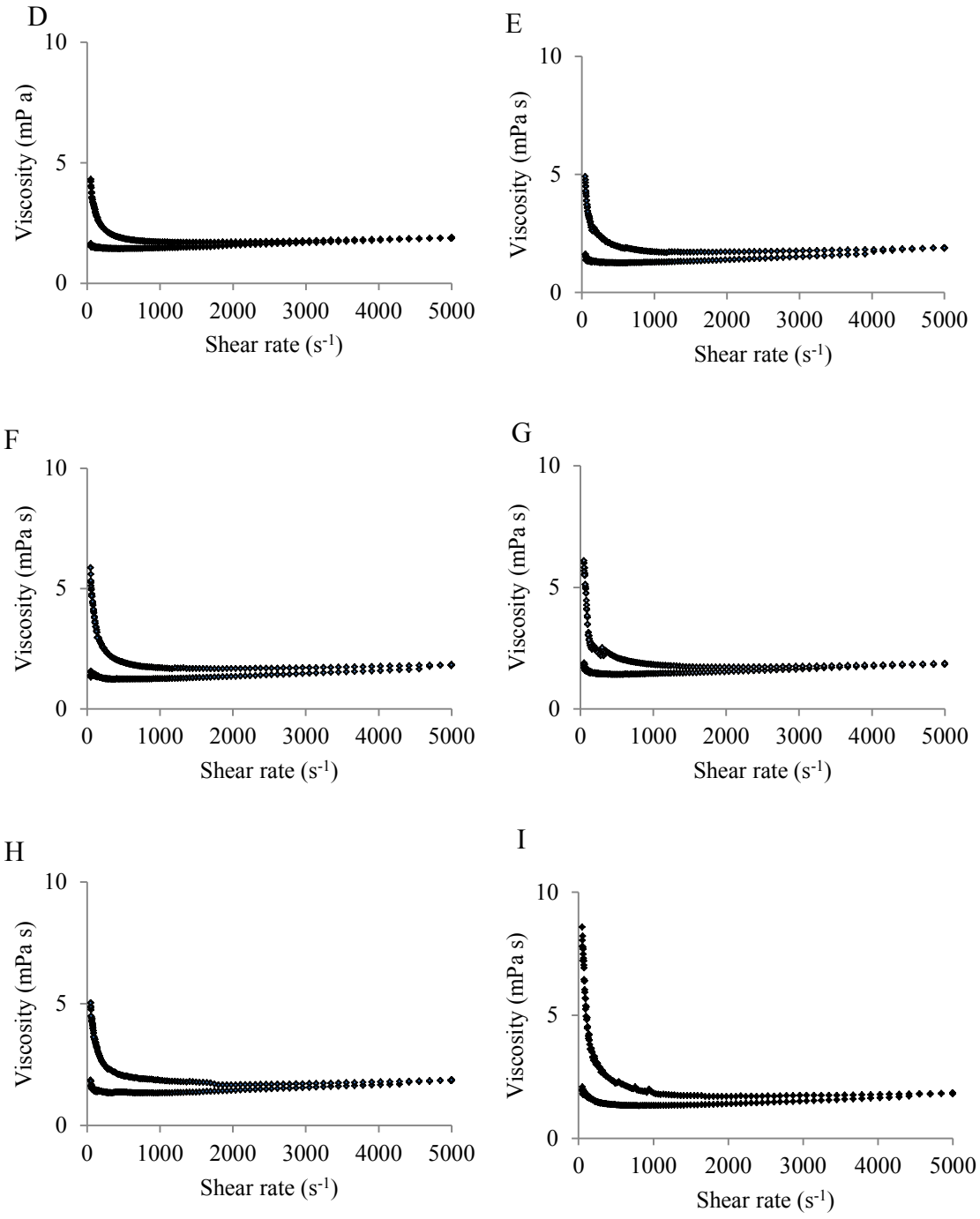

Figure 3.1. Changes in viscosity of Fn in solution exposed to shear (cont.).

Soluble plasma Fn, at different concentrations (10, 50, and 100 µg/ml), was added to plates pre-coated with BSA, collagen, or soluble Fn. Subsequently, Fn solutions were exposed to stepwise increasing shear rates from 50 s^{-1} to 5000 s^{-1} within 5 min (lower curves) and subsequently decreasing from 5000 s^{-1} to 50 s^{-1} within 5 min (upper curves) generated by untreated cones. 50 µg/ml Fn on BSA (D). 100 µg/ml Fn on BSA (E). 50 µg/ml Fn on collagen (F). 100 µg/ml Fn on collagen (G). 50 µg/ml Fn on Fn (H). 100 µg/ml Fn on Fn (I). Depicted are data of at least 4 independent experiments.

It is reported that under static conditions, platelets adherent to Fn-, fibrin-, laminin-, or collagen-coated surfaces support Fn assembly, whereas platelets adherent to vitronectin- or Fg-coated surfaces do not (Cho et al., 2005; Cho and Mosher, 2005; Olorundare et al., 2001). Therefore, in this work, 3 different immobilized surfaces, BSA, collagen, and Fn, were used to examine whether flow shear forces induce conformational changes of Fn in surface-dependent manner. It is observed that, the increases in viscosity of Fn solution added to BSA-immobilized plates were 2.76 ± 1.59 mPas (50 μg/ml) and 3.3 ± 1.94 mPas (100 μg/ml), while higher increases were observed on collagen surfaces (4.5 ± 3.2 mPas and 4.24 ± 1.75 mPas, respectively) or Fn surfaces (3.16 ± 1.34 mPas and 6.60 ± 6.22 mPas, respectively) (Figure 3.1 and Table 3.1). The correlation between increase in viscosity and protein unfolding has been recognized for many years (Tu and Breedveld, 2005; Williams et al., 1982). Hence, the change in viscosities observed in this study could indicate conformational changes of Fn.

Table 3.1. Changes in viscosity of Fn solutions exposed to shear.

Soluble plasma Fn, at different concentrations (10, 50, and 100 μg/ml), was added to plates pre-coated with BSA, collagen, or soluble Fn and subsequently exposed to shear. Flow conditions were simulated by dynamic shear rates stepwise increasing from 50 s^{-1} to 5000 s^{-1} within 5 min and subsequently decreasing from 5000 s^{-1} to 50 s^{-1} within 5 min. Depicted are data of at least 4 independent experiments.

	Initial viscosity (mPa s)	Viscosity at shear rate 5000 s^{-1} (mPa s)	Ultimate viscosity (mPa s)	p-value between initial and ultimate viscosity
10 μg/ml Fn on BSA	1.49 ± 0.23	1.88 ± 0.25	1.39 ± 0.38	0.71
10 μg/ml Fn on collagen	1.44 ± 0.12	1.78 ± 0.07	1.25 ± 0.18	0.24
10 μg/ml Fn on Fn	1.53 ± 0.39	1.79 ± 0.29	1.42 ± 0.29	0.73
50 μg/ml Fn on BSA	1.55 ± 0.11	1.88 ± 0.06	4.31 ± 1.70	0.01
50 μg/ml Fn on collagen	1.37 ± 0.48	1.82 ± 0.09	5.87 ± 3.11	0.03
50 μg/ml Fn on Fn	1.87 ± 0.87	1.85 ± 0.27	5.03 ± 1.86	0.02
100 μg/ml Fn on BSA	1.61 ± 0.70	1.88 ± 0.18	4.92 ± 1.80	0.01
100 μg/ml Fn on collagen	1.85 ± 0.19	1.84 ± 0.06	6.09 ± 1.93	0.00
100 μg/ml Fn on Fn	1.98 ± 1.41	1.84 ± 0.35	8.58 ± 5.66	0.03

(A)

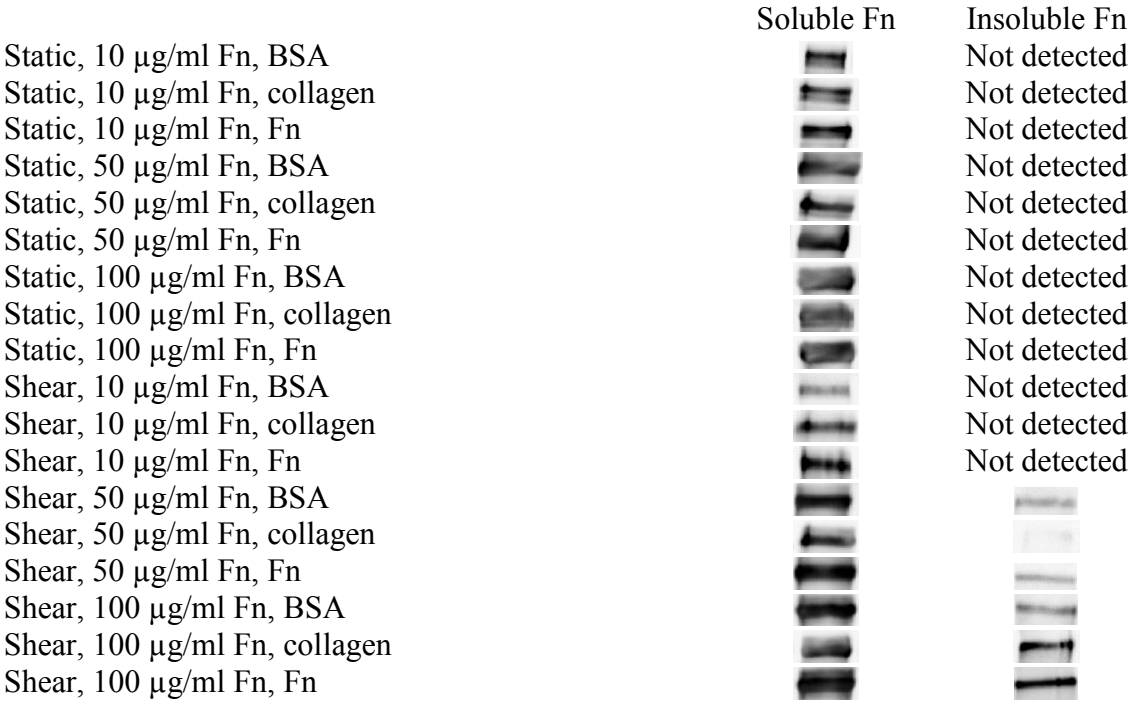

(B)

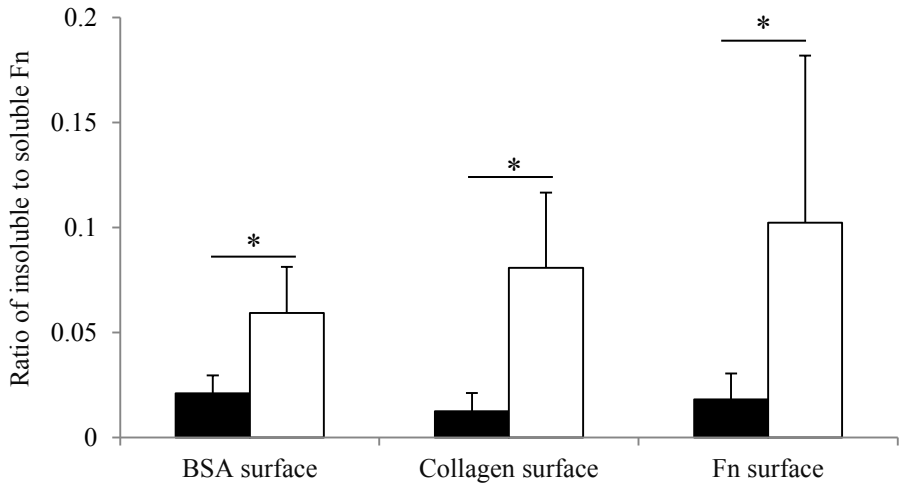

Figure 3.2. Shear induces fibril formation of Fn.

(A) Western blot analysis of insoluble and soluble Fn fractions which were separated by DOC solubility assay after exposed to shear generated by bare stainless cone. An illustration of the 6% SDS-PAGE blotted on nitrocellulose membrane and analysed by Western blotting was shown. Complete blots were shown in Supplemental data 1, 2 and 3. (B) Densitometric analysis of Western blots to quantify the amount of Fn fibrils (ratio of insoluble to soluble Fn) after dynamic shear rates were generated. Prior exposure to shear conditions, Fn solution at the concentration of 50 µg/ml (black column) or 100 µg/ml (white column) was added to the BSA, collagen, or Fn coated plates. Depicted are data of at least 4 independent experiments. (*) $p < 0.05$.

The assembly process of Fn matrix can be monitored by following the conversion of Fn fibrils from a detergent DOC-soluble form into a DOC-insoluble fibrillar network (McKeown-Longo and Mosher, 1983; Mosher, 1993). This conversion provides a useful method for quantifying matrix assembly through analysis of DOC insoluble Fn. Hence, shear-exposed Fn solutions were further subjected to DOC solubility assay. Fibril formation of Fn upon shear was calculated as ratio of DOC-insoluble Fn to DOC-soluble Fn. At the concentration of 10 µg/ml Fn, no fibrils were detected (Figure 3.2A). In contrast, fibril formation increased 2.8-fold on BSA surfaces, 6.4-fold on collagen surfaces, and 6.7-fold on Fn surfaces ($p < 0.05$), when the concentration of added soluble Fn was elevated from 50 µg/ml to 100 µg/ml (Figure 3.2). In addition, at the same concentration conditions (i.e., 50 µg/ml or 100 µg/ml of Fn), there was no difference among coated surfaces (i.e., BSA, collagen, and Fn) in terms of fibril formation. Hence, in further experiments, soluble Fn at the concentration of 100 µg/ml were used.

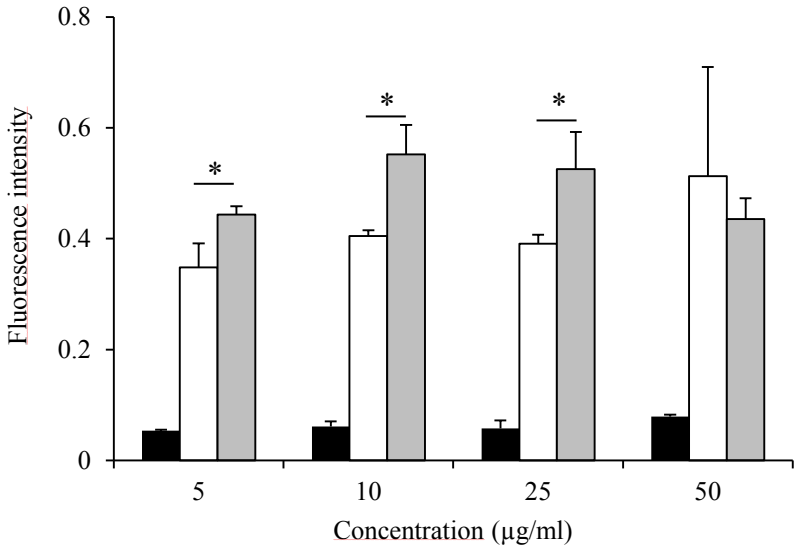

Figure 3.3. Platelet adhesion onto immobilized Fn, which was exposed or not exposed to shear.

CMFDA-labeled platelets (10^7/ml) in HEPES Tyrode's buffer containing 2 mM $CaCl_2$ were placed on wells coated with Fn which was not exposed to shear (white columns) or with Fn which was exposed to shear (gray columns) and incubated for 30 min at 37°C. For control experiments, platelets were placed onto immobilized BSA-coated (black columns) wells. Depicted are data of 3 independent experiments. (*) $p < 0.05$.

It has been reported that Fn assembly into fibrillar Fn supports cell adhesion (Morla et al., 1994). Therefore, platelet adhesion assay was conducted as an indirect proof to demonstrate fibril formation of Fn upon shear. Briefly, 100 µg/ml plasma Fn was exposed

to shear and subsequently these shear-induced Fn solutions were adjusted to different concentrations and immobilized onto 96 well plates. As depicted in Figure 3.3, at concentration of 5, 10, or 25 μg/ml Fn, the extent of platelet adhesion was significantly higher onto surfaces coated with Fn that had been exposed to shear than onto surfaces also coated with Fn but had not been exposed to shear.

Taken together, these results indicate that flow-simulated shear could modulate Fn unfolding in concentration-dependent and surface-independent manner. In addition, shear-induced Fn matrix supports platelet adhesion.

3.2. Physical properties of stainless steel induce Fn unfolding

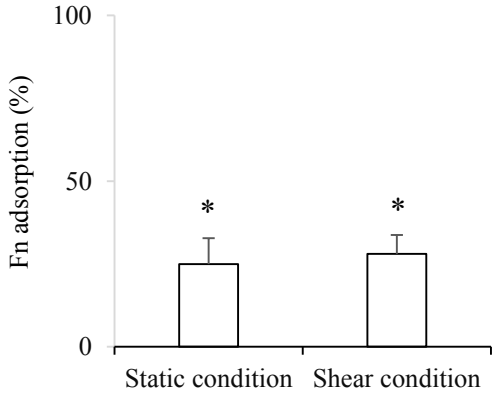

Figure 3.4. Chemical modification of stainless steel surface could reduce Fn adsorption onto cone surfaces.

Percentage of Fn adsorption, as determined by Western blot and densitometry, onto different cone surfaces under static conditions and upon exposure to dynamic shear (50 s^{-1} - 5000 s^{-1}). Two cone surfaces, bare stainless steel and stainless steel grafted with PEG (white columns), were used. The results obtained with uncoated surfaces were set at 100% and the other measures were referred to this. Depicted are data of 3 independent experiments. (*) indicates significant lower than the uncoated surfaces in terms of Fn adsorption ($p < 0.05$).

The cones in cone – plate apparatus used to generate shear in this work are made of stainless steel, which the bare surface is hydrophobic. Kang and Lee (2007) reported that covalently grafting PEG, a hydrophilic polymer, onto the cone surface could reduce protein adsorption. Western blot and densitometric analysis (Figure 3.4) showed that the adsorption of plasma Fn onto the PEG-grafted cones decreased by 75% as compared to untreated cones, thus confirming that surface modification was achieved.

To study the effect of physical properties of stainless steel on Fn fibril formation, stainless steel cones with different physical properties, bare stainless steel and PEG-grafted, were used to generate shear. Fn (100 µg/ml) was added to the plates pre-coated with BSA or collagen and subsequently exposed to shear generated by different stainless steel cones. As shown in Table 3.2, upon exposure to dynamic shear for 10 min, the viscosities of Fn solutions increased, indicative of Fn fibrillogenesis. Interestingly, the increase in viscosity in the samples exposed to shear generated by PEG-grafted cones was higher than samples in which uncoated cones were used.

Table 3.2. Changes in viscosity of Fn solutions (100 µg/ml) exposed to shear generated by cones with different surface characteristics.

b.s: bare surface, p.g.: PEG-grafted. Depicted are data of 4 independent experiments. (*) indicates significant difference, compared to corresponding immobilized surfaces ($p < 0.05$)

	Initial viscosity (mPa s) (1)	Viscosity at shear rate 5000 s^{-1} (mPa s)	Ultimate viscosity (mPa s) (2)	Increase in viscosity upon shear (mPa s)	p-value between (1) and (2)
b.s cone, BSA	1.61 ± 0.70	1.88 ± 0.18	4.92 ± 1.80	3.3 ± 1.94	0.01
b.s cone, collagen	1.85 ± 0.19	1.84 ± 0.06	6.09 ± 1.93	4.24 ± 1.75	0.00
g.s cone, BSA	4.82 ± 0.62	1.95 ± 0.05	11.30 ± 0.57	6.48 ± 0.58*	0.00
g.s cone, collagen	3.36 ± 0.97	2.01 ± 0.04	11.48 ± 2.14	8.13 ± 2.78*	0.00

Western blot and densitometric analysis (Figure 3.5) showed that chemical modification of cone surface resulted in considerably lower fibril formation, as compared to bare stainless steel. In addition, upon exposed to shear generated by PEG-grafted cones, collagen-immobilized surfaces resulted in a higher amount of Fn fibril formation, as compared to BSA surfaces. Chemical modification of metallic biomaterial by means of covalently grafting of hydrophilic polymer can prevent Fn adsorption and fibril formation. Hence, in further experiments, cones grafted with PEG were used to generate shear.

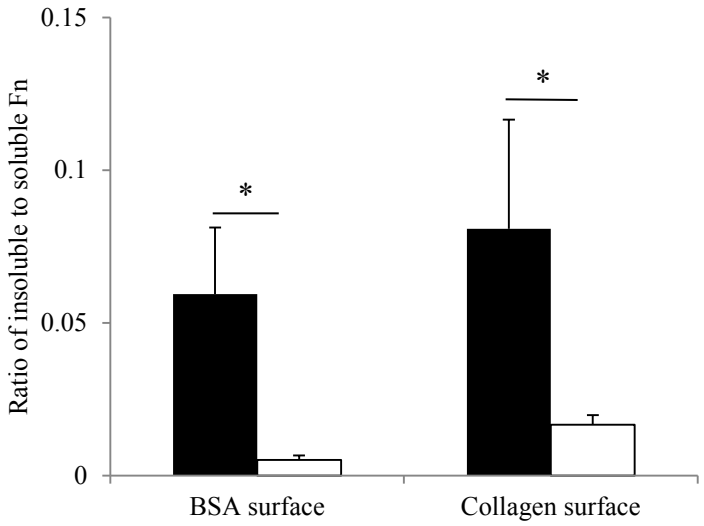

Figure 3.5. Physical properties of stainless steel modulate Fn unfolding.

Conformational changes of Fn in solution interacting with plates coated with BSA or collagen after dynamic shear rates were generated. Different stainless steel cones, bare stainless steel (black columns) and PEG grafted (white columns), were used to generate shear. Prior exposure to shear conditions, Fn solutions at the concentrations of 100 µg/ml were added to the coated plates. Densitometric analysis of Western blots was performed to quantify the amount of Fn fibrils (calculated as ratio of insoluble to soluble Fn). Depicted are data of 4 independent experiments. (*): $p < 0.05$.

Taken together, these results (Figure 3.2 and Figure 3.5) demonstrate that physical characteristic of metallic biomaterial could modulate shear-induced Fn fibrillogenesis in surface-independent manner. In addition, shear alone could induce Fn unfolding in surface-dependent manner.

3.3. Fn fibrillogenesis is stimulated by shear and platelets

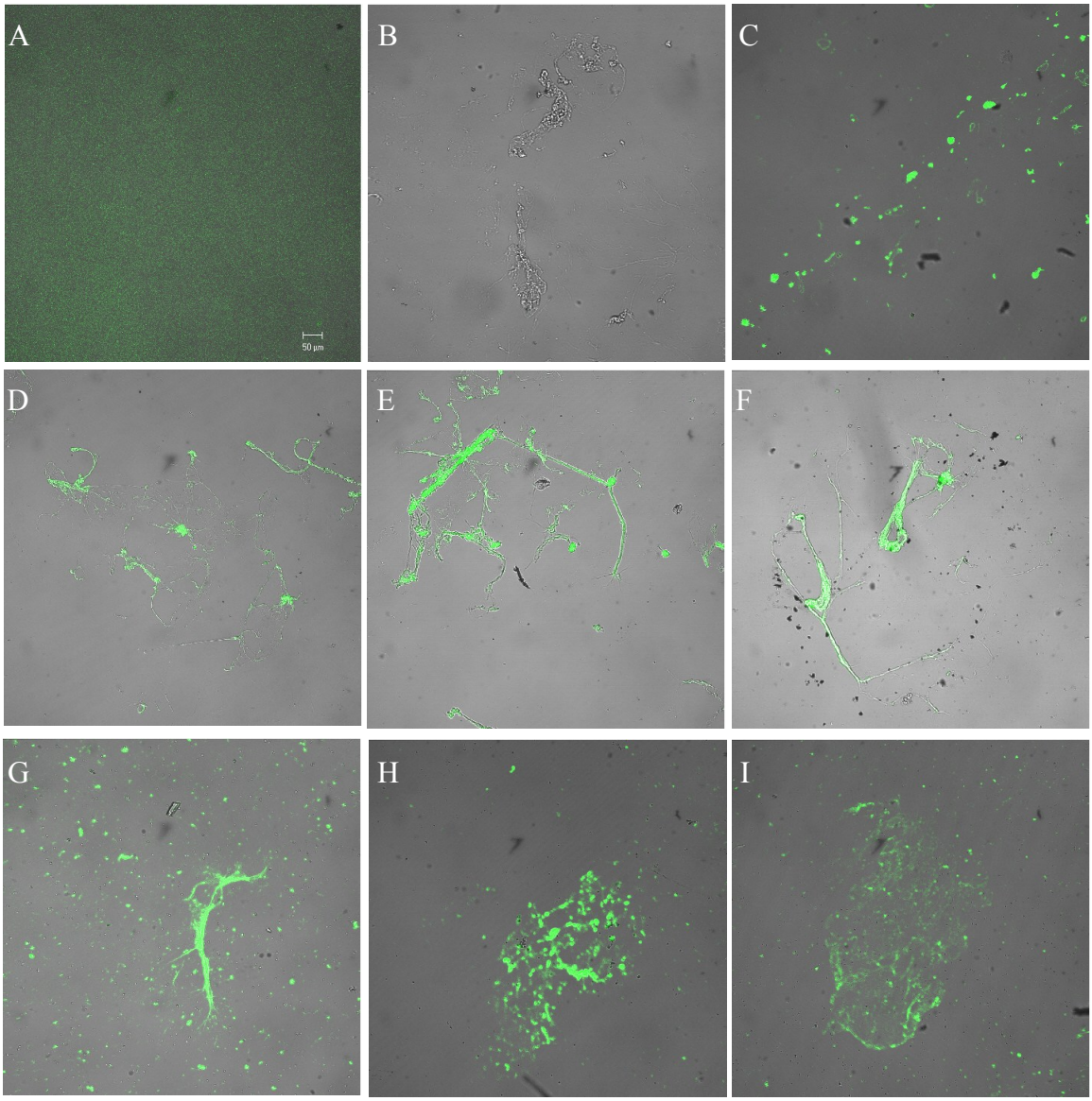

Figure 3.6. Platelets induce Fn unfolding exposed to shear.

An illustration of fluorescence microscopic images of Fn solutions, in the absence or presence of platelets, after shear exposure. Fn488 was added to Fn surface, static condition (A). Unlabeled Fn was added to Fn surface and subsequently exposed to shear (B). Fn488, in the presence of 70KDa Fn fragments, was added to Fn surface and subsequently exposed to shear (C). Fn488, in the absence of washed platelets, was added to BSA- (D), collagen- (E), or Fn-immobilized surface (F) and subsequently exposed to shear. Fn488, in the presence of washed platelets, was added to BSA- (G), collagen- (H), or Fn-immobilized surface (I) and subsequently exposed to shear. Scale bars represent 50 µm. Control experiments conducted at static condition were shown in Supplemental data 4.

It has been reported that fibril formation of plasma Fn is mediated by cells (Mao and Schwarzbauer, 2005a). The structures of shear-induced Fn fibrils (100 μg/ml) in the presence or absence of washed platelets were then examined by laser scanning microscopy (LSM). As depicted in Figure 3.6, Fn fibril diameter varied from 0.5 to 5 μm. Observed fibrils were linked with each other and varied in length (from 50 to 300 μm). In the absence of washed platelets, shear exposure of Fn solutions interacting with plates coated with collagen- or Fn-coated plates resulted in fibril matrix in which fibrils linked with one another. In contrast, short and discrete Fn fibrils were formed on BSA surfaces. It should be stressed that, as mentioned in section 3.2, upon exposed to shear generated by PEG-grafted cone, viscosity of Fn solutions increased (Table 3.2), indicative of conformational changes of Fn. Treatment of soluble Fn with the N-terminal 70 kDa fragment of Fn, which is known to inhibit Fn matrix assembly (Cho and Mosher, 2005; McKeown-Longo and Mosher, 1985; Tomasini-Johansson et al., 2006), blocked the fibril formation of Fn (Figure 3.6C). Addition of platelets resulted in a higher intertwined matrix of shear-induced fibrils (Figure 3.6G – I) as compared to sample without platelets (Figure 3.6D – F). Under static condition, no fibrils were observed (Supplemental data 4).

To confirm these microscopic observations (Figure 3.6), after shear exposure, Fn solutions, in the presence or absence of washed platelets, were subjected to DOC solubility assay. Western blot and densitometric analysis (Figure 3.7) revealed that washed platelets (2.5 x 10^7/ml) resulted in significant increases of 9-, 7- and 20-fold in fibril formation of Fn, generated by shear on BSA-, collagen- and Fn-immobilized plates, respectively. Using platelets at the concentration of 2.5x 10^6/ml caused roughly similar effect. It is worthy to notice that collagen and Fn surfaces significantly enhanced Fn assembly (Figure 3.6 H & I and Figure 3.7) mediated by cell and shear stress, compared with BSA surfaces (Figure 3.6 G and Figure 3.7). Thus, shear stress and platelets could modulate fibril formation of Fn in a surface-dependent manner and platelet concentration-independent manner.

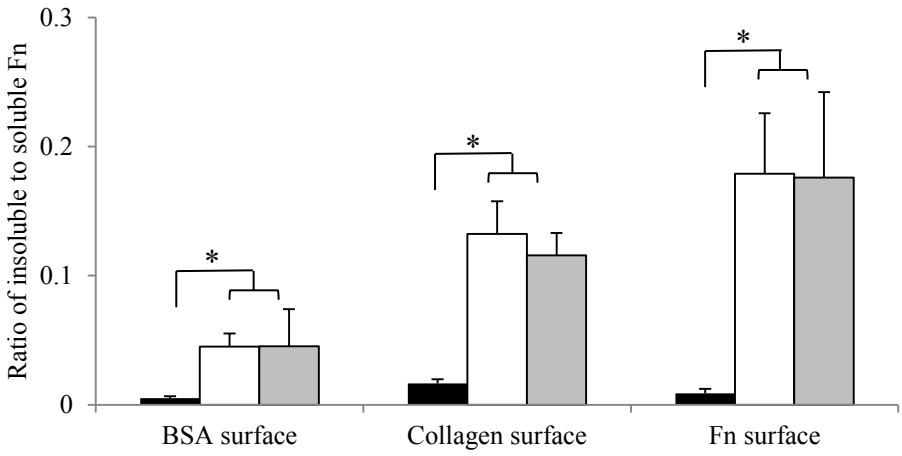

Figure 3.7. Platelets modulate Fn matrix assembly induced by fluid shear.

Plasma Fn (100 µg/ml), in the absence (black column) or presence ($2.5x10^6$/ml: white column or $2.5x10^7$/ml: gray column) of washed platelets, was exposed to shear generated by PEG-grafted cones. Subsequently, the solutions were subjected to DOC solubility assay. Densitometric analysis of Western blots was performed to quantify the amount of Fn fibrils (ratio of insoluble to soluble Fn) after dynamic shear rates were generated. Depicted are data of at least 3 independent experiments. (*): $p < 0.05$.

3.4. Fn-binding integrins differentially modulate Fn fibrillogenesis

Platelet integrins αIIbβ3, αvβ3, and α5β1 have been reported to interact with Fn (Cho and Mosher, 2006c). At static condition, β3 integrins had a major impact on the interaction of Fn on platelets (Huynh Khon et al., 2013). Integrin α5β1 is known to play a role in initiation of matrix assembly (Schwarzbauer, 1991). Hence, in this work I determined whether these integrins cause similar effects on Fn fibrillogenesis induced by shear. Platelets in suspension were preincubated with abciximab (C7E3 Fab), P1D6, 10E5, or LM609 prior to addition of soluble Fn. As depicted in Figure 3.8 C & D, αIIbβ3-blocking antibodies 10E5 or C7E3 resulted only in a slightly increase, from 9.34 (mPa s) ± 1.29 to 10.33 ± 0.74 or from 8.77 ± 0.99 to 10.5 ± 1.00 in viscosity of samples. In contrast, higher increases, 9.87 mPa s and 3.42 mPa s, were observed when platelets were preincubated with P1D6 and LM609, respectively (Figure 3.8 A & B). Control experiments in which Fn, in the presence of antibody-untreated platelets, was exposed to shear were shown in Supplemental data 5.

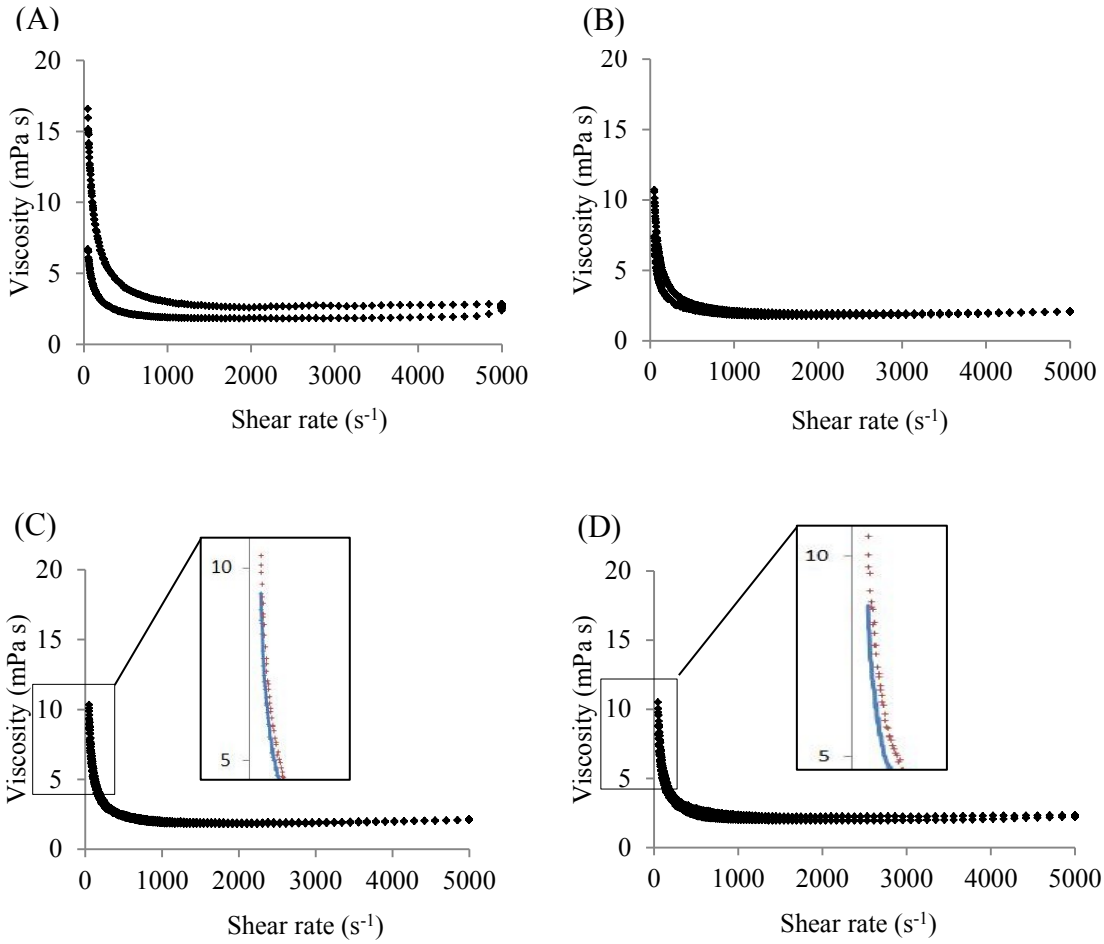

Figure 3.8. Distinct Fn-binding integrins modulate changes in viscosity of Fn solution exposed to shear.

Changes in viscosity of Fn solution, in presence of washed platelets, exposed to shear generated using PEG-grafted cones. Washed platelets were preincubated with the monoclonal antibodies P1D6 blocking α5β1 (A), LM609 blocking αvβ3 (B), 10E5 blocking αIIbβ3 (C), or C7E3 blocking both αIIbβ3 and αvβ3 (D) (10 µg/ml, each), prior to the addition of Fn and shear exposure. Depicted are pooled data from 3 independent experiments. Control experiments in which platelets were not treated with antibody were shown in Supplemental data 5.

Consistent with the data in regarding the viscosity of solution upon shear (Figure 3.8), Western blot and densitometric analysis (Figure 3.9) revealed that using 10E5 to block αIIbβ3 or C7E3 to block both αIIbβ3 and αvβ3 caused a significant reduction by 82% or 74% in fibril formation of Fn, in comparison to samples without antibodies. In contrast, when α5β1 or αvβ3 was blocked by P1D6 or LM609, Fn fibrils were formed 17% or 56% less than those in control experiments. Thus, the data demonstrate that the formation of fibrils is modulated by platelet integrins. Hereby, αIIbβ3 plays a predominant role, while

α5β1 has a minor part among the three examined platelet integrins, in terms of fibril formation.

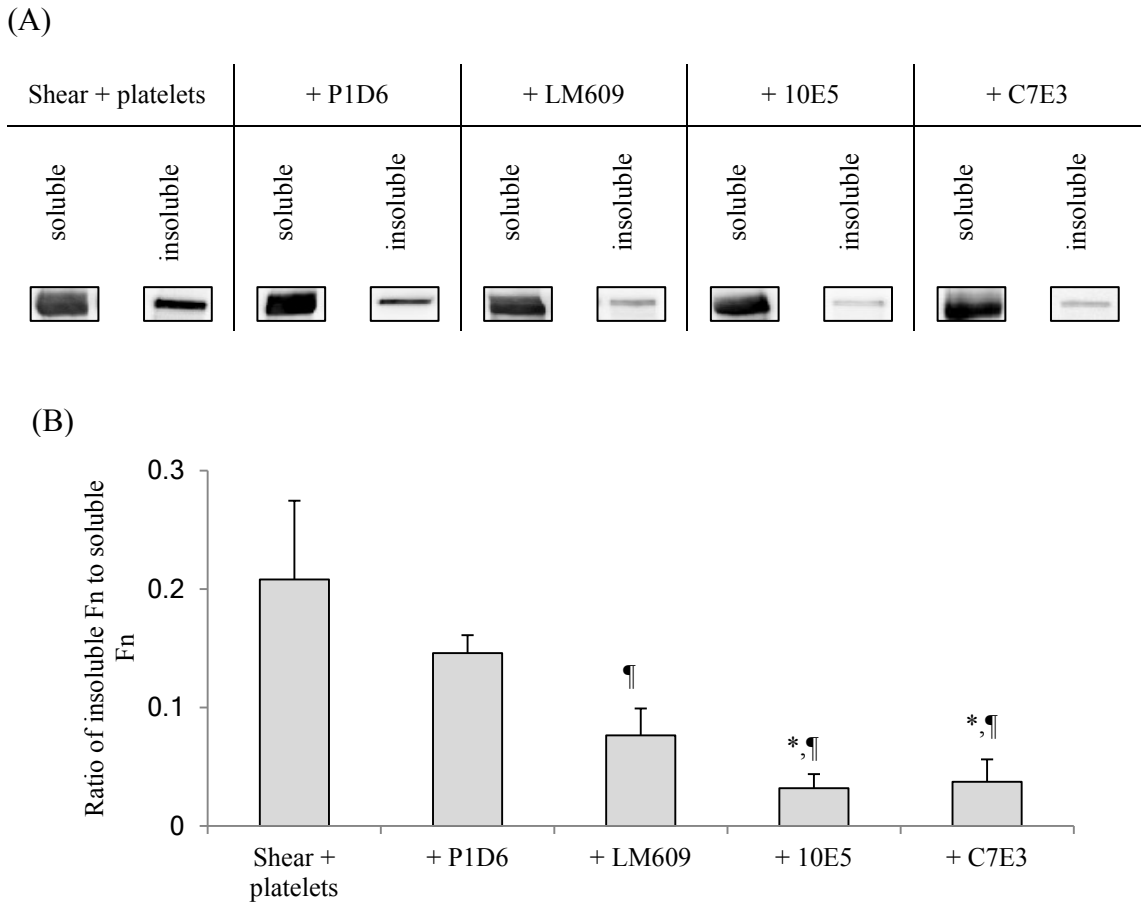

Figure 3.9. Distinct Fn-binding integrins modulate Fn unfolding exposed to shear.

Western blot analysis of insoluble and soluble Fn, which were separated using DOC solubility assay after shear exposure. Fn, in presence of washed platelets, exposed to shear generated using PEG-grafted cones. Washed platelets were preincubated with the monoclonal antibodies P1D6 blocking α5β1, LM609 blocking αvβ3, 10E5 blocking αIIbβ3, or C7E3 blocking both αIIbβ3 and αvβ3(10 μg/ml, each), prior to the addition of Fn and shear exposure (A). Densitometric analysis of Western blots to quantify the amount of Fn fibrils (ratio of insoluble to soluble Fn) after dynamic shear rates were generated (B). Depicted are pooled data from 3 independent experiments. (*) indicates significant difference ($p < 0.05$), as compared to the samples without antibodies. (¶) indicates significant difference ($p < 0.05$) as compared to "P1D6" group.

3.5. Platelet cytoskeleton regulates fibril formation of Fn

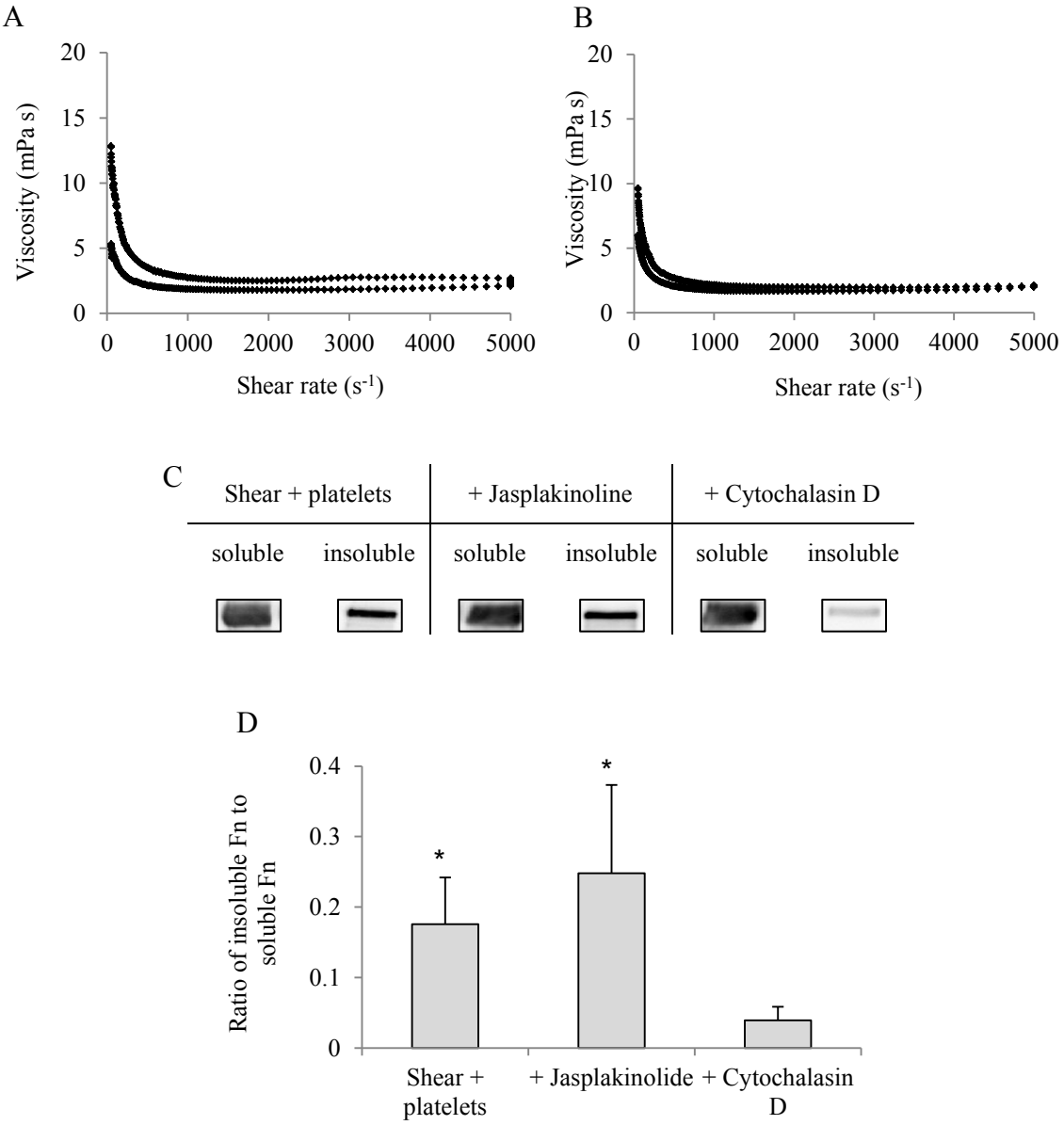

Figure 3.10. Cytoskeleton regulates Fn unfolding exposed to shear.

Changes in viscosity of solution exposed to shear. Fn solutions, in the presence of washed platelet, were exposed to shear. Washed platelets were preincubated with jasplakinoline (A) or cytochalasin D (B), prior to the addition of Fn and shear exposure. Control experiments were shown in Supplemental data 5. Western blot analysis of insoluble and soluble Fn, which were separated using DOC solubility assay (C). Densitometric analysis of Western blots to quantify the conformational changes of Fn in solution interacting with plates coated with Fn after dynamic shear rates were generated (D). Depicted are data of at least 3 independent experiments. (*) indicates significant difference ($p < 0.05$), as compared to the "cytochalasin D" group.

In addition to their roles in adhesion to ECM ligands, integrins serve as transmembrane biomechanical links from those extracellular contacts to the cytoskeleton inside cells (Hynes, 2002). Actin, a highly conserved and abundant cytoskeletal protein, is implicated in a number of cellular activities, including reorganization of cell shape and cell motility (Lauffenburger and Horwitz, 1996; Mitchison and Cramer, 1996). Many of these processes require the dynamic behavior of the actin cytoskeleton which involves the polymerization and depolymerization of actin filaments (Welch et al., 1997). Hence, interactions between Fn binding integrins and an intact actin cytoskeleton are crucial for the assembly of a Fn matrix (Wu, 1997). To examine the effect of platelet cytoskeleton on Fn fibrillogenesis induced by shear, platelets were preincubated with cytoskeleton drugs, i.e., jasplakinolide to stabilize actin or cytochalasin D to disrupt actin polymerization. As depicted in Figure 3.10 A and B, changes in viscosities of samples, indicative of Fn conformational changes, depended on the actin cytoskeleton since treatment with cytochalasin D resulted in a lower increase in viscosity, in comparison with control experiments (Supplemental data 5). Densitometric analysis has supported this observation by depecting that jasplakinolide caused an increase by 41% in fibril formation of Fn, as compared to control experiments. In contrast, disruption of actin by cytochalasin D resulted in a decrease by 86% (Figure 3.10D). Hence, the dynamic to polymerization of actin, rather than depolymerization, is necessary for fibril formation of Fn.

3.6. Mimetic peptides

The above results prompted us to further investigate changes of shear-induced Fn fibrillogenesis on platelets upon blocking the interaction of Talin-1 or Kindlin-3 with the β cytoplasmic tail of integrins in platelets. To inhibit the interaction between adaptor proteins (Talin-1 and Kindlin-3) and the β cytoplasmic tail of platelet integrins, we used synthetic peptides with sequences derived from regions of β3 cytoplasmic tail that contain specific binding site for Talin or Kindlin. Peptide sequences and the nomenclature used are set out in Material and Methods (2.1.4). Specific binding between the synthetic β3 tail mimetic peptides and Talin or Kindlin from platelets was confirmed by means of Western blot (Supplemental data 9). In addition, FACS analysis indicated that our TAT(47-57)-conjugated peptides can penetrate the platelet membrane (Supplemental data 8) and do not activate platelets in the absence of agonists (Supplemental data 10).

3.6.1. Effect of mimetic peptides on platelet adhesion and aggregation

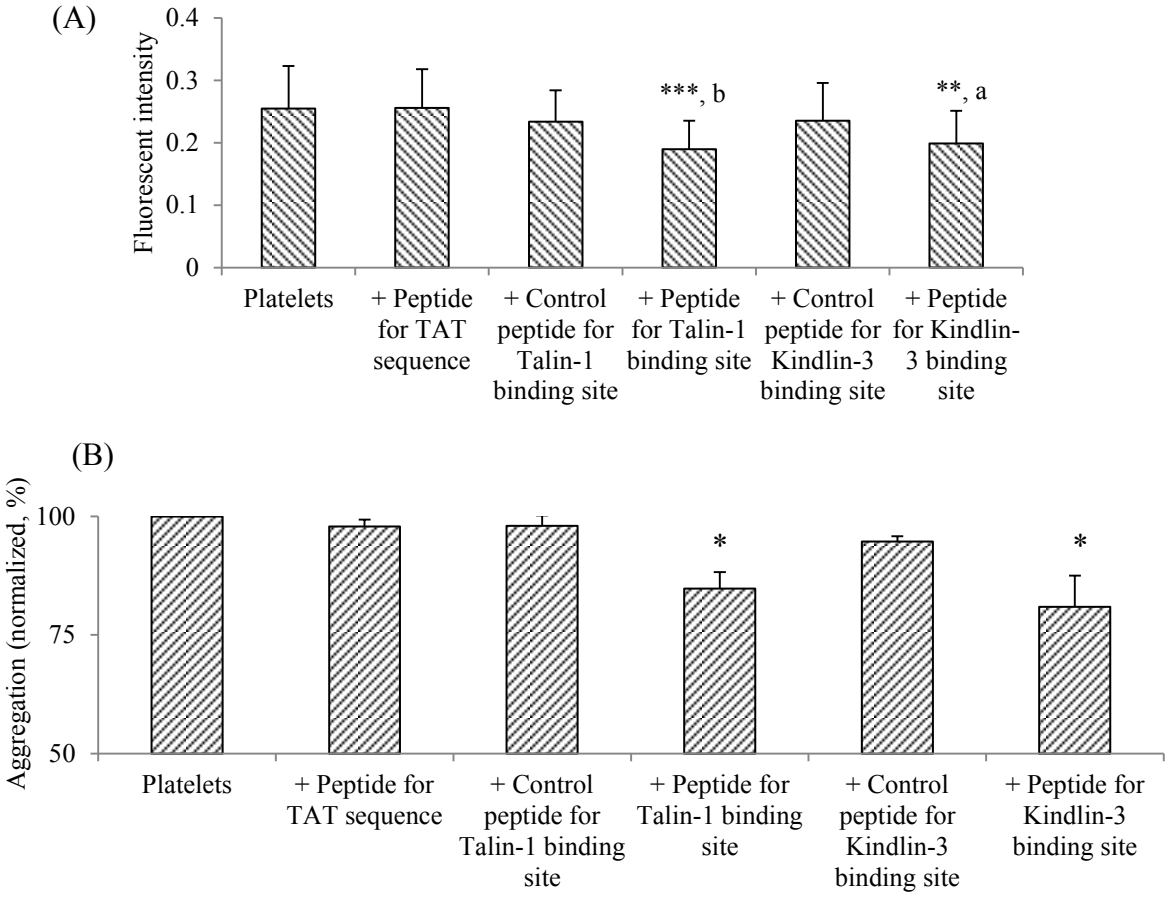

Figure 3.11. Impact of β3 mimetic peptides on platelet function.

(A) Platelet adhesion onto immobilized Fn. After treating with mimetic peptides, CMFDA-labeled platelets in HEPES Tyrode's buffer containing 2 mM $CaCl_2$ were placed on wells coated with Fn, incubated for 30 min at 37°C. (B) Platelet aggregation in PRP induced by ADP. The maximum aggregations obtained with untreated samples were set at 100% and the other measures were referred to this. For control experiments, platelets were not treated with peptides or treated with control peptides. (*) $p < 0.05$, (**) $p < 0.01$, as compared to samples without peptide treatment. (a) $p < 0.05$, (b) $p < 0.01$, as compared to sample treated with control peptides.

To study the effect of mimetic peptides on platelet adhesion, fluorescent-labeled platelets were incubated with peptides and subsequently adhered onto Fn surface. Fluorescent signal (Figure 3.11A) revealed that treating washed platelets with mimetic peptides to inhibit Talin-1 or Kindlin-3 binding resulted in a significant decrease in platelet adhesion by 26% or 22%, as compared to control experiments. In addition, microscopic images (Supplemental data 11) further supported this observation by showing that platelets treated with peptides containing Kindlin binding site exhibited a defect in the adhesion

onto immobilized Fg, in comparison to samples treated with TAT peptides. Platelets penetrated with control peptides adhered as similar as samples in the absence of peptides.

To examine the impact of mimetic peptides on platelet aggregation, peptide-treated platelets in PRP were stimulated by ADP. In the presence of ADP, mimetic peptides caused significant reductions by 15 % (peptide for Talin-1 binding site) and 19% (peptide for Kindlin-3 binding site) in terms of aggregation (Figure 3.11B). As it was expected all the control peptides did not inhibit platelet aggregation induced by ADP.

3.6.2. Effect of mimetic peptides on activation of αIIbβ3

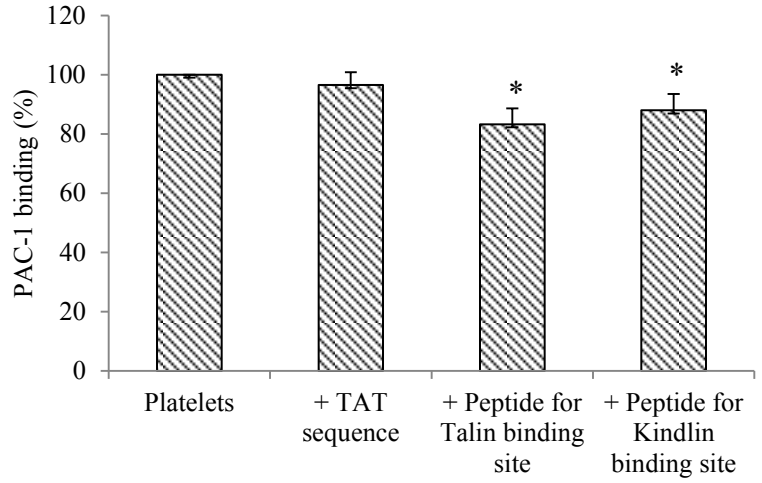

Figure 3.12. Effect of β3 mimetic peptides on ADP-induced αIIbβ3 activation.

Flow cytometry assay were performed to evaluate the binding of PAC-1 to ADP-induced platelets in PRP. The fluorescent signal obtained with untreated samples were set at 100% and the other measures were referred to this. For control experiments, platelets were not treated with peptides or treated with control peptides. (*) $p < 0.05$, as compared to control experiments.

When platelets are activated, the αIIbβ3 receptor undergoes conformational changes, from the inactive to active state. PAC-1 is a monoclonal antibody that recognizes an epitope on αIIbβ3 expressed only in its activated state (Dimitriou et al., 2009). PAC-1 binding assay was performed by means of flow cytometry to examine the impact of mimetic peptides on αIIbβ3 activation. ADP-induced platelets in PRP, pretreated with peptides, were incubated with FITC-conjugated PAC-1. The level of PAC-1 binding was subsequently measured by flow cytometry. FACS analysis showed that specific mimetic peptides for Talin-1 and Kindlin-3 binding sites resulted in a significant decrease by 16 ±

5% and 12 ± 5% in terms of PAC-1 binding to ADP-activated platelets, as compared to control experiments. Platelets penetrated with peptide contains TAT sequence only bound to PAC-1 antibody as similar as samples in the absence of peptides. All data indicate that β3 cytoplasmic tail mimetic peptides for Talin-1 or Kindlin-3 binding sites can reduce activation of αIIbβ3 in response to agonists and impair platelet functions.

3.6.3. Impact of mimetic peptide on Fn fibril formation induced by fluid shear forces

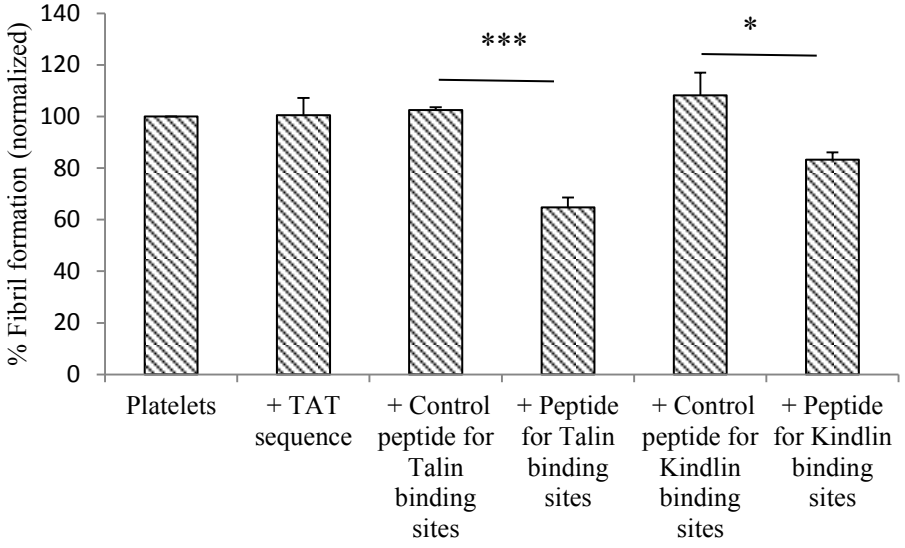

Figure 3.13. Role of mimetic peptides derived from the β3 cytoplasmic tail in fibril formation of plasma Fn exposed to shear.

Plasma Fn (100 μg/ml), in the presence of washed platelets, was exposed to shear generated by PEG-grafted cones. Washed platelets were pretreated with peptides prior the addition of Fn. Densitometric analysis of Western blots were performed to quantify the conformational changes of Fn in solutions. The amount of fibril formation obtained with untreated samples were set at 100% and the other measures were referred to this. For control experiments, platelets were not treated with peptides or treated with control peptides. Depicted are data of at least 3 independent experiments. (*) $p < 0.05$, (***) $p < 0.001$.

We have observed that the engagement between cytoskeleton and Fn via platelet integrins regulates Fn fibril assembly (Section 3.5). In addition, β3 mimetic peptides, which disrupt the interaction between integrin and adaptor proteins, can regulate αIIbβ3 activation and function. Therefore, we next examine the involvements of integrin-regulatory adaptor proteins Talin-1 and Kindlin-3 in Fn fibrillogenesis. As depicted in Figure 3.13, mimetic peptide corresponding to the binding sites of Talin-1 or Kindlin-3 could inhibit fibril

formation of Fn by 35.3 ± 3.91 % and 16.79 ± 2.92 %, respectively, as compared to samples with untreated platelets. Pretreatment of platelets with control peptides did not show any difference in Fn fibrillogenesis upon shear, as compared to samples with untreated platelets.

Taken together, these results indicate that mimetic peptides for Talin-1 and Kindlin-3 binding sites impaired platelet function and activation of αIIbβ3 in response to agonists, resulting a reduction in Fn unfolding.

4. Discussion

Platelets circulate freely in the blood and, for a correct role in hemostasis, they must be activated by sequential and coordinated mechanisms. In pathological situations, a loss of strict controls of these processes can lead to an occlusive platelet thrombus in blood vessels, possibly resulting in myocardial infarction and stroke or causing platelet dysfunction and bleeding syndrome. One of the subtle processes that must be particularly well controlled is platelet integrin αIIbβ3 activation. The cytoplasmic tail of the β3 subunit is linked to the adaptor proteins Kindlin-3 and Talin-1 both of which are connected with the cytoskeleton (Smith et al., 2007). Binding of adaptor proteins, Talin-1 and Kindlin-3, to the β3 integrin tail is critical for agonist induced αIIbβ3 activation *in vivo*. ECM ligand Fn, an adhesive protein which binds to integrin receptors, also plays a role in hemostasis and thrombosis (Schwarzbauer and Sechler, 1999).

Several agents that block signaling through ADP receptors (e.g., clopidogrel) or through the generation of thromboxane A2 (e.g., aspirin) have been used in the chronic prevention of arterial thrombosis (Bhatt and Topol, 2003). However, chronic blockade of αIIbβ3 by orally administered antagonists is ineffective in thrombosis protection, possibly because of the need to limit dosage to avoid pathological bleeding (Bhatt and Topol, 2003). Hence, in this research, we intend to develop β3 mimetic peptides that disrupt the β3-adaptor proteins interactions, consequently imparting antithrombotic effects while preserving primary hemostasis. Fn unfolding induced by shear was used as a tool to evaluate the inhibitory effect of these mimetic peptides on αIIbβ3 activation and functions. To understand the contribution of integrin-regulatory adaptor proteins Talin-1 and Kindlin-3 to Fn fibrillogenesis by platelet integrins exposed to fluid shear forces, we addressed the following questions: (1) How flow and resulting shear contribute to Fn fibrillogenesis? (2) Distinct role of Fn-binding integrins (αIIbβ3, αvβ3, and α5β1) in inducing fibril formation of Fn upon shear. (3) What are the quantitative changes in Fn fibrils formed on platelets upon pretreatment with peptides?

4.1. Fn fibrillgenesis in cell-free system

4.1.1. Flow-simulated shear contributes to Fn unfolding

Several studies (Siediecki et al., 1996; Singh et al., 2009) have shown a correlation between shear stress and structural changes of vWF, a plasma protein which plays a central role in regulating hemostasis and thrombosis (Hassan et al., 2012). Exposure of

vWF to shear rates above 2000 – 5000 s^{-1} can trigger transition from a folded to a stretched conformation. Only two reports studied the effect of shear on the conformational changes of Fn in the context of extracellular matrices (Smith et al., 2007; Steward et al., 2011). Our report is the first study which investigates the contribution of fluid flow and its resulting shear over a broad range of physiological and pathological rates (50 - 5000 s^{-1}) on Fn fibrillogenesis in a cell-free system.

It is observed that upon shear exposure, viscosity of Fn-containing solutions (50 μg/ml and 100 μg/ml) increased, while at the concentration of 10 μg/ml, Fn solutions did not show any change in term of viscosity (Figure 3.1 and Table 3.1). The correlation between increase in viscosity and protein unfolding has been recognized for decades (Tu and Breedveld, 2005; Williams et al., 1982). Therefore, changes in viscosity, as depicted, can be indicative of conformational changes in Fn. It was then confirmed by observation (Figure 3.2) showing that fluid shear up to 5000 s^{-1} could induce conformational changes in plasma Fn in concentration-dependent manner. Two groups (Barg et al., 2007; Schneider et al., 2007) also reported similar observation that the assembly of immobilized fibers from multimeric soluble vWF requires a critical protein concentration (50 μg/ml) and application of a sufficient shear rate (≥ 5000 s^{-1}). In addition, theoretical studies have proposed that the β-strand structure of Fn type III modules may be capable of unraveling under tension (Erickson, 1994). Atomic force microscopic (AFM) data also revealed that the Fn modules III10 and III13 are mechanically the weakest domains with low unfolding forces (~80 pN) (Oberhauser et al., 2002). Hence, the application of shear up to 5000 s^{-1}, as used in this work, could disrupt weak interdomain interactions between type III repeats (Leahy et al., 1996) and modulate unfolding of these type III modules of Fn. As a consequence, cryptic binding domains may be exposed, promoting the binding of other molecules, including Fn, collagen, and cell surface receptors (Oberhauser et al., 2002) and facilitating intermolecular association and fibril growth (Gao et al., 2003; Hocking et al., 1994; Zhong et al., 1998).

In this work, soluble Fn in solution was added to 3 different immobilized surfaces, BSA, collagen, and Fn, before exposed to shear, in the absence of platelets. It was found that there was no difference among immobilized surfaces in terms of increase in viscosity and fibril formation of Fn (Figure 3.1, 3.2 and Table 3.1). Hence, in cell-free system, flow

shear forces probably induce conformational changes of Fn in surface-independent manner.

The observation showing that fluid shear up to 5000 s^{-1} could induce conformational changes in plasma Fn (Figure 3.2) was then confirmed by platelet adhesion assays. As depicted in Figure 3.3, Fn exposed to shear supported better platelet adhesion compared to soluble Fn. This result is consistent with previous studies reported that Fn assembly into fibrillar Fn supports cell adhesion (Morla et al., 1994). Hence, the adhesion of platelet onto shear-exposed Fn surfaces, observed here, indirectly indicated that upon shear exposure, soluble plasma Fn changed the conformational structure to an unfolded form while exposing the intrinsic binding sites. As depicted in Figure 3.3, coating the well surfaces with Fn at a concentration of 50 μg/ml, the extent of platelet adhesion onto surfaces coated with shear-exposed Fn did not differ from that onto surfaces coated with Fn which had not been exposed to shear. This result is probably due to saturation of the ligand. A similar observation was made with Fg-coated surfaces (Jen and Lin, 1991).

Several blood components have been reported to be involved in negative and positive regulation of Fn assembly. Fragment containing the C-terminal two-thirds of Fn module III1 (anastellin) could induce Fn polymerization in the absence of cells (Morla et al., 1994), while the N-terminal 70kDa fragments of Fn can inhibit Fn matrix assembly by competing for Fn assembly sites (Bourdoulous et al., 1998). In addition, high concentrations of vitronectin have an inhibitory effect on the Fn-matrix assembly (Hocking et al., 1999; Zheng et al., 2007). Hence, those components could act as a feedback system to regulate the amount of Fn on the cell surface and physiological Fn fibrillogenesis in circulatory system.

Taken together, shear alone could induce assembly of Fn matrix, supporting platelet adhesion. These force-triggered and dose-response events might be important for the activation of Fn fibrillogenesis and matrix assembly (Oberhauser et al., 2002).

4.1.2. Physical properties of stainless steel induce Fn matrix assembly

Stainless steel is being widely used in many biomedical devices, such as surgical implants and vascular stents. It has been reported that the bare surface of stainless steel can reduce the partial thromboplastin time by 50%, indicative of activated coagulation (Oeveren et

al., 2000). Generally, metallic materials are regarded as thrombogenic due to their positively charged surface and the high surface free energy. Adsorption of plasma Fn onto surface of metallic material initiates their conformational changes (Salmeron-Sanchez et al., 2011), that promote their prothrombotic properties (Hong et al., 2005).

PEG is well known as one of the most suitable coating agents because of its biocompatibility (Deible et al., 1998; Jo and Park, 2000). This polymer has been reported extensively in the literature as having inherent capabilities to reduce non-specific protein binding. Hence it has become more attractive for biomedical research, biosensors, and pharmaceutical applications (Kang and Lee, 2007). In this study, stainless steel cones were used to generate shear. Upon treatment with PEG, the surface properties of the stainless steel cone were modified. Western blotting and densitometry analysis revealed that Fn adsorption onto the bare surface of stainless steel was higher than on the surface-modified cones (Figure 3.4). This observation is consistent with a previous report by Kang and Lee (2007). The adsorption of Fn onto the bare surface is presumably caused by electrostatic or hydrophobic forces. In the circulation, the rapid adsorption of plasma proteins onto metallic surfaces is regarded as first step of interaction upon contact of blood with artificial surfaces followed by platelet adhesion and subsequent aggregation. Chemical modification by means of covalently grafting of hydrophilic polymer can prevent adsorption of Fn. It is presumably because that the grafted polymers prevent the protein from approaching the surfaces. It has been reported that water molecules situated between the proteins and the surface take part in reducing the protein-substrate attraction. The stability and thickness of the interfacial water layers largely and negatively affect the protein adsorption (Kang and Lee, 2007).

As depicted in Table 3.2, the initial viscosity of solutions exposed to shear generated by cones coated with PEG was higher than those exposed to shear generated by uncoated cones. In addition, the increase in viscosity in the samples exposed to shear generated by PEG-grafted cones was higher than samples in which uncoated cones were used. It is due to two effects (Zalipsky and Harris, 1997):

- First, attachment of PEG to cone surfaces alters the electrical nature of the surfaces that were subsequently exposed to aqueous environment.
- Second, the PEG layers act like a gel with high viscosity, even at the tip of the cone where it can be in contact with plates (cone-plate space is 0.053 mm).

Generating shear by bare stainless steel resulted in a higher amount of Fn fibril formation (Figure 3.5), indicating that bare surface of stainless steel can induce considerable Fn unfolding upon shear. Hence, flow-dynamic conditions and/or physical properties of steel surface may modulate Fn fibrillogenesis, as documented previously (Nguyen et al., 2013). This observation corresponds to the *in vivo* situation in which the contact of metallic biomedical devices, such as needles and implant stents, with circulating blood initiates hemostasis. Upon this, platelet adhesion and aggregation occur at the injured vascular sites. Platelet adhesion is accentuated by increased shear rate (Triplett, 2000). At moderate shear rates ($\leq$ 1250 s^{-1}), Fn assembly enhances platelet adhesion (Cho and Mosher, 2006c) onto surfaces, such as nonfibrillar collagens and the subendothelium of the vessel wall (Beumer et al., 1995). Themistou et al. (2009) pointed out that vasoconstriction (a step in hemostasis process) and high shear rates associated with arterial stenosis may enhance conformational changes of vWF. However, no such studies have been conducted with regard to plasma Fn.

As depicted in Figure 3.5 and Figure 3.2, when using cones which have bare stainless steel surfaces to generate shear, there was no difference among immobilized surfaces in terms of Fn fibrillogenensis. In contrast, when using PEG-grafted cones to generate shear, collagen coated plates resulted in a higher amount of fibril formation, as compared to BSA surfaces. Several groups (Cho et al., 2005; Cho and Mosher, 2005; Olorundare et al., 2001) have reported that platelets adherent to Fn-, fibrin-, laminin-, or collagen-coated surfaces support Fn assembly, whereas platelets adherent to vitronectin- or Fg-coated surfaces do not.

Taken together, shear alone could induce Fn fibrillogenesis in surface-dependent manner, while physical properties of metallic material modulate fibril formation of Fn induced by shear in surface-independent and concentration-dependent manner.

4.2. Shear-induced Fn matrix assembly is modulated by platelet integrins

Studies in cell free system (Section 3.1 and 3.2) have revealed that flow-simulated shear and physical properties of metallic biomedical devices could induce Fn fibrillogenesis. The importance of shear forces in regulating platelet function has long been recognized. In addition, fibril formation of Fn has been well known as a cell-mediated process. We therefore further examined the role of platelet and its surface receptors in the

conformational changes of Fn upon shear.

4.2.1. Morphology of Fn fibrils induced by fluid shear forces and platelets

Microscopic analysis (Figure 3.6) showed that upon shear, Fn fibrils were formed, in the presence or absence of platelet. Chen et al. (1997) and Peters et al. (1998) observed that Fn fibrils formed in the cell-free system have similar structural and biochemical features as in cell cultures. The thickness of observed fibrils (Figure 3.6) varied from 500 to 5000 nm, while Mao and Schwarzbauer (2005a) reviewed that the Fn fibril diameter is ranging from 10 to 1000nm. The fibrillar Fn patterns are affected by multiple factors, including Fn concentration, incubation time, and force direction. Concentrated Fn solution (100 μg/ml) usually yielded thick bundles of Fn fiber (Ulmer et al., 2008). Phase contrast and epifluorescent images of cells exposed to shear fluid flow also appeared to form thicker Fn fibrils (Steward et al., 2011). Difference along the length of fibrils indicated that Fn dimers vary in their degrees of expansion from the compact to the extended form. The most likely regions in Fn dimers that could undergo conformational changes and influence the conformation of the fibril are the two sets of type III 15-17 repeats in Fn. These repeats not only comprise more than 60% of the molecule, but their β-strand structure and the strength of interdomain interactions between them are likely to contribute to the overall flexibility of Fn fibrils (Peters et al., 1998).

The interaction of platelets with soluble Fn may be different depending on whether platelets are activated or inactivated. At static condition, we observed no fibril formation when soluble plasma Fn was added to washed platelets in suspension (Supplemental data 4). Our result is consistent with previous studies showed that Fn does not reveal any binding to platelets in suspension in the absence of agonists (Huynh Khon et al., 2013). At normal wall shear rates (20 – 2000 s^{-1}), shear does not stimulate the activation of platelets in suspension. However pathologically elevated shear stress may trigger the activation of platelets (Savage et al., 1996). The addition of platelets resulted in a significant increase in fibril formation, as demonstrated in Figure 3.6, indicating that flow-simulated shear up to 5000 s^{-1} could induce platelet activation and subsequent Fn fibrillogenesis. Several studies (Cho et al., 2005; Cho and Mosher, 2005; Olorundare et al., 2001) reported that assembly of plasma Fn by adherent platelets depends on the adhesive protein surfaces under both static and flow conditions. Fn possesses adhesive sites for various substances, including collagen, Fn, Fg, heparin, factor XIII (Magnusson

and Mosher, 1998). Hence, observation in which Fn and collagen surfaces could enhance Fn unfolding upon shear is consistent with previous studies. It is worthy to notice that collagen, an extracellular matrix component that interacts directly with platelets (Watson, 2009), could induce platelet activation through the Ig receptor, GPVI (Nieswandt and Watson, 2003). It is reported that platelets adherent to collagen assembled plasma Fn under static and moderately high shear (1250 s^{-1}) conditions. Thrombus formation at 1250 s^{-1} was enhanced by perfused Fn in a concentration-dependent manner and accompanied by deposition of Fn in developing thrombi (Cho and Mosher, 2006b).

Upon exposed to shear up to 5000 s^{-1}, platelet can become activated (Savage et al., 1996). Activation consequently causes platelets to change shape, secrete their intracellular granules, and aggregate with each other (Gordon, 1976). Platelet alpha granules contain polypeptides such as coagulation proteins (e.g., Fg, factor V), soluble adhesion molecules (e.g., vWF, vitronectin), growth factors, protease inhibitors, and membrane adhesion molecules (Holmsen, 1994). In addition, fibrillar Fn matrix could modulate Fg assembly into a complex matrix fibrils (Pereira et al., 2002). Hence, fibril matrix observed in Figure 3.6 G-I could be involved the assembly of those platelet-secreted proteins.

4.2.2. Distinct role of platelet integrins in Fn fibrillogenesis

The initiation of Fn fibril formation, so-called fibrillogenesis, is induced by the interaction of Fn with cellular surface integrin receptors via RGD sequence (Wu et al., 1995). Integrin activation is required for Fn matrix assembly (Wu et al., 1996; Wu et al., 1995). Tzima et al. (2001) reported that shear stress induced conformational activation of integrins followed by their increased binding to ECM ligands. These results indicate that the ability of cells to assemble Fn matrix is controlled by both the type and the activation state of the integrins (Wu et al., 1995). Therefore, we examined the contribution of these three integrins, αIIbβ3, αvβ3 and α5β1, in Fn fibrillogenesis upon shear. The finding that C7E3 reduced more than 78% in Fn fibril formation (Figure 3.9) is in correlation with previous data which showed that this β3-antibody causes a reduction of 40% in Fn binding to platelets (Huynh Khon et al., 2013). Despite its low expression on the platelet surface, αvβ3 had the same contribution to Fn binding as αIIbβ3 on platelets in suspension (Huynh Khon et al., 2013) but showed a smaller contribution to Fn unfolding modulated by shear (as depicted in Figure 3.9), similar to previous study at static condition (Huynh Khon et al., 2013). α5β1 is known as a major receptor for Fn and has

been implicated in Fn fibril formation by fibroblast and endothelial cells (Singh et al., 2010). Our data demonstrated that α5β1 also participates in the interaction, unfolding, and assembly of Fn by platelets, but to a lesser extent, than β3 integrins. The appearance of Fn fibrils mediated by activated αIIbβ3 and by α5β1 was similar (Wu et al., 1995). It should be stressed again that the distinct integrins involved in the binding and assembly of Fn on the platelet surface have significantly different expression levels ranging from a few hundreds (αvβ3) up to 80 000 (αIIbβ3) copies per platelet. Therefore, these differences must be taken into account for a direct comparison of the platelet receptors involved in the interactions with Fn (Huynh Khon et al., 2013). The data on the increase in viscosity of the Fn solutions and Western blot analysis (Figure 3.7) corresponded with each other, showing a correlation between changes in viscosity and conformational changes, consistent with Tu and Breedveld's study (2005).

Taken together, these results demonstrate that flow-simulated shear and platelets could modulate Fn unfolding in surface-dependent manner and platelet concentration-independent manner. β3 integrins play predominant role in this event. In addition, beside Fn assembly, formed fibril matrix could be involved the assembly of platelet-secreted proteins.

4.3. Actin cytoskeleton promotes Fn fibril formation

In addition to their roles in adhesion to ECM ligands, integrins serve as transmembrane biomechanical links from those extracellular contacts to the cytoskeleton inside cells (Hynes, 2002). Integrins link Fn to the actin cytoskeleton through interactions between their cytoplasmic domains and cytoskeletal-associated proteins (Wu et al., 1995). As depicted in Figure 3.10, disrupting actin polymerization by cytochalasin D resulted in a significant decrease in fibril formation. This observation correlates with previous fluorescence resonance energy transfer (FRET) studies showed that cell-generated force is required to maintain Fn in partially unfolded conformations (Baneyx et al., 2002). Initially, integrin-bound Fn is diffusely localized at the cell surface. Receptor clustering by dimeric Fn helps to organize Fn into short fibrils that are soluble in detergent. The cytoplasmic domains of integrins become associated with the actin cytoskeletal network forming a connection that is essential for Fn matrix assembly (Wu et al., 1995). Our finding in this study is consistent with previous reports showing that the binding of Fn to integrins is not sufficient to initiate fibril formation, instead cells must also exert

cytoskeleton-generated traction force, resulting in Fn adhesions to promote Fn fibril assembly (Wu et al., 1995; Zhong et al., 1998).

4.4. Adaptor proteins, Talin-1 and Kindlin-3, regulate αIIbβ3 integrin activation and shear-induced Fn unfolding

Stefanini et al. (2014) has reported that platelet Talin mutant mice were protected from thrombosis, but exhibited only a modest reduction in hemostasis function. Integrin activation of Talin mutant platelet was reduced but not abolished. Hence, deceleration of αIIbβ3 activation could be a safe strategy to prevent arterial thrombosis (Stefanini et al., 2014). Therefore, we proposed a strategy to synthesized β3 mimetic peptide analogs which can partially disrupt the interaction of adaptor proteins and integrins, consequently regulating integrin activation and subsequent signaling events. This partial inhibition imparts antithrombotic effects while preserving primary hemostasis.

TAT (47-57) sequence that derives from the HIV-1 TAT protein was used to facilitate peptide penetration into cells. As depicted in Supplemental data 8 and 9, peptide analogs of the β3 intracellular domain conjugated to TAT (47-57) sequence were platelet permeable and bound specifically to corresponding adaptor proteins. An important feature characteristic of TAT cell penetrating peptide is that it possesses low cytotoxicity in various cell types (Futaki et al., 2003; Futaki et al., 2001). It is not clear how this strongly cationic and hydrophilic TAT sequence is able to penetrate the cell membrane. A direct transport through the lipid bilayer of membranes has been proposed as a possible mechanism of translocation (Derossi et al., 1996; Vivès et al., 1997). However, there are several other studies supporting the involvement of endocytosis as the major route for the internalization of TAT peptide carrier (Richard et al., 2003).

Several studies reported that HIV-1 TAT protein could activate platelets via interaction with integrin αvβ3 (through RGD motif) and the chemokine (C-C motif) receptors CCR3 (through CCF/Y and SYXR motif). TAT-induced platelet activation requires both chemokine receptor CCR3 and integrin β3 (Wang et al., 2011). As denoted in section 2.1.4, TAT (47-57) peptide and mimetic peptides containing TAT (47-57) sequence do not contain neither RGD motif nor binding sites for chemokine receptors. Hence, peptides used in this work did not activate platelets (Supplemental data 10), as expected.

4.4.1. Effect of of mimetic peptides on β3 integrin activation and functions

Cellular control of integrin activation is essential for virtually all cells, including platelets, which seal injured vessels and stop bleeding. Activated αIIbβ3 integrins bind adhesive protein such as Fg and Fn, thus allowing firm platelet adhesion and platelet aggregation (Moser et al., 2008). As depicted in Figure 3.11 and fluorescent microscopic images (Supplemental data 11), the mimetic peptides have effects on platelet activation and functions, while control peptides showed no reduction. According to previously published results, a peptide analog containing β3755–762 sequence (containing Kindlin binding sites) mediated a 25% reduction in platelet adhesion onto Fg-coated surface (Litjens et al., 2003). Liu et al. (1996) also reported that peptides encompassing the entire integrin β3 cytoplasmic sequence selectively exerted an inhibitory effect on adhesion of human erythroleukemia cell line (HEL) or vein endothelial cell line *(*ECV) to immobilized Fg. Tyrosine mutation in peptides involving conservative replacements Tyr747Ala and Tyr759Ala resulted in the loss of inhibitory function of peptide. Tyr747 and Tyr759 are critically important for the inhibitory activity of the cell-permeable peptide (Liu et al., 1996). Hence, our findings are consistent with previous studies showing that inside-out and outside-in signalings of αIIbβ3 integrin are abrogated in Talin- or Kindlin-deficient platelets (Nieswandt et al., 2007).

Interestingly, we observed that the inhibitory effect of mimetic peptides in PRP is lower than that in washed platelets. Previous studies have shown that synthetic peptides are susceptible to degradation by plasma proteases which make them lose their biological potency (Brinckerhoff et al., 1999; Chen et al., 2007; Papamichael et al., 2009). In addition, Dimitriou et al. (2009) also reported that incubation of the β3 analog peptide with PRP for a time period higher than one min significantly abolished its inhibitory effect.

It is reported that complete lack of integrin function in Talin-1- or Kindlin-3-deficient platelets resulted in defective hemostasis and abrogated platelet adhesion, and thrombus formation in injured vessels *in vivo* (Moser et al., 2008; Nieswandt et al., 2007; Petrich et al., 2007b). Loss of αIIbβ3 in humans, due to mutation in either αIIb or β3 integrin genes (Glanzmann thrombasthenia), or complete lack of αIIbβ3 function is associated with an increased risk of pathological bleeding (Quinn et al., 2003). Chronic blockade of ligand

binding to αIIbβ3 by orally administered antagonists is ineffective in thrombosis protection, possibly because of the need to limit dosage to avoid pathological bleeding (Bhatt and Topol, 2003). In contrast, blockade of Talin binding to αIIbβ3 inhibits thrombosis with less pathological bleeding than complete lack of αIIbβ3 function. Outside-in signaling, which is sufficient for hemostasis in the microcirculation (Coller, 2001), may account for the lack of pathological bleeding (Tahiliani et al., 1997). Hence, mimetic peptides disrupting adaptor proteins-αIIbβ3 interaction could be potential antithrombotic agents.

4.4.2. Shear-induced Fn fibrillogenesis is regulated by β3 mimetic peptides

Adaptor proteins connect the β3 cytoplasmic tail of integrins to the actin cytoskeleton. Thereby, cellular tension forces are generated by cytoskeletal reinforcement and transmitted through integrins to bound ligands on cell surface. As depicted in Figure 3.11, treating platelets with mimetic peptide derived from β3 cytoplasmic tail caused a reduction in terms of Fn matrix assembly. Peptide for Talin-1 binding site showed a higher inhibitory effect than peptide for Kindlin-3 binding site in terms of Fn fibril formation. It is consistent with previous study show that blocking Talin binding to β-integrin tails blocks both Talin- and Kindlin-driven integrin activation, whereas inhibiting Kindlin binding still permits Talin-mediated activation (Ye et al., 2010). Hence, it confirms that Kindlins have little effect in the absence of Talin (Harburger et al., 2009; Ma et al., 2008). Talins, which increase the affinity of individual integrins, and Kindlins, which promote integrin clustering, can synergize with each other in activating integrins (Harburger et al., 2009; Ma et al., 2008; Ye et al., 2013). Integrin clustering and conformational changes then can synergistically enhance multivalent ligand binding to cellular integrins (Hato et al., 1998).

It is worthy to notice that concentrations of mimetic peptides used in this work were relatively high, as compared to other reports (Dimitriou et al., 2009). In addition, inhibitory effect of β3 mimetic peptides was not pronounced, as expected. This is probably because mimetic peptides did not form an optimal structure facilitating the interaction to adaptor proteins. Circular dichroism data regarding the secondary structure of mimetic peptides were shown in Supplemental data 6 and 7. Nuclear magnetic resonance (NMR) dynamics studies showed that before forming a complex with Talin, the β tails are essentially disordered (Tompa et al., 2009). Disordered protein regions

often act as ‘hubs’ for promiscuous interactions with several different partners; the disorder gives rise to weak but specific interactions because of an entropic cost in forming the complex (Tompa et al., 2009). The interaction is optimal when the β subunit cytoplasmic tail is presented on a hydrophilic negatively charged surface such as the inner leaflet of plasma membranes. Small changes in cytoplasmic tail of the β subunit sequences have been shown to significantly increase their affinities for Talin family FERM domains (Anthis et al., 2010). Crystallography and NMR data on β3 cytoplasmic domain also reveal that, when bound to the PTB-like domain of Talin, the β3 tail NPLY motif forms a β turn and the preceding seven residues form a β-strand that augments the β sandwich present in Talin (García-Alvarez et al., 2003; Ulmer et al., 2001). Thus, integrin tails might rely on interaction with intracellular factors to stabilize their structure (Ulmer et al., 2003; Ulmer et al., 2001). Hence, molecular dynamic simulations need to be performed to determine and improve the structural stability of mimetic peptides, resulting a lower concentration needed.

5. Conclusions

This study focuses on the impact of adaptor proteins Talin-1 and Kindlin-3 on Fn fibrillogenesis induced by flow shear forces. By using a cone-plate rheometer to generate flow-simulated shear, I demonstrated that the conformational changes of Fn could be monitored by viscosity. Dynamic shear rates simulating venous or arterial flow conditions and physical properties of stainless steel can trigger fibrillogenesis of plasma Fn in a concentration-dependent manner, while shear alone could induce Fn unfolding in surface-dependent manner. In addition, the formation of fibrils upon shear is modulated by platelet integrins and actin polymerization. Hereby, αIIbβ3 plays a predominant role, while α5β1 has a minor part among the three examined platelet integrins, in terms of fibril formation. By introducing β3 mimetic peptides which can bind to Talin-1 or Kindlin-3, the data observed in this report support the hypothesis that disrupting the interaction between β3 cytoplasmic tail and adaptor proteins Talin-1 and Kindlin-3 could impair platelet activation and functions, resulting a reduction in Fn matrix assembly. Talin-1 shows a more important role in regulating Fn unfolding, while Kindlin-3 plays as a coactivator. Taken together, I observed roles of these adaptors proteins in modulating Fn fibrillogenesis. Furthermore, the process of Fn unfolding and assembly depends on the type of integrin, actin polymerization and fluid shear forces. To our knowledge, this is the first study reporting shear-induced conformational changes in Fn.

In an attempt to develop an antithrombotic agent, which can prevent thrombosis while preserving hemostasis, we have developed β3 mimetic peptides which can regulate αIIbβ3 activation and function. Although the inhibitory effects of these mimetic peptides have not been impressive, they still exhibit as potential therapeutics aimed at specifically disrupting integrin activation in platelets. The insights of my data raise some questions for further studies:

1. What are the consequences in terms of qualitative changes of Fn fibrils formed on platelets pretreated with Talin or Kindlin binding peptides under different flow dynamic conditions?
2. Does improved structural stability of the mimetic peptides (by mean of molecular dynamic simulation) lead to enhanced activities in disrupting Talin-integrin or Kindlin-integrin interactions and, thereby, cause more profound changes in the fibrillogenesis of Fn on platelets?

3. What are the consequences regarding platelet function when combination of both peptides were used?

Such studies contribute a better understanding of the role of Talin-1 and Kindlin-3 in modulating Fn fibrillogenesis on platelets exposed to biomechanical stress. Moreover, the use of specific peptides mimicking the binding sites for Talin-1 and Kindlin-3 offers a novel strategy for antithrombotic intervention.

SUPPLEMENTS

1. Chemical modification of stainless steel

Acid treatment and silanization. The cones (Diameter: 60 mm, Cone angle: 1.016^{o}, Truncation: 0.051 mm) were acid-treated using a piranha solution composed of H_2SO_4 and H_2O_2 (4:1) for 1 h to remove any contaminants and expose the reactive hydroxyl groups on the surface. The acid-treated cones were subsequently cleaned by ultrasonication in deionized water, ethanol and acetone for 10 min in a sequential manner, dried by nitrogen steam, and immediately subjected to silanization. Silanization was performed with epoxy-functionalized silane (GPTS, Aldrich, Steinheim, Germany) in a 10% (v/v) GPTS/toluene solution at 55°C for 48 h. Subsequently, to eliminate the non-covalently adsorbed silane compounds, ultrasonication in toluene and methylene chloride was performed two times for 5 min each. The cones were then dried gently under a steam of argon gas and thermally cured in an oven at 70°C for 3 h.

Polymer grafting on the silanized surface. Grafting of the PEG polymer was carried out in a 10 mM PEG/n-methyl-2-pyrrolidone solution. Six equivalents of diisopropylethylamine with respect to the polymer were added. This step was performed in a shaking incubator at 50°C for 24 h. To eliminate any ungrafted polymer, ultrasonication was carried out sequentially in the grafting solvent and methylene chloride twice and for 10 min each time. The polymer-grafted cones were dried gently using nitrogen gas and then stored in a vacuum desiccator until required. This polymer-grafting step was conducted twice.

2. Western blot images (Section 3.1, Figure 3.2A)

(A)

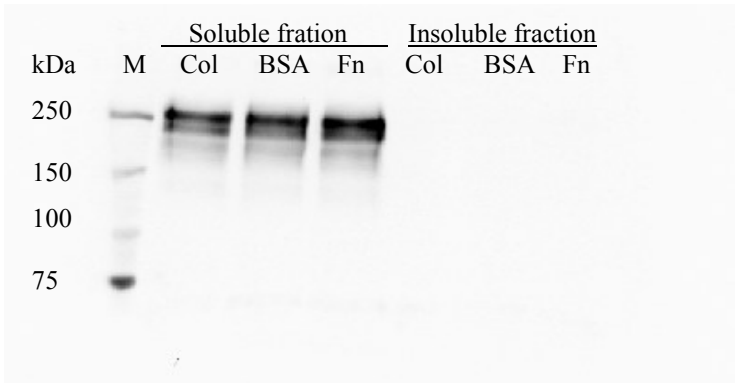

(B)

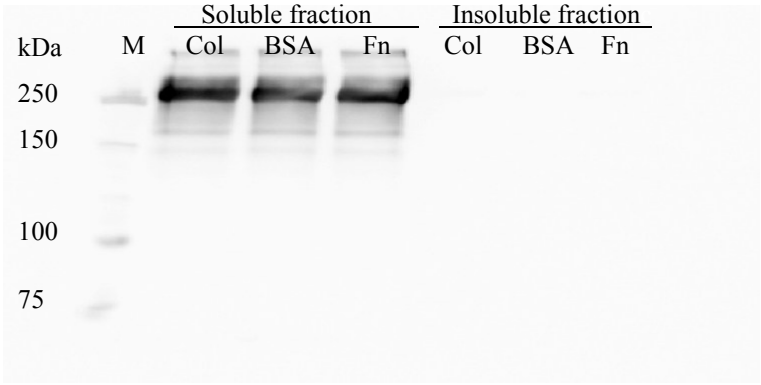

(C)

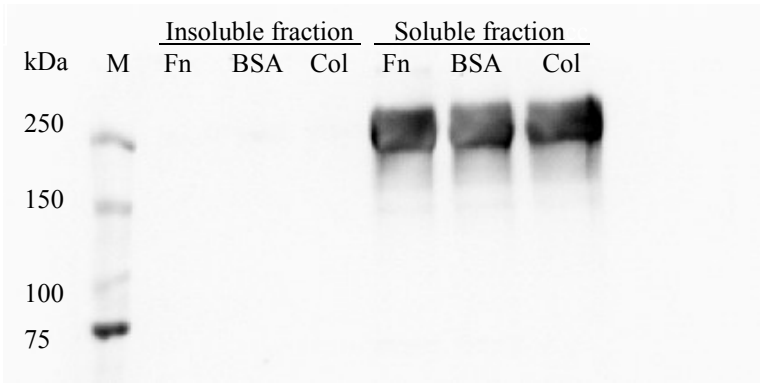

Supplemental data 1. Western blot analysis of insoluble and soluble Fn fractions.

Soluble plasma Fn, at the concentration of 10 µg/ml (A), 50 µg/ml (B), or 100 µg/ml (C) was added to coated plates. Fn in solution was at static conditions for 10 min and subsequently subjected to DOC solubility assay and Western blot analysis. An illustration of the 6% SDS-PAGE blotted on nitrocellulose membrane and analyzed by Western blotting was shown. (M) protein marker, (Col) collagen surface, (BSA) BSA surface, (Fn) Fn surface.

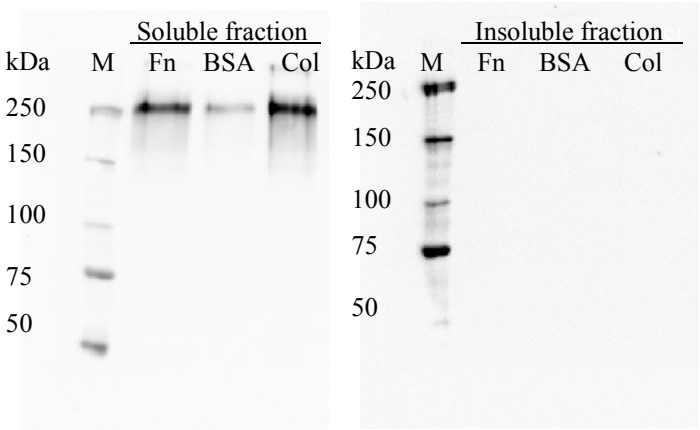

Supplemental data 2. Western blot analysis of insoluble and soluble Fn fractions.

Soluble plasma Fn, at the concentration of 10 µg/ml was added to coated plates. Upon shear exposure, Fn in solutions was subjected to DOC solubility assay and Western blot analysis. An illustration of the 6% SDS-PAGE blotted on nitrocellulose membrane and analyzed by Western blotting was shown. (M) protein marker, (Col) collagen surface, (BSA) BSA surface, (Fn) Fn surface.

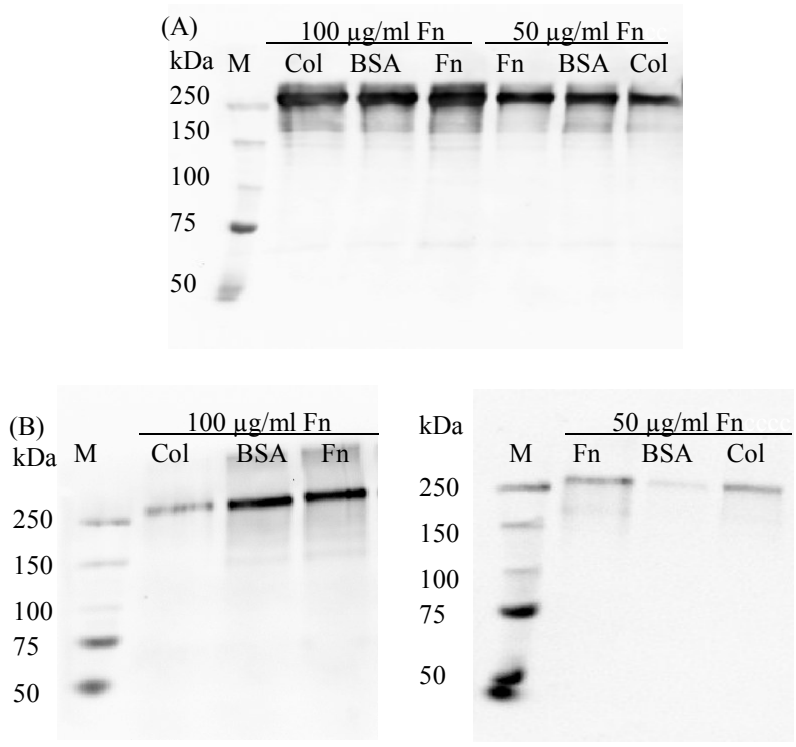

Supplemental data 3. Western blot analysis of insoluble and soluble Fn fractions.

Soluble plasma Fn, at the concentration of 50 µg/ml (B), or 100 µg/ml (C) was added to coated plates. Fn in solution was at static conditions for 10 min and subsequently subjected to DOC solubility assay. Soluble (A) and insoluble (B) fractions of Fn exposed to shear were subsequently analyzed by Western blot. An illustration of the 6% SDS-PAGe blotted on nitrocellulose membrane and analyzed by Western blotting was shown. (M) protein marker, (Col) collagen surface, (BSA) BSA surface, (Fn) Fn surface.

3. Fn, in the presence or absence of washed platelets, at static conditions (Section 3.3, Figure 3.6)

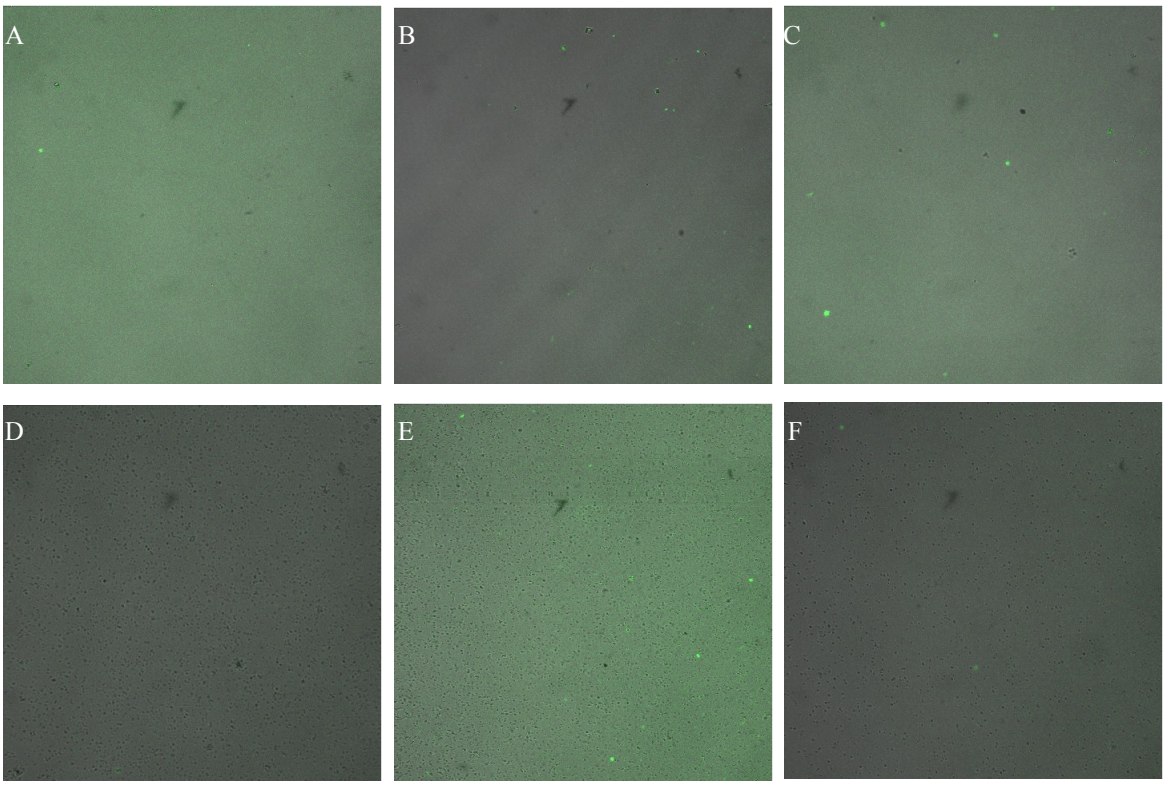

Supplemental data 4. Fn, in the presence or absence of washed platelets, at static conditions.

An illustration of fluorescence microscopic images of Fn solutions, in the absence or presence of platelets, at static conditions. Fn488, in the absence of washed platelets, was added to BSA- (A), collagen- (B), or Fn-immobilized surface (C). Fn488, in the presence of $2.5x10^7$/ml washed platelets, was added to BSA- (D), collagen- (E), or Fn-immobilized surface (F).

4. Changes in viscosity of Fn in solution, in the presence of washed platelets, exposed to shear (Section 3.4, Figure 3.8 and Section 3.5, Figure 3.10)

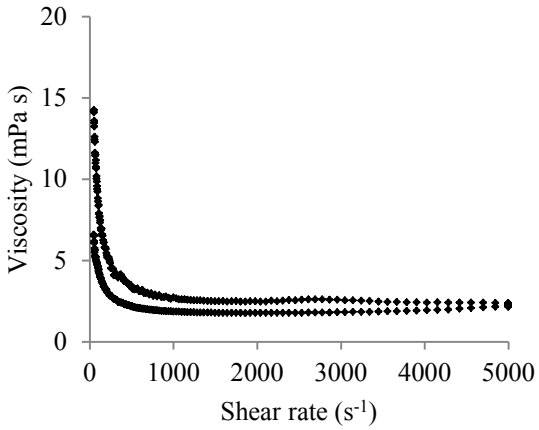

Supplemental data 5. Changes in viscosity of Fn in solution, in the presence of washed platelets, exposed to shear.

100 µg/ml Fn, in presence of washed platelets (2.5 x 10^7/ml), was added to plates precoated with Fn. Subsequently, solutions were exposed to shear generated by PEG-grafted cones. Depicted are pooled data from 3 independent experiments.

5. Secondary structure of mimetic peptides (Section 4.4.2)

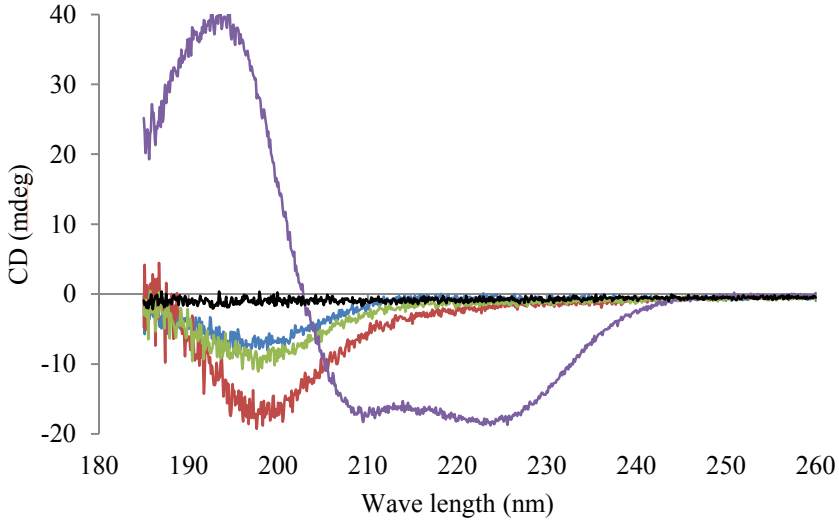

Supplemental data 6. Circular dichroism (CD) spectra of mimetic peptides in 10 mM phosphate buffer pH 7.0.

0.1 mg/ml of peptide containing TAT sequence only (blue), peptide for Talin-1 binding sites (red), or peptide for Kindlin-3 (green) was subjected to CD measurement in 1 cm pathlength cell. Spectra were acquired over the wavelength range 185 to 260 nm, with 0.1 nm step size at 0.25 seconds per data point. Myoglobin (violet) and phosphate buffer pH 7.0 (black) were used as control. Depicted are pooled data from 5 accumulations.

Supplemental data 7. Analyses of the structure of peptides from the CD data in Supplemental data 6.

Data were analyzed by program CONTINLL (CDPro package). Reference set was SMP50

	Fraction of each secondary structure						
	Regular α-helix	Distorted α-helix	Regular β strand	Distorted β-strand	Turns	Random coils	RMSD
Myoglobin	53.4%	22.2%	0%	0.2%	8.7%	15.6%	0.20
TAT sequence	0.3 %	6.4%	19.9%	13.1%	23.1%	37.1%	0.26
Peptide for Talin-1	0.6%	7.6%	13.9%	12.1%	25.5%	40.3%	0.43
Peptide for Kindlin-3	0.5%	5.7%	19.3%	12.6%	23.3%	38.6%	0.18

6. Peptide penetration (Section 3.6)

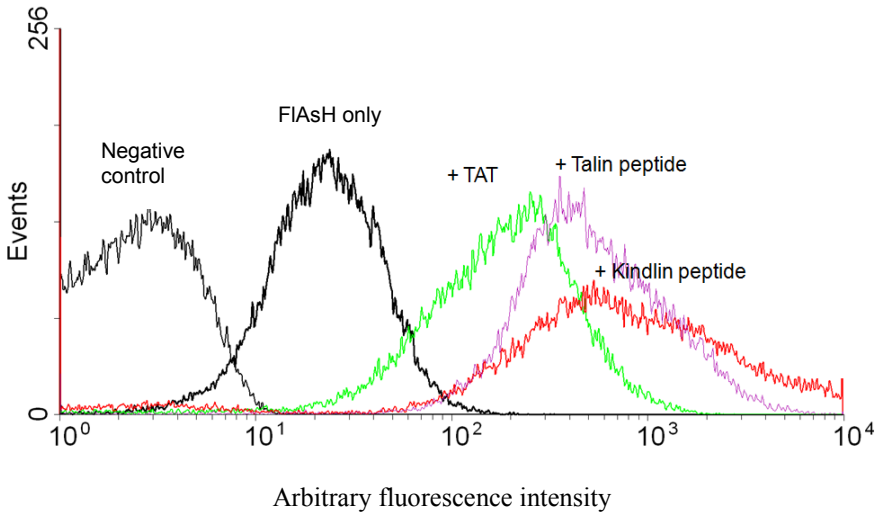

Supplemental data 8. Penetration of mimetic peptides into platelet cytoplasm

TAT-conjugated peptides were incubated with 1.6 µM FlAsH for 15 min, at room temperature. Platelets (2.5 x 10^8/ml) were incubated with FlAsH-preincubated peptides (360 µM) for 15 min. The penetration of mimetic peptides was subsequently measured by FACS.

A tetracysteine sequence (CCPGCC) was put into the peptides' sequence and was used in combination with a membrane-permeant fluorogenic biarsenical dye named FlAsH (Fluorescein Arsenical Hairpin binder). FlAsH is used as a nonfluorescent complex with ethanedithiol, and it becomes fluorescent on binding to this tetracysteine sequence (Hoffmann et al., 2010). As shown in Supplemental data 8, platelets pretreated with mimetic peptides or control peptides exhibited a strong fluorescence signal, indicating the penetration of mimetic peptides into platelet cytoplasm.

7. Specificity of peptide binding (Section 3.6)

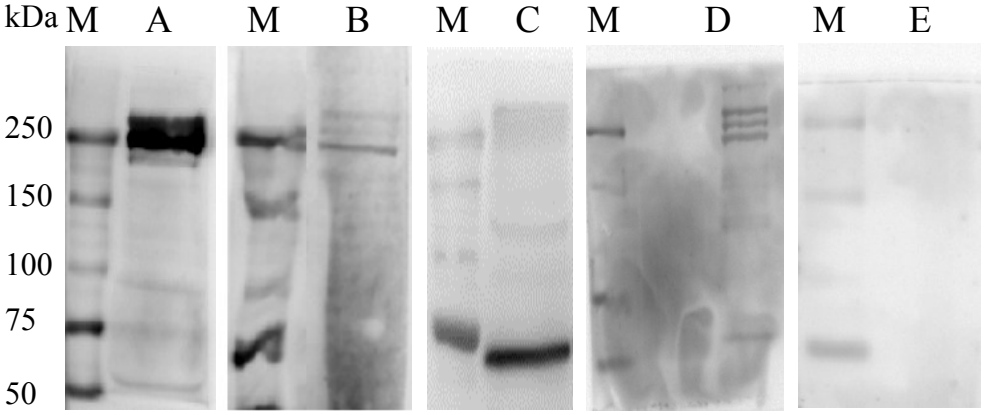

Supplemental data 9. Specific binding of synthetic peptides with Talin, Kindlin detected by Western blotting.

Platelets lysates were subjected to SDS-PAGE and transferred to nitrocellulose membranes. M: molecular marker. Membranes were probed with rabbit polyclonal antibodies raised against Talin-1 (A), biotinylated peptide for Talin binding site (B), rabbit polyclonal antibodies raised against Kindlin-3 (C), biotinylated peptide for Kindlin binding site (D), or biotinylated peptide containing TAT sequence only (E) as primary antibodies. Anti-rabit antibody or Streptavidin was used as secondary antibodies.

To confirm that the specific binding between the synthetic peptides and Talin, or Kindlin from platelets, Western blot experiments were performed. Lysates derived from human washed platelets were subjected to SDS-PAGE and transferred to a nitrocellulose membrane. Mimetic peptides corresponding to Talin or Kindlin binding site were conjugated with biotin and used as primary antibodies for detecting Talin and Kindlin, respectively. Control experiments were performed by using rabbit polyclonal antibodies raised against Talin-1 (Abcam) and Kindlin-3 (Millipore), respectively, as primary antibodies. As depicted in Supplemental data 9**,** a unique band that migrated around the 250 kDa molecular weight marker which corresponds to the molecular weight of Talin

(270 kDa) was present on membranes probed with peptides for Talin binding site (B) and rabbit anti-Talin polyclonal antibody (A). Membranes probed with peptides for Kindlin binding site (D) and rabbit anti-Kindlin polyclonal antibody (C) showed a band between 75 kDa and 50 kDa which corresponds to Kindlin. No specific band was observed in control experiments in which the membranes were directly incubated with anti-rabbit secondary antibody or streptavidin (data not shown). In another control experiment, there is no band observed when peptide containing TAT sequence only was used as primary antibody (E). Taken together, these results confirm the specific binding of the sythetic β3 tail mimetic peptides for the two adaptor proteins (Talin or Kindlin).

8. TAT (47-57) does not activate platelet (Section 3.6)

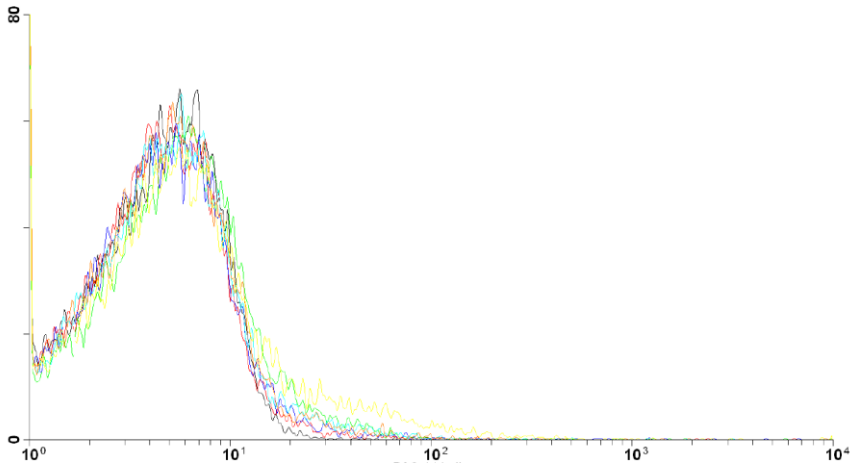

Supplemental data 10. TAT (47 – 57) does not activate platelet.

FACS histogram of PAC-1 binding assay after peptide treatments. Platelets in whole blood were incubated with 800 µM mimetic peptides for Talin (dark blue) or Kindlin (orange) binding sites or 15 min. Subsquently, treated platelets were incubated with 0.5 µg/ml FITC-conjugated PAC-1 antibody for 1 hour in the dark; diluted (1:10, v/v) with 10 mM PBS, pH 7.4 and immediately analyzed by flow cytometry. Platelets were gated according to staining for the platelet specific antigen CD42a. As control experiments, platelets treated with TAT peptide (red), control peptide for Talin binding site (light blue), or control peptide for Kindlin binding site (yellow) were used. Isotype control (black) or platelets without peptides (green) also were used.

Several studies reported that HIV-1 TAT protein could activate platelets via interaction with integrin αvβ3 (through RGD motif) and the chemokine (C-C motif) receptors CCR3 (through CCF/Y and SYXR motif). TAT-induced platelet activation requires both chemokine receptor CCR3 and integrin β3 (Wang et al., 2011). As denoted in section

2.1.4, TAT peptide and mimetic peptides containing TAT (47-57) sequence do not contain neither RGD motif nor binding sites for chemokine receptors. Hence, I hypothesized that peptides used in this work did not activate platelets. All peptides containing TAT sequence were subjected to PAC-1 binding assay to support this hypothesis. As depicted in Supplemental data 10, peptides containing TAT (47-57) sequence used in this work do not activate platelets, in the absence of agonists.

9. Fluorescence microscopic images of platelet adhesion onto immobilized Fg after peptide treatment (Section 3.6.1)

For fluorescence microscopic imaging, a tetracysteine sequence (CCPGCC) was put into the peptides' sequence and was used in combination with the green FlAsH to visualize by laser scanning microscopy. As shown in Supplemental data 11, platelets pretreated with peptides containing only TAT sequence exhibited a strong green fluorescence signal as well as adhered on immobilized Fg. In parallel experiments in which the peptide for Kindlin binding site was used, peptide-carried platelets (green platelets) showed a defect in the adhesion onto immobilized Fg. Only platelets with no peptide penetration (non-fluorescence platelets) could adhere onto Fg. These results confirmed the biofunctionality of the synthetic peptides.

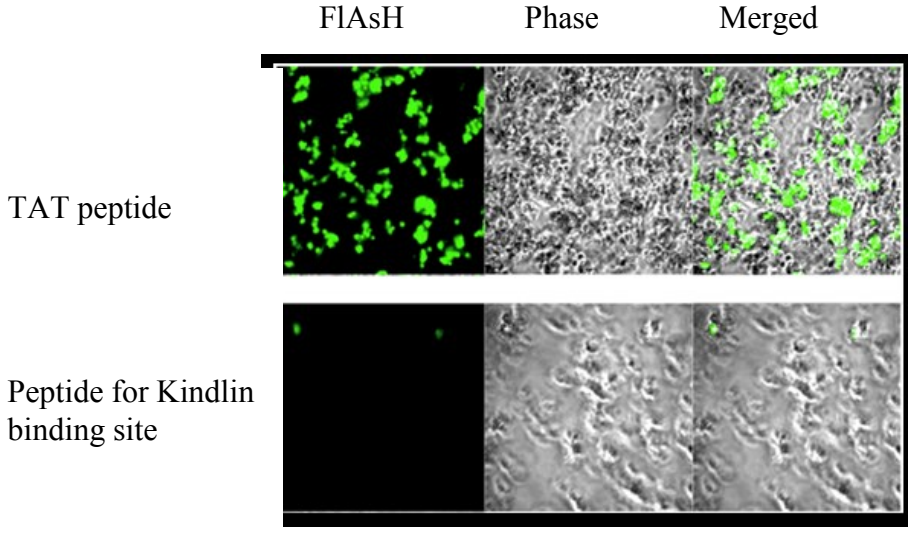

Supplemental data 11. Effect of peptide for Kindlin binding site on platelet adhesion onto immobilized ligand.

Laser scanning microscopic images of platelets adherent onto immobilized Fg (50 μg/ml) after penetration of peptide for Kindlin binding site or TAT sequence added with a tetracysteine sequence.

REFERENCES

Acharya, S.S., and Dimichele, D.M. (2008). Rare inherited disorders of fibrinogen. Haemophilia *14*, 1151-1158.

Anthis, N.J., Wegener, K.L., Critchley, D.R., and Campbell, I.D. (2010). Structural Diversity in Integrin/Talin Interactions. Structure *18*, 1654-1666.

Anthis, N.J., Wegener, K.L., Ye, F., Kim, C., Goult, B.T., Lowe, E.D., Vakonakis, I., Bate, N., Critchley, D.R., Ginsberg, M.H. (2009). The structure of an integrin/talin complex reveals the basis of inside-out signal transduction. The EMBO Journal *28*, 3623-3632.

Baneyx, G., Baugh, L., and Vogel, V. (2002). Fibronectin extension and unfolding within cell matrix fibrils controlled by cytoskeletal tension. Proceedings of the National Academy of Sciences *99*, 5139-5143.

Banno, A., and Ginsberg, M. (2008). Integrin activation. Biochem Soc Trans *36*, 229 - 234.

Barg, A., Ossig, R., Goerge, T., Schneider, M.F., Schillers, H., Oberleithner, H., and Schneider, S.W. (2007). Soluble plasma-derived von Willebrand factor assembles to a haemostatically active filamentous network. Thrombosis and Haemostasis *97*, 514-526.

Bergkvist, M., Carlsson, J., and Oscarsson, S. (2003). Surface-dependent conformations of human plasma fibronectin adsorbed to silica, mica, and hydrophobic surfaces, studied with use of Atomic Force Microscopy. Journal of Biomedical Materials Research Part A *64A*, 349-356.

Beumer, S., Heijnen, H., IJsseldijk, M., Orlando, E., de Groot, P., and Sixma, J. (1995). Platelet adhesion to fibronectin in flow: the importance of von Willebrand factor and glycoprotein Ib. Blood *86*, 3452-3460.

Beumer, S., IJsseldijk, M., de Groot, P., and Sixma, J. (1994). Platelet adhesion to fibronectin in flow: dependence on surface concentration and shear rate, role of platelet membrane glycoproteins GP IIb/IIIa and VLA-5, and inhibition by heparin. Blood *84*, 3724-3733.

Bhatt, D.L., and Topol, E.J. (2003). Scientific and therapeutic advances in antiplatelet therapy. Nature Reviews Drug Discovery *2*, 15-28.

Bialkowska, K., Byzova, T.V., and Plow, E.F. (2015). Site-specific phosphorylation of Kindlin-3 protein regulates its capacity to control cellular responses mediated by Integrin αIIbβ3. Journal of Biological Chemistry *290*, 6226-6242.

Bledzka, K., Liu, J., Xu, Z., Perera, H.D., Yadav, S.P., Bialkowska, K., Qin, J., Ma, Y.Q., and Plow, E.F. (2012). Spatial coordination of kindlin-2 with talin head domain in interaction with integrin beta cytoplasmic tails. Journal of Biological Chemistry *287*, 24585-24594.

Bledzka, K., Smyth, S.S., and Plow, E.F. (2013). Integrin αIIbβ3: From discovery to efficacious therapeutic target. Circulation Research *112*, 1189-1200.

Bourdoulous, S., Orend, G., MacKenna, D.A., Pasqualini, R., and Ruoslahti, E. (1998). Fibronectin matrix regulates activation of RHO and CDC42 GTPases and cell cycle progression. Journal of Cell Biology *143*, 267-276.

Bowditch, R.D., Hariharan, M., Tominna, E.F., Smith, J.W., Yamada, K.M., Getzoff, E.D., and Ginsberg, M.H. (1994). Identification of a novel integrin binding site in fibronectin. Differential utilization by beta 3 integrins. Journal of Biological Chemistry *269*, 10856-10863.

Brem, H., and Tomic-Canic, M. (2007). Cellular and molecular basis of wound healing in diabetes. The Journal of clinical investigation *117*, 1219-1222.

Brinckerhoff, L.H., Kalashnikov, V.V., Thompson, L.W., Yamshchikov, G.V., Pierce, R.A., Galavotti, H.S., Engelhard, V.H., and Slingluff, C.L. (1999). Terminal modifications inhibit proteolytic degradation of an immunogenic mart-127–35 peptide: Implications for peptide vaccines. International Journal of Cancer *83*, 326-334.

Broos, K., Feys, H., De Meyer, S., Vanhoorelbeke, K., and Deckmyn, H. (2011). Platelets at work in primary hemostasis. Blood Reviews *4*, 155 - 167.

Bultmann, H., Santas, A.J., and Peters, D.M.P. (1998). Fibronectin fibrillogenesis involves the Heparin II binding domain of fibronectin. Journal of Biological Chemistry *273*, 2601-2609.

Bushuev, V.N., Metsis, M.L., Morozkin, A.D., Ruuge, E.K., Sepetov, N.F., and Koteliansky, V.E. (1985). A comparative study of structural properties of fibronectin and its 180 kDa fragment. FEBS Letters *189*, 276-280.

Calderwood, D.A. (2004). Integrin activation. Journal of Cell Science *117*, 657-666.

Calderwood, D.A., Campbell, I.D., and Critchley, D.R. (2013). Talins and kindlins: partners in integrin-mediated adhesion. Nature Reviews Molecular Cell Biology *14*, 503-517.

Calderwood, D.A., Shattil, S.J., and Ginsberg, M.H. (2000). Integrins and actin filaments: Reciprocal regulation of cell adhesion and signaling. Journal of Biological Chemistry *275*, 22607-22610.

Calderwood, D.A., Yan, B., de Pereda, J.M., Alvarez, B.G., Fujioka, Y., Liddington, R.C., and Ginsberg, M.H. (2002). The phosphotyrosine binding-like domain of talin activates integrins. The Journal of biological chemistry *277*, 21749-21758.

Calderwood, D.A., Zent, R., Grant, R., Rees, D.J.G., Hynes, R.O., and Ginsberg, M.H. (1999). The Talin head domain binds to integrin β subunit cytoplasmic tails and regulates integrin activation. Journal of Biological Chemistry *274*, 28071-28074.

Chen, H., and Mosher, D.F. (1996). Formation of Sodium Dodecyl Sulfate-stable Fibronectin Multimers: Failure to detect products of thiol-disulfide exchange in cyanogen bromide or limited acid digests of stabilized matrix fibronectin. Journal of Biological Chemistry *271*, 9084-9089.

Chen, J., Yu, L., Wang, L., Fang, X., Li, L., and Li, W. (2007). Stability of Synthetic Exendin-4 in Human Plasma In Vitro. Protein & Peptide Letters *14*, 19-25.

Chen, L.B., Murray, A., Segal, R.A., Bushnell, A., and Walsh, M.L. (1978). Studies on intercellular LETS glycoprotein matrices. Cell *14*, 377-391.

Chen, Y., Zardi, L., and Peters, D.M.P. (1997). High-resolution cryo-scanning electron microscopy study of the macromolecular structure of fibronectin fibrils. Scanning *19*, 349-355.

Chew, D.P., Bhatt, D.L., Sapp, S., and Topol, E.J. (2001). Increased Mortality With Oral Platelet Glycoprotein IIb/IIIa Antagonists: A Meta-Analysis of Phase III Multicenter Randomized Trials. Circulation *103*, 201-206.

Cho, J., Degen, J.L., Coller, B.S., and Mosher, D.F. (2005). Fibrin but not adsorbed fibrinogen supports fibronectin assembly by spread platelets. Effects of the interaction of alphaIIb beta3 with the C terminus of the fibrinogen gamma-chain. The Journal of biological chemistry *280*, 35490-35498.

Cho, J., and Mosher, D.F. (2005). Characterization of fibronectin assembly by platelets adherent to adsorbed laminin-111. Journal of Thrombosis and Haemostasis *4*, 943 - 951.

Cho, J., and Mosher, D.F. (2006a). Enhancement of thrombogenesis by plasma fibronectin cross-linked to fibrin and assembled in platelet thrombi. Blood *107*, 3555-3563.

Cho, J., and Mosher, D.F. (2006b). Impact of fibronectin assembly on platelet thrombus formation in response to type I collagen and von Willebrand factor. Blood *108*, 2229-2236.

Cho, J., and Mosher, D.F. (2006c). Role of fibronectin assembly in platelet thrombus formation. Journal of Thrombosis and Haemostasis *4*, 1461-1469.

Coller, B.S. (2001). Anti-GPIIb/IIIa Drugs: Current Strategies and Future Directions. Thrombosis and Haemostasis *86*, 427-443.

Davies, P.F., Barbee, K.A., Volin, M.V., Robotewskyj, A., Chen, J., Joseph, L., Griem, M.L., Wernick, M.N., Jacobs, E., Polacek, D.C. (1997). Spatial relationships in early signaling events of flow-mediated endothelial mechanotransduction. Annual Review of Physiology *59*, 527-549.

Deible, C.R., Beckman, E.J., Russell, A.J., and Wagner, W.R. (1998). Creating molecular barriers to acute platelet deposition on damaged arteries with reactive polyethylene glycol. Journal of Biomedical Materials Research *41*, 251-256.

Derossi, D., Calvet, S., Trembleau, A., Brunissen, A., Chassaing, G., and Prochiantz, A. (1996). Cell Internalization of the Third Helix of the Antennapedia Homeodomain Is Receptor-independent. Journal of Biological Chemistry *271*, 18188-18193.

Dimitriou, A.A., Stathopoulos, P., Mitsios, J.V., Sakarellos-Daitsiotis, M., Goudevenos, J., Tsikaris, V., and Tselepis, A.D. (2009). Inhibition of platelet activation by peptide analogs of the β3-intracellular domain of platelet integrin αIIbβ3 conjugated to the cell-penetrating peptide Tat(48–60). Platelets *20*, 539-547.

Doyle, P.S., Ladoux, B., and Viovy, J.L. (2000). Dynamics of a Tethered Polymer in Shear Flow. Phys Rev Lett *84*, 4769-4772.

Dzamba, B.J., Jakab, K.R., Marsden, M., Schwartz, M.A., and DeSimone, D.W. (2009). Cadherin Adhesion, Tissue Tension, and Noncanonical Wnt Signaling Regulate Fibronectin Matrix Organization. Developmental Cell *16*, 421-432.

Dzamba, B.J., and Peters, D.M. (1991). Arrangement of cellular fibronectin in noncollagenous fibrils in human fibroblast cultures. Journal of Cell Science *100*, 605-612.

Engvall, E., and Ruoslahti, E. (1977). Binding of soluble form of fibroblast surface protein, fibronectin, to collagen. International Journal of Cancer *20*, 1-5.

Erickson, H.P. (1994). Reversible unfolding of fibronectin type III and immunoglobulin domains provides the structural basis for stretch and elasticity of titin and fibronectin. Proceedings of the National Academy of Sciences *91*, 10114-10118.

Erickson, H.P., and Carrell, N.A. (1983). Fibronectin in extended and compact conformations. Electron microscopy and sedimentation analysis. Journal of Biological Chemistry *258*, 14539-14544.

Evans, E.A., and Calderwood, D.A. (2007). Forces and Bond Dynamics in Cell Adhesion. Science *316*, 1148-1153.

Futaki, S., Goto, S., and Sugiura, Y. (2003). Membrane permeability commonly shared among arginine-rich peptides. Journal of Molecular Recognition *16*, 260-264.

Futaki, S., Suzuki, T., Ohashi, W., Yagami, T., Tanaka, S., Ueda, K., and Sugiura, Y. (2001). Arginine-rich Peptides: An abundant source of membrane-permeable peptides having potential as carriers for intracellular protein delivery. Journal of Biological Chemistry *276*, 5836-5840.

Gao, M., Craig, D., Lequin, O., Campbell, I.D., Vogel, V., and Schulten, K. (2003). Structure and functional significance of mechanically unfolded fibronectin type III1 intermediates. Proceedings of the National Academy of Sciences of the United States of America *100*, 14784-14789.

García-Alvarez, B., de Pereda, J.M., Calderwood, D.A., Ulmer, T.S., Critchley, D., Campbell, I.D., Ginsberg, M.H., and Liddington, R.C. (2003). Structural Determinants of Integrin Recognition by Talin. Molecular Cell *11*, 49-58.

George, E.L., Georges-Labouesse, E.N., Patel-King, R.S., Rayburn, H., and Hynes, R.O. (1993). Defects in mesoderm, neural tube and vascular development in mouse embryos lacking fibronectin. Development *119*, 1079-1091.

Ginsberg, M.H., Partridge, A., and Shattil, S.J. (2005). Integrin regulation. Current Opinion in Cell Biology *17*, 509-516.

Gordon, J. (1976). Platelets in Biology and Pathology (New York: North Holland Publishing).

Harburger, D.S., Bouaouina, M., and Calderwood, D.A. (2009). Kindlin-1 and -2 directly bind the C-terminal region of beta integrin cytoplasmic tails and exert integrin-specific activation effects. The Journal of biological chemistry *284*, 11485-11497.

Harburger, D.S., and Calderwood, D.A. (2009). Integrin signalling at a glance. Journal of Cell Science *122*, 159-163.

Hassan, M.I., Saxena, A., and Ahmad, F. (2012). Structure and function of von Willebrand factor. Blood Coagulation & Fibrinolysis *23*, 11-22.

Hato, T., Pampori, N., and Shattil, S.J. (1998). Complementary Roles for Receptor Clustering and Conformational Change in the Adhesive and Signaling Functions of Integrin αIIbβ3. The Journal of cell biology *141*, 1685-1695.

Hocking, D.C., Smith, R.K., and McKeown-Longo, P.J. (1996). A novel role for the integrin-binding III-10 module in fibronectin matrix assembly. The Journal of cell biology *133*, 431-444.

Hocking, D.C., Sottile, J., and McKeown-Longo, P.J. (1994). Fibronectin's III-1 module contains a conformation-dependent binding site for the amino-terminal region of fibronectin. Journal of Biological Chemistry *269*, 19183-19187.

Hocking, D.C., Sottile, J., Reho, T., Fässler, R., and McKeown-Longo, P.J. (1999). Inhibition of Fibronectin Matrix Assembly by the Heparin-binding Domain of Vitronectin. Journal of Biological Chemistry *274*, 27257-27264.

Hoffmann, C., Gaietta, G., Zurn, A., Adams, S.R., Terrillon, S., Ellisman, M.H., Tsien, R.Y., and Lohse, M.J. (2010). Fluorescent labeling of tetracysteine-tagged proteins in intact cells. Nat Protocols *5*, 1666-1677.

Holmsen, H. (1994). Platelet secretion and energy metabolism. In Hemostasis and Thrombosis: Basic Principles and Clinical Practice, R. Colman, J. Hirsch, V. Marder, and E. Salzman, eds. (Philadephia: JB Lippincott), pp. 524-525.

Hong, J., Azens, A., Ekdahl, K.N., Granqvist, C.G., and Nilsson, B. (2005). Material-specific thrombin generation following contact between metal surfaces and whole blood. Biomaterials *26*, 1397-1403.

Humphries, M.J. (1996). Integrin activation: the link between ligand binding and signal transduction. Current Opinion in Cell Biology *8*, 632-640.

Huynh Khon, C., Stoldt Volker, R., and Scharf Rudiger, E. (2013). Contribution of distinct platelet integrins to binding, unfolding, and assembly of fibronectin. Biological Chemistry *394*, 1485.

Hynes, R.O. (1990). Fibronectin (New York: Springer-Verlag).

Hynes, R.O. (2002). Integrins: Bidirectional, Allosteric Signaling Machines. Cell *110*, 673-687.

Ingham, K.C., Brew, S.A., Huff, S., and Litvinovich, S.V. (1997). Cryptic Self-association Sites in Type III Modules of Fibronectin. Journal of Biological Chemistry *272*, 1718-1724.

Jen, C.J., and Lin, J.S. (1991). Direct observation of platelet adhesion to fibrinogen- and fibrin-coated surfaces. American Journal of Physiology - Heart and Circulatory Physiology *261*, H1457-H1463.

Jo, S., and Park, K. (2000). Surface modification using silanated poly(ethylene glycol)s. Biomaterials *21*, 605-616.

Johnson, K.J., Sage, H., Briscoe, G., and Erickson, H.P. (1999). The Compact Conformation of Fibronectin Is Determined by Intramolecular Ionic Interactions. Journal of Biological Chemistry *274*, 15473-15479.

Kahner, B.N., Kato, H., Banno, A., Ginsberg, M.H., Shattil, S.J., and Ye, F. (2012). Kindlins, Integrin Activation and the Regulation of Talin Recruitment to aIIb3. PLoS ONE *7*, e34056 - e34067.

Kalli, A.C., Campbell, I.D., and Sansom, M.S.P. (2011). Multiscale simulations suggest a mechanism for integrin inside-out activation. Proceedings of the National Academy of Sciences *108*, 11890-11895.

Kang, C.K., and Lee, Y.S. (2007). The surface modification of stainless steel and the correlation between the surface properties and protein adsorption. Journal of materials science Materials in medicine *18*, 1389-1398.

Khan, M.Y., Jaikaria, N.S., Frenz, D.A., Villanueva, G., and Newman, S.A. (1988). Structural changes in the NH2-terminal domain of fibronectin upon interaction with heparin. Relationship to matrix-driven translocation. Journal of Biological Chemistry *263*, 11314-11318.

Kloeker, S., Major, M.B., Calderwood, D.A., Ginsberg, M.H., Jones, D.A., and Beckerle, M.C. (2004). The Kindler Syndrome Protein Is Regulated by Transforming Growth Factor-β and Involved in Integrin-mediated Adhesion. Journal of Biological Chemistry *279*, 6824-6833.

Krammer, A., Lu, H., Isralewitz, B., Schulten, K., and Vogel, V. (1999). Forced unfolding of the fibronectin type III module reveals a tensile molecular recognition switch. Proceedings of the National Academy of Sciences *96*, 1351-1356.

Kroll, M.H., Hellums, J.D., Mclntire, L.V., Schafer, A.I., and Moake, J.L. (1996). Platelets and Shear Stress. The Journal of The American Society of Hematology *88*, 1525 - 1541.

Langenbach, K.J., and Sottile, J. (1999). Identification of Protein-disulfide Isomerase Activity in Fibronectin. Journal of Biological Chemistry *274*, 7032-7038.

Lauffenburger, D.A., and Horwitz, A.F. (1996). Cell Migration: A Physically Integrated Molecular Process. Cell *84*, 359-369.

Leahy, D.J., Aukhil, I., and Erickson, H.P. (1996). 2.0 Å Crystal Structure of a Four-Domain Segment of Human Fibronectin Encompassing the RGD Loop and Synergy Region. Cell *84*, 155-164.

Lerman, O.Z., Galiano, R.D., Armour, M., Levine, J.P., and Gurtner, G.C. (2003). Cellular Dysfunction in the Diabetic Fibroblast: Impairment in Migration, Vascular Endothelial Growth Factor Production, and Response to Hypoxia. The American Journal of Pathology *162*, 303-312.

Litjens, P.E.M.H., Kroner, C.I., Akkerman, J.W.N., and Van Willigen, G. (2003). Cytoplasmic regions of the β3 subunit of integrin αIIbβ3 involved in platelet adhesion on fibrinogen under flow conditions. Journal of Thrombosis and Haemostasis *1*, 2014-2021.

Liu, J., Fukuda, K., Xu, Z., Ma, Y.-Q., Hirbawi, J., Mao, X., Wu, C., Plow, E.F., and Qin, J. (2011). Structural Basis of Phosphoinositide Binding to Kindlin-2 Protein Pleckstrin Homology Domain in Regulating Integrin Activation. Journal of Biological Chemistry *286*, 43334-43342.

Liu, K.Y., Timmons, S., Lin, Y.Z., and Hawiger, J. (1996). Identification of a functionally important sequence in the cytoplasmic tail of integrin beta 3 by using cell-permeable peptide analogs. Proceedings of the National Academy of Sciences *93*, 11819-11824.

Luo, B.-H., Carman, C.V., and Springer, T.A. (2007). Structural Basis of Integrin Regulation and Signaling. Annual Review of Immunology *25*, 619-647.

Ma, Y.-Q., Yang, J., Pesho, M.M., Vinogradova, O., Qin, J., and Plow, E.F. (2006). Regulation of Integrin αIIbβ3 Activation by Distinct Regions of Its Cytoplasmic Tails†. Biochemistry *45*, 6656-6662.

Ma, Y.Q., Qin, J., Wu, C., and Plow, E.F. (2008). Kindlin-2 (Mig-2): a co-activator of beta3 integrins. The Journal of cell biology *181*, 439-446.

Magnusson, M.K., and Mosher, D.F. (1998). Fibronectin: Structure, Assembly, and Cardiovascular Implications. Arteriosclerosis, Thrombosis, and Vascular Biology *18*, 1363-1370.

Malinin, N.L., Plow, E.F., and Byzova, T.V. (2010). Kindlins in FERM adhesion. Blood *115*, 4011-4017.

Mao, Y., and Schwarzbauer, J.E. (2005a). Fibronectin fibrillogenesis, a cell-mediated matrix assembly process. Matrix biology : journal of the International Society for Matrix Biology *24*, 389-399.

Mao, Y., and Schwarzbauer, J.E. (2005b). Stimulatory effects of a three-dimensional microenvironment on cell-mediated fibronectin fibrillogenesis. Journal of Cell Science *118*, 4427-4436.

Maurer, L.M., Tomasini-Johansson, B.R., and Mosher, D.F. (2010). Emerging roles of fibronectin in thrombosis. Thrombosis Research *125*, 287-291.

McKeown-Longo, P.J., and Mosher, D.F. (1983). Binding of plasma fibronectin to cell layers of human skin fibroblasts. The Journal of cell biology *97*, 466-472.

McKeown-Longo, P.J., and Mosher, D.F. (1985). Interaction of the 70,000-mol-wt amino-terminal fragment of fibronectin with the matrix-assembly receptor of fibroblasts. The Journal of cell biology *100*, 364-374.

Mitchison, T.J., and Cramer, L.P. (1996). Actin-Based Cell Motility and Cell Locomotion. Cell *84*, 371-379.

Monkley, S.J., Pritchard, C.A., and Critchley, D.R. (2001). Analysis of the Mammalian Talin2 Gene TLN2. Biochemical and Biophysical Research Communications *286*, 880-885.

Morla, A., Zhang, Z., and Ruoslahti, E. (1994). Superfibronectin is a functionally distinct form of fibronectin. Nature *367*, 193-196.

Moser, M., Legate, K.R., Zent, R., and Fassler, R. (2009). The tail of integrins, talin, and kindlins. Science *324*, 895-899.

Moser, M., Nieswandt, B., Ussar, S., Pozgajova, M., and Fassler, R. (2008). Kindlin-3 is essential for integrin activation and platelet aggregation. Nature medicine *14*, 325-330.

Mosher, D.F. (1993). Assembly of fibronectin into extracellular matrix. Current Opinion in Structural Biology *3*, 214-222.

Nguyen, H.T., Huynh, K.C., Scharf, R.E., and Stoldt, V.R. (2013). Shear-related fibrillogenesis of fibronectin. Biol Chem *394*, 1495-1503.

Ni, H., Denis, C.V., Subbarao, S., Degen, J.L., Sato, T.N., Hynes, R.O., and Wagner, D.D. (2000). Persistence of platelet thrombus formation in arterioles of mice lacking both von Willebrand factor and fibrinogen. The Journal of clinical investigation *106*, 385-392.

Ni, H., Papalia, J.M., Degen, J.L., and Wagner, D.D. (2003). Control of thrombus embolization and fibronectin internalization by integrin αIIbβ3 engagement of the fibrinogen γ chain. Blood *102*, 3609-3614.

Nieswandt, B., Moser, M., Pleines, I., Varga-Szabo, D., Monkley, S., Critchley, D., and Fässler, R. (2007). Loss of talin1 in platelets abrogates integrin activation, platelet aggregation, and thrombus formation in vitro and in vivo. The Journal of Experimental Medicine *204*, 3113-3118.

Nieswandt, B., and Watson, S.P. (2003). Platelet-collagen interaction: is GPVI the central receptor?, Vol 102.

Oberhauser, A.F., Badilla-Fernandez, C., Carrion-Vazquez, M., and Fernandez, J.M. (2002). The Mechanical Hierarchies of Fibronectin Observed with Single-molecule AFM. Journal of Molecular Biology *319*, 433-447.

Oeveren, W.V., Schoen, P., and Maijers, C.A. (2000). Blood Compatibility of Metals and Alloys Used in Medical Devices. Progress in Biomedical Research *5*, 211 - 214.

Olorundare, O.E., Peyruchaud, O., Albrecht, R.M., and Mosher, D.F. (2001). Assembly of a fibronectin matrix by adherent platelets stimulated by lysophosphatidic acid and other agonists. Blood *98*, 117 - 124.

Pankov, R., Cukierman, E., Katz, B.-Z., Matsumoto, K., Lin, D.C., Lin, S., Hahn, C., and Yamada, K.M. (2000). Integrin Dynamics and Matrix Assembly: Tensin-Dependent Translocation of α5β1 Integrins Promotes Early Fibronectin Fibrillogenesis. The Journal of cell biology *148*, 1075-1090.

Pankov, R., and Yamada, K.M. (2002). Fibronectin at a glance. Journal of Cell Science *115*, 3861 - 3863.

Papamichael, N.D., Stathopoulou, E.M., Roussa, V.D., Tsironis, L.D., Kotsia, A.P., Stanica, R.-M., Moussis, V., Tsikaris, V., Katsouras, C.S., Tselepis, A.D. (2009). Effect of a Synthetic Peptide Corresponding to Residues 313 to 320 of the αIIb Subunit of the Human Platelet Integrin αIIbβ3 on Carotid Artery Thrombosis in Rabbits. Journal of Pharmacology and Experimental Therapeutics *329*, 634-640.

Pereira, M., Rybarczyk, B.J., Odrljin, T.M., Hocking, D.C., Sottile, J., and Simpson-Haidaris, P.J. (2002). The incorporation of fibrinogen into extracellular matrix is dependent on active assembly of a fibronectin matrix. Journal of Cell Science *115*, 609-617.

Perera, H.D., Ma, Y.-Q., Yang, J., Hirbawi, J., Plow, Edward F., and Qin, J. (2011). Membrane Binding of the N-Terminal Ubiquitin-Like Domain of kindlin-2 Is Crucial for Its Regulation of Integrin Activation. Structure *19*, 1664-1671.

Peters, D.M.P., Chen, Y., Zardi, L., and Brummel, S. (1998). Conformation of Fibronectin Fibrils Varies: Discrete Globular Domains of Type III Repeats Detected. Microscopy and Microanalysis *4*, 385-396.

Petersen, T.E., Thogersen, H.C., Skorstengaard, K., Vibe-Pedersen, K., Sahl, P., Sottrup-Jensen, L., and Magnusson, S. (1983). Partial primary structure of bovine plasma fibronectin: Three types of internal homology. Proceedings of the National Academy of Sciences *80*, 137-141.

Petrich, B.G., Fogelstrand, P., Partridge, A.W., Yousefi, N., Ablooglu, A.J., Shattil, S.J., and Ginsberg, M.H. (2007a). The antithrombotic potential of selective blockade of talin-dependent integrin αIIbβ3 (platelet GPIIb–IIIa) activation. The Journal of clinical investigation *117*, 2250-2259.

Petrich, B.G., Marchese, P., Ruggeri, Z.M., Spiess, S., Weichert, R.A.M., Ye, F., Tiedt, R., Skoda, R.C., Monkley, S.J., Critchley, D.R. (2007b). Talin is required for integrin-mediated platelet function in hemostasis and thrombosis. The Journal of Experimental Medicine *204*, 3103-3111.

Piotr, S., and Marek, C. (2011). Hydrodynamic effects in proteins. Journal of Physics: Condensed Matter *23*, 033102.

Qian, Y., Feldman, E., Pennathur, S., Kretzler, M., and Brosius, F.C. (2008). From Fibrosis to Sclerosis: Mechanisms of Glomerulosclerosis in Diabetic Nephropathy. Diabetes *57*, 1439-1445.

Quinn, M.J., Byzova, T.V., Qin, J., Topol, E.J., and Plow, E.F. (2003). Integrin αIIbβ3 and Its Antagonism. Arteriosclerosis, Thrombosis, and Vascular Biology *23*, 945-952.

Ratnikov, B.I., Partridge, A.W., and Ginsberg, M.H. (2005). Integrin activation by talin. Journal of Thrombosis and Haemostasis *3*, 1783-1790.

Richard, J.P., Melikov, K., Vives, E., Ramos, C., Verbeure, B., Gait, M.J., Chernomordik, L.V., and Lebleu, B. (2003). Cell-penetrating Peptides: A reevaluation of the mechanism of cellular uptake. Journal of Biological Chemistry *278*, 585-590.

Roberts, G.C., and Critchley, D.R. (2009). Structural and biophysical properties of the integrin-associated cytoskeletal protein talin. Biophysical reviews *1*, 61-69.

Salmeron-Sanchez, M., Rico, P., Moratal, D., Lee, T.T., Schwarzbauer, J.E., and Garcia, A.J. (2011). Role of material-driven fibronectin fibrillogenesis in cell differentiation. Biomaterials *32*, 2099-2105.

Savage, B., Almus-Jacobs, F., and Ruggeri, Z.M. (1998). Specific Synergy of Multiple Substrate–Receptor Interactions in Platelet Thrombus Formation under Flow. Cell *94*, 657-666.

Savage, B., Saldívar, E., and Ruggeri, Z.M. (1996). Initiation of Platelet Adhesion by Arrest onto Fibrinogen or Translocation on von Willebrand Factor. Cell *84*, 289-297.

Schneider, S.W., Nuschele, S., Wixforth, A., Gorzelanny, C., Alexander-Katz, A., Netz, R.R., and Schneider, M.F. (2007). Shear-induced unfolding triggers adhesion of von Willebrand factor fibers. Proceedings of the National Academy of Sciences *104*, 7899-7903.

Schroeder, C.M., Teixeira, R.E., Shaqfeh, E.S.G., and Chu, S. (2005). Characteristic Periodic Motion of Polymers in Shear Flow. Phys Rev Lett *95*, 018301.

Schwarzbauer, J.E. (1991). Identification of the fibronectin sequences required for assembly of a fibrillar matrix. The Journal of cell biology *113*, 1463-1473.

Schwarzbauer, J.E., and Sechler, J.L. (1999). Fibronectin fibrillogenesis: a paradigm for extracellular matrix assembly. Current Opinion in Cell Biology *11*, 622–627.

Shattil, S.J., Kim, C., and Ginsberg, M.H. (2010). The final steps of integrin activation: the end game. Nat Rev Mol Cell Biol *11*, 288-300.

Siediecki, C., Lestini, B., Kottke-Marchant, K., Eppell, S., Wilson, D., and Marchant, R. (1996). Shear-dependent changes in the three-dimensional structure of human von Willebrand factor. Blood *88*, 2939-2950.

Singer, I.I. (1979). The fibronexus: a transmembrane association of fibronectin-containing fibers and bundles of 5 nm microfilaments in hamster and human fibroblasts. Cell *16*, 675-685.

Singh, I., Themistou, E., Porcar, L., and Neelamegham, S. (2009). Fluid Shear Induces Conformation Change in Human Blood Protein von Willebrand Factor in Solution. Biophysical Journal *96*, 2313-2320.

Singh, P., Carraher, C., and Schwarzbauer, J.E. (2010). Assembly of fibronectin extracellular matrix. Annual review of cell and developmental biology *26*, 397-419.

Smith, D.E., Babcock, H.P., and Chu, S. (1999). Single-Polymer Dynamics in Steady Shear Flow. Science *283*, 1724-1727.

Smith, M.L., Gourdon, D., Little, W.C., Kubow, K.E., Eguiluz, R.A., Luna-Morris, S., and Vogel, V. (2007). Force-Induced Unfolding of Fibronectin in the Extracellular Matrix of Living Cells. PLoS Biol *5*, e268.

Stefanini, L., Ye, F., Snider, A.K., Sarabakhsh, K., Piatt, R., Paul, D.S., Bergmeier, W., and Petrich, B.G. (2014). A talin mutant that impairs talin-integrin binding in platelets decelerates alphaIIbbeta3 activation without pathological bleeding. Blood *123*, 2722-2731.

Steward, R.L., Cheng, C.-M., Ye, J.D., Bellin, R.M., and LeDuc, P.R. (2011). Mechanical stretch and shear flow induced reorganization and recruitment of fibronectin in fibroblasts. Sci Rep *1*, 147 - 158.

Tadokoro, S., Shattil, S.J., Eto, K., Tai, V., Liddington, R.C., de Pereda, J.M., Ginsberg, M.H., and Calderwood, D.A. (2003). Talin Binding to Integrin ß Tails: A Final Common Step in Integrin Activation. Science *302*, 103-106.

Tahiliani, P.D., Singh, L., Auer, K.L., and LaFlamme, S.E. (1997). The Role of Conserved Amino Acid Motifs within the Integrin β3 Cytoplasmic Domain in Triggering Focal Adhesion Kinase Phosphorylation. Journal of Biological Chemistry *272*, 7892-7898.

Tanentzapf, G., and Brown, N.H. (2006). An interaction between integrin and the talin FERM domain mediates integrin activation but not linkage to the cytoskeleton. Nat Cell Biol *8*, 601-606.

Teixeira, R.E., Babcock, H.P., Shaqfeh, E.S.G., and Chu, S. (2004). Shear Thinning and Tumbling Dynamics of Single Polymers in the Flow-Gradient Plane. Macromolecules *38*, 581-592.

Themistou, E., Singh, I., Shang, C., Balu-Iyer, S.V., Alexandridis, P., and Neelamegham, S. (2009). Application of Fluorescence Spectroscopy to Quantify Shear-Induced Protein Conformation Change. Biophysical Journal *97*, 2567-2576.

Thurlow, P.J., D, A.K., and Connellan, J.M. (1990). The role of fibronectin in platelet aggregation. British Journal of Haernatology *75*, 549-556.

To, W.S., and Midwood, K.S. (2011). Plasma and cellular fibronectin: distinct and independent functions during tissue repair. Fibrogenesis & tissue repair *4*, 21.

Tomasini-Johansson, B.R., Annis, D.S., and Mosher, D.F. (2006). The N-terminal 70-kDa fragment of fibronectin binds to cell surface fibronectin assembly sites in the absence of intact fibronectin. Matrix Biology *25*, 282-293.

Tompa, P., Fuxreiter, M., Oldfield, C.J., Simon, I., Dunker, A.K., and Uversky, V.N. (2009). Close encounters of the third kind: disordered domains and the interactions of proteins. BioEssays *31*, 328-335.

Triplett, D.A. (2000). Coagulation and Bleeding Disorders: Review and Update. Clinical Chemistry *46*, 1260-1269.

Tsilibary, E.C. (2003). Microvascular basement membranes in diabetes mellitus. The Journal of Pathology *200*, 537-546.

Tu, R.S., and Breedveld, V. (2005). Microrheological detection of protein unfolding. Physical Review E *72*, 041914.

Tzima, E., del Pozo, M.A., Shattil, S.J., Chien, S., and Schwartz, M.A. (2001). Activation of integrins in endothelial cells by fluid shear stress mediates Rho-dependent cytoskeletal alignment. The EMBO Journal *20*, 4639-4647.

Ugarova, T.P., Zamarron, C., Veklich, Y., Bowditch, R.D., Ginsberg, M.H., Weisel, J.W., and Plow, E.F. (1995). Conformational Transitions in the Cell Binding Domain of Fibronectin. Biochemistry *34*, 4457-4466.

Ulmer, J., Geiger, B., and Spatz, J.P. (2008). Force-induced fibronectin fibrillogenesis in vitro. Soft Matter *4*, 1998-2007.

Ulmer, T.S., Calderwood, D.A., Ginsberg, M.H., and Campbell, I.D. (2003). Domain-Specific Interactions of Talin with the Membrane-Proximal Region of the Integrin β3 Subunit. Biochemistry *42*, 8307-8312.

Ulmer, T.S., Yaspan, B., Ginsberg, M.H., and Campbell, I.D. (2001). NMR Analysis of Structure and Dynamics of the Cytosolic Tails of Integrin αIIbβ3 in Aqueous Solution†. Biochemistry *40*, 7498-7508.

Ussar, S., Wang, H.-V., Linder, S., Fässler, R., and Moser, M. (2006). The Kindlins: Subcellular localization and expression during murine development. Experimental Cell Research *312*, 3142-3151.

Vincentelli, A., Susen, S., Thierry Le Tourneau, Six, I., Fabre, O., Juthier, F., Bauters, A., Decoene, C., Goudemand, J., Prat, A. (2003). Acquired von Willebrand Syndrome in Aortic Stenosis. The new england journal of medicine *349*, 343 - 349.

Vivès, E., Brodin, P., and Lebleu, B. (1997). A Truncated HIV-1 Tat Protein Basic Domain Rapidly Translocates through the Plasma Membrane and Accumulates in the Cell Nucleus. Journal of Biological Chemistry *272*, 16010-16017.

Wang, J., Zhang, W., Nardi, M.A., and Li, Z. (2011). HIV-1 Tat-induced platelet activation and release of CD154 contribute to HIV-1-associated autoimmune thrombocytopenia. J Thromb Haemost *9*, 562-573.

Watson, S.P. (2009). Platelet Activation by Extracellular Matrix Proteins in Haemostasis and Thrombosis Current Pharmaceutical Design *15*, 1358-1372

Wegener, K.L., Partridge, A.W., Han, J., Pickford, A.R., Liddington, R.C., Ginsberg, M.H., and Campbell, I.D. (2007). Structural Basis of Integrin Activation by Talin. Cell *128*, 171-182.

Welch, M.D., Mallavarapu, A., Rosenblatt, J., and Mitchison, T.J. (1997). Actin dynamics in vivo. Current Opinion in Cell Biology *9*, 54-61.

Wierzbicka-Patynowski, I., and Schwarzbauer, J.E. (2003). The ins and outs of fibronectin matrix assembly. Journal of Cell Science *116*, 3269-3276.

Williams, E.C., Janmey, P.A., Ferrylll, J.D., and Masher, D. (1982). Conformational States of Fibronectin. The Journal of biological chemistry *257*, 14973 - 14978.

Wu, C. (1997). Roles of integrins in fibronectin matrix assembly. Histology and Histopathology *12*, 233-240.

Wu, C., Hughes, P., Ginsberg, M., and McDonald, J. (1996). Identification of a new biological function for the integrin alpha v beta 3: initiation of fibronectin matrix assembly. Cell adhesion Commun *4*, 149-158.

Wu, C., Keivenst, V.M., O'Toole, T.E., McDonald, J.A., and Ginsberg, M.H. (1995). Integrin activation and cytoskeletal interaction are essential for the assembly of a fibronectin matrix. Cell *83*, 715-724.

Xi, X., Bodnar, R.J., Li, Z., Lam, S.C.-T., and Du, X. (2003). Critical roles for the COOH-terminal NITY and RGT sequences of the integrin β3 cytoplasmic domain in inside-out and outside-in signaling. The Journal of cell biology *162*, 329-339.

Xu, J., and Mosher, D. (2011). Fibronectin and Other Adhesive Glycoproteins. In The Extracellular Matrix: an Overview, R.P. Mecham, ed. (Springer Berlin Heidelberg), pp. 41-75.

Yates, L.A., Füzéry, A.K., Bonet, R., Campbell, I.D., and Gilbert, R.J.C. (2012a). Biophysical Analysis of Kindlin-3 Reveals an Elongated Conformation and Maps Integrin Binding to the Membrane-distal β-Subunit NPXY Motif. Journal of Biological Chemistry *287*, 37715-37731.

Yates, L.A., Lumb, C.N., Brahme, N.N., Zalyte, R., Bird, L.E., De Colibus, L., Owens, R.J., Calderwood, D.A., Sansom, M.S.P., and Gilbert, R.J.C. (2012b). Structural and Functional Characterization of the Kindlin-1 Pleckstrin Homology Domain. Journal of Biological Chemistry *287*, 43246-43261.

Ye, F., Hu, G., Taylor, D., Ratnikov, B., Bobkov, A.A., McLean, M.A., Sligar, S.G., Taylor, K.A., and Ginsberg, M.H. (2010). Recreation of the terminal events in physiological integrin activation. The Journal of cell biology *188*, 157-173.

Ye, F., Petrich, Brian G., Anekal, P., Lefort, Craig T., Kasirer-Friede, A., Shattil, Sanford J., Ruppert, R., Moser, M., Fässler, R., and Ginsberg, Mark H. (2013). The Mechanism of Kindlin-Mediated Activation of Integrin αIIbβ3. Current Biology *23*, 2288-2295.

Zalipsky, S., and Harris, J.M. (1997). Introduction to chemistry and biological application of poly(ethylen glycol). In Poly(Ethylen Glycol) Chemistry and Biological Applications, J.M. Harris, and S. Zalipsky, eds. (Washington DC: American Chemistry Society), pp. 1-13.

Zardi, L., Cecconi, C., Barbieri, O., Carnemolla, B., Picca, M., and Santi, L. (1979). Concentration of Fibronectin in Plasma of Tumor-bearing Mice and Synthesis by Ehrlich Ascites Tumor Cells. Cancer Research *39*, 3774-3779.

Zheng, M., Ambesi, A., Yu, L., and McKeown-Longo, P.J. (2007). Quantification of fibronectin matrix assembly sites using a novel ELISA assay. Matrix Biology *26*, 330-333.

Zhong, C., Chrzanowska-Wodnicka, M., Brown, J., Shaub, A., Belkin, A.M., and Burridge, K. (1998). Rho-mediated Contractility Exposes a Cryptic Site in Fibronectin and Induces Fibronectin Matrix Assembly. The Journal of cell biology *141*, 539-551.